

1. Report Number FHWA/TX - 91/1123-3		2. Government Accession No.		3. Recipient's Catalog No.	
4. Title and Subtitle MODULUS 4.0: Expansion and Validation of the MODULUS Backcalculation System				5. Report Date November, 1990	
				6. Performing Organization Code	
7. Author(s) G. T. Rohde and T. Scullion				8. Performing Organization Report No. Research Report 1123-3	
9. Performing Organization Name and Address Texas Transportation Institute Texas A&M University System College Station, Texas 77843-3135				10. Work Unit No. Study No. 2-18-87-1123	
				11. Contract or Grant No.	
12. Sponsoring Agency Name and Address Texas State Department of Highways and Public Transportation, Transportation Planning Division, P. O. Box 5051, Austin, Texas 77876				13. Type of Report and Period Covered Final Report September 88 - September 90	
				14. Sponsoring Agency Code	
15. Supplementary Notes Research performed in cooperation with DOT, FHWA Research Study Title "Nondestructive Test Procedures for Analyzing the Structural Conditions of Pavements"					
16. Abstract This report describes the Texas Transportation Institute's continuing efforts to upgrade the MODULUS backcalculation system. Enhancements have been made in several areas, including: <ol style="list-style-type: none"> 1. Inclusion of a procedure to estimate the depth to a stiff layer. 2. A method of assessing the non-linearity of the subgrade and computation of the optimum number of sensors to use in the backcalculation routine. 3. The replacement of the BISAR linear elastic procedure with the WES5 procedure recently developed by the US Corps of Engineers. <p>The new MODULUS 4.0 is evaluated with monthly deflection data collected on 10 experimental sites for which all the layer materials have been tested in the laboratory. Validation of the system is attempted by using pavement sections instrumented with Multidepth Deflectometers. By simultaneously monitoring surface and depth deflections it is possible to quantify the effectiveness of the backcalculation system. Results show that the linear elastic model used in MODULUS produces reasonable layer moduli for pavements with thick asphalt surfacing. However, errors may result in using the linear elastic approach on thin pavements. The use of a stress dependent model which includes dilation substantially improves the match of measured and computed depth deflections on thin pavements. Preliminary results from a finite element backcalculation system have also been included.</p>					
17. Key Words Modulus, Backcalculation, Falling Weight Deflectometer, Depth to Bedrock			18. Distribution Statement No Restrictions Available through the National Technical Information Service 5285 Port Royal Road Springfield, Virginia 22161		
19. Security Classif.(of this report) Unclassified		20. Security Classif.(of this page) Unclassified		21. No. of Pages 128	22. Price

**MODULUS 4.0: EXPANSION AND VALIDATION OF THE MODULUS
BACKCALCULATION SYSTEM**

by

G. T. Rohde
T. Scullion

Research Report 1123-3
Research Study Number 2-18-87-1123
Study Title: "Nondestructive Test Procedures
for Analyzing the Structural
Condition of Pavements"

Conducted for

Texas State Department of Highways
and Public Transportation
in Cooperation with US DOT
FHWA

by

Texas Transportation Institute

November, 1990

**MODULUS 4.0: EXPANSION AND VALIDATION OF THE MODULUS
BACKCALCULATION SYSTEM**

ABSTRACT

This report describes the Texas Transportation Institute's continuing efforts to upgrade the MODULUS backcalculation system. Enhancements have been made in several areas, including:

1. Inclusion of a procedure to estimate the depth to a stiff layer.
2. A method of assessing the non-linearity of the subgrade and computation of the optimum number of sensors to use in the backcalculation routine.
3. The replacement of the BISAR linear elastic procedure with the WES5 procedure recently developed by the US Corps of Engineers.

The new MODULUS 4.0 is evaluated with monthly deflection data collected on 10 experimental sites for which all the layer materials have been tested in the laboratory. Validation of the system is attempted by using pavement sections instrumented with Multidepth Deflectometers. By simultaneously monitoring surface and depth deflections it is possible to quantify the effectiveness of the backcalculation system. Results show that the linear elastic model used in MODULUS produces reasonable layer moduli for pavements with thick asphalt surfacing. However, errors may result in using the linear elastic approach on thin pavements. The use of a stress dependent model which includes dilation substantially improves the match of measured and computed depth deflections on thin pavements. Preliminary results from a finite element backcalculation system have also been included.

METRIC (SI*) CONVERSION FACTORS

APPROXIMATE CONVERSIONS TO SI UNITS

Symbol	When You Know	Multiply By	To Find	Symbol
LENGTH				
in	inches	2.54	centimetres	cm
ft	feet	0.3048	metres	m
yd	yards	0.914	metres	m
mi	miles	1.61	kilometres	km

AREA				
in ²	square inches	645.2	centimetres squared	cm ²
ft ²	square feet	0.0929	metres squared	m ²
yd ²	square yards	0.836	metres squared	m ²
mi ²	square miles	2.59	kilometres squared	km ²
ac	acres	0.395	hectares	ha

MASS (weight)				
oz	ounces	28.35	grams	g
lb	pounds	0.454	kilograms	kg
T	short tons (2000 lb)	0.907	megagrams	Mg

VOLUME				
fl oz	fluid ounces	29.57	millilitres	mL
gal	gallons	3.785	litres	L
ft ³	cubic feet	0.0328	metres cubed	m ³
yd ³	cubic yards	0.0765	metres cubed	m ³

NOTE: Volumes greater than 1000 L shall be shown in m³.

TEMPERATURE (exact)

°F	Fahrenheit temperature	5/9 (after subtracting 32)	Celsius temperature	°C
----	------------------------	----------------------------	---------------------	----

APPROXIMATE CONVERSIONS TO SI UNITS

Symbol	When You Know	Multiply By	To Find	Symbol
LENGTH				
mm	millimetres	0.039	inches	in
m	metres	3.28	feet	ft
m	metres	1.09	yards	yd
km	kilometres	0.621	miles	mi

AREA				
mm ²	millimetres squared	0.0016	square inches	in ²
m ²	metres squared	10.764	square feet	ft ²
km ²	kilometres squared	0.39	square miles	mi ²
ha	hectares (10 000 m ²)	2.53	acres	ac

MASS (weight)				
g	grams	0.0353	ounces	oz
kg	kilograms	2.205	pounds	lb
Mg	megagrams (1 000 kg)	1.103	short tons	T

VOLUME				
mL	millilitres	0.034	fluid ounces	fl oz
L	litres	0.264	gallons	gal
m ³	metres cubed	35.315	cubic feet	ft ³
m ³	metres cubed	1.308	cubic yards	yd ³

TEMPERATURE (exact)

°C	Celsius temperature	9/5 (then add 32)	Fahrenheit temperature	°F

These factors conform to the requirement of FHWA Order 5190.1A.

* SI is the symbol for the International System of Measurements

DISCLAIMER

This report is not intended to constitute a standard, specification, or regulation, and does not necessarily represent the views or policy of the Federal Highway Administration or the Texas State Department of Highways and Public Transportation.

PREFACE

Other Reports in the 1123 series include:

Report 1123-1 "A Microcomputer Based Procedure to Backcalculate Layer Moduli from FWD Data" which describes the calculation procedure in MODULUS 2.0, and the segmentation procedures.

Report 1123-2 "Field Evaluation of the Multidepth Deflectometer" describes the MDD, the installation procedure and typical results obtained. This device provides the best means of validating modulus backcalculation procedures.

Report 1123-4F "MODULUS 4.0; User Guide"

TABLE OF CONTENTS

	Page
ABSTRACT	i
DISCLAIMER	iii
PREFEACE	iv
I. INTRODUCTION	1
II. DESCRIPTION OF ENHANCEMENTS TO MODULUS 4.0	3
2.1 Depth to an Apparent Rigid Layer	3
2.2 Sensor Weighing Factors	10
2.3 Sensor Selection Criteria	14
2.4 Inclusion of the WES5 Layered Elastic Program	16
III. FIELD VALIDATION PROCEDURES OF MODULUS 4.0	18
3.1 The Experimental Sections	18
3.2 Multidepth Deflection Testing	26
IV. DATA ANALYSIS	35
4.1 Analysis of Surface Deflection Data	35
4.2 Analysis of Multidepth Deflection Testing	61
V. CONCLUSIONS AND RECOMMENDATIONS.	81
REFERENCES	82
APPENDIX A SUBGRADE INFORMATION	84
APPENDIX B LABORATORY RESULTS	90
APPENDIX C MONTHLY DEFLECTION DATA	101
APPENDIX D BACKCALCULATION RESULTS	107

LIST OF TABLES

	Page
1. Comparing Predicted and Measured Depth to Bedrock	11
2. Typical Deflection Matching Results	13
3. The Location and Pavement Structure of the 10 Test Sites.	20
4. Base Course Coefficients for Equation 3.1	24
5. Subgrade Coefficients for Equation 3.1	25
6. Subgrade Coefficients for the Bilinear Model on Sections with Clay Subgrades	26
7. The Measured Surface and In-Depth Deflections Under an FWD Load for Section A	32
8. The Measured Surface and In-Depth Deflections Under an FWD Load for Section B	34
9. Stiffness Ratio of the Average Backcalculated Base Moduli for Sites 1 through 12	60
10. Results of the Deflection Analysis for Section A Using a Backcalculation Model with a Rigid Layer at a Depth of 20 feet	63
11. Results of the Deflection Analysis for Section A Using a Backcalculation Model with an Apparent Rigid Layer at a Depth of 16 feet	66
12. Results of the Deflection Analysis for Section B Using a Backcalculation Model with a Rigid Layer at a Depth of 20 feet.	69
13. Results of the Deflection Analysis for Section B Using a Backcalculation Model with an Apparent Rigid Layer at a Depth of 5.5 feet	70
14. Results of the Deflection Analysis for Section B Using a Backcalculation Model with an Apparent Rigid Layer at a Depth of 5.5 feet and a Subgrade Divided into Two Layers.	73
15. Material Properties Used in the Finite Element Model for Section B	75
16. Results of the Nonlinear Deflection Analysis for Section B.	76
A1. Subgrade Information for Site 1	85

LIST OF TABLES (Continued)

	Page
A2. Subgrade Information for Site 2	85
A3. Subgrade Information for Site 4	86
A4. Subgrade Information for Site 5	86
A5. Subgrade Information for Site 6	87
A6. Subgrade Information for Site 7	87
A7. Subgrade Information for Site 8	88
A8. Subgrade Information for Site 9	88
A9. Subgrade Information for Site 11.	89
A10. Subgrade Information for Site 12.	89
B1. The Laboratory Results for Site 1	91
B2. The Laboratory Results for Site 2	92
B3. The Laboratory Results for Site 4	93
B4. The Laboratory Results for Site 5	94
B5. The Laboratory Results for Site 6	95
B6. The Laboratory Results for Site 7	96
B7. The Laboratory Results for Site 8	97
B8. The Laboratory Results for Site 9	98
B9. The Laboratory Results for Site 11.	99
B10. The Laboratory Results for Site 12.	100
C1. Average Normalized Monthly Deflection Data for Site 1	102
C2. Average Normalized Monthly Deflection Data for Site 2	102
C3. Average Normalized Monthly Deflection Data for Site 4	103
C4. Average Normalized Monthly Deflection Data for Site 5	103
C5. Average Normalized Monthly Deflection Data for Site 6	104
C6. Average Normalized Monthly Deflection Data for Site 7	104
C7. Average Normalized Monthly Deflection Data for Site 8	105
C8. Average Normalized Monthly Deflection Data for Site 9	105
C9. Average Normalized Monthly Deflection Data for Site 11.	106
C10. Average Normalized Monthly Deflection Data for Site 12.	106
D1. Summary of the Backcalculation Results for Site 1	108
D2. Summary of the Backcalculation Results for Site 2	109
D3. Summary of the Backcalculation Results for Site 4	110

LIST OF TABLES (Continued)

	Page
D4. Summary of the Backcalculation Results for Site 5	111
D5. Summary of the Backcalculation Results for Site 6	112
D6. Summary of the Backcalculation Results for Site 7	113
D7. Summary of the Backcalculation Results for Site 8	114
D8. Summary of the Backcalculation Results for Site 9	115
D9. Summary of the Backcalculation Results for Site 11.	116
D10. Summary of the Backcalculation Results for Site 12.	117

LIST OF FIGURES

	Page
1. A Schematic of the Stress Distribution Below an FWD Load	4
2. Deflection vs. the Inverse of Offset (1/r) for a Number of Hypothetical Pavement Structures	6
3. An Illustration of the Method to Determine the Effective Depth to a Rigid Layer	8
4. A Schematic Illustrating the Procedure to Select the Number of Sensors to Use During Deflection Analysis	15
5. Location of the Test Pavement Sections	19
6. The Layout of a Typical Test Section	21
7. The Arithmetic Model (Bilinear Model) Describing the Nonlinear Resilient Modulus of a Fine Grained Soil	27
8. A Schematic of the Multidepth Deflectometer.	28
9. A Typical MDD Signal Under an FWD Load Before and After Noise Filtering	29
10. A Schematic Illustrating How One of the FWD Geophones can be Used to Measure the Anchor Deflection of the MDD System.	30
11. Monthly Backcalculation Results for Site 1	37
12. Monthly Backcalculation Results for Site 2	38
13. Monthly Backcalculation Results for Site 4	39
14. Monthly Backcalculation Results for Site 5	40
15. Monthly Backcalculation Results for Site 6	41
16. Monthly Backcalculation Results for Site 7	42
17. Monthly Backcalculation Results for Site 8	43
18. Monthly Backcalculation Results for Site 9	44
19. Monthly Backcalculation Results for Site 11.	45
20. Monthly Backcalculation Results for Site 12.	46
21. Comparison Between Backcalculation and Laboratory Results for the Asphalt Concrete and Subgrade of Site 1.	48
22. Comparison Between Backcalculation and Laboratory Results for the Asphalt Concrete and Subgrade of Site 2.	49
23. Comparison Between Backcalculation and Laboratory Results for the Asphalt Concrete and Subgrade of Site 4.	50

LIST OF FIGURES (Continued)

	Page
24. Comparison Between Backcalculation and Laboratory Results for the Asphalt Concrete and Subgrade of Site 5.	51
25. Comparison Between Backcalculation and Laboratory Results for the Asphalt Concrete and Subgrade of Site 6.	52
26. Comparison Between Backcalculation and Laboratory Results for the Asphalt Concrete and Subgrade of Site 7.	53
27. Comparison Between Backcalculation and Laboratory Results for the Asphalt Concrete and Subgrade of Site 8.	54
28. Comparison Between Backcalculation and Laboratory Results for the Asphalt Concrete and Subgrade of Site 9.	55
29. Comparison Between Backcalculation and Laboratory Results for the Asphalt Concrete and Subgrade of Site 11	56
30. Comparison Between Backcalculation and Laboratory Results for the Asphalt Concrete and Subgrade of Site 12	57
31. Measured and Predicted Deflections for Section A Based on a Pavement Model with a Rigid Layer at a Depth of 20 feet. . . .	65
32. Measured and Predicted Deflections for Section A Based on a Pavement Model with an Apparent Rigid Layer at a Depth of 16 feet	67
33. Measured and Predicted Deflections for Section B Based on a Pavement Model with an Apparent Rigid Layer at a Depth of 5.5 feet	71
34. Measured and Predicted Deflections for Section A Based on a Pavement Model with an Apparent Rigid Layer at a Depth of 5.5 feet and a Subgrade Divided into Two Layers	74
35. Measured and Predicted Deflections for Section B Based on a Nonlinear Elastic Pavement Model	77
36. The Backcalculated Moduli for Section B Based on a Nonlinear Elastic Pavement Model	78

CHAPTER I INTRODUCTION

The work presented in this report represents the continuing efforts of the Texas Transportation Institute to improve and validate the modulus backcalculation scheme (MODULUS) first published in Research Report 1123-1. (Uzan, et al., 1988). It is acknowledged that there does not exist a single backcalculation scheme that gives realistic layer moduli values under all test conditions for all pavement types. However, it is by undertaking continuing studies that efforts can be made to improve and expand existing systems.

The enhancements made to the MODULUS system include the following:

1. A procedure has been included to estimate the depth of a stiff layer within the pavement structure.
2. A method of assessing the non-linearity of the subgrade and computing the optimum number of sensors to be used in the backcalculation routine.
3. The replacement of the BISAR linear elastic procedure with the WES5 procedure recently developed by the Corps of Engineers.

In all phases of the work, efforts were made to validate the process. Seismic refraction test and mini cone borings were used to validate the theoretically developed depth to bedrock equations. The effectiveness of the system to generate realistic moduli values was validated using Multidepth Deflectometers. Furthermore, monthly deflection data were collected and processed on ten inservice pavements around the State of Texas. The procedures described in this report have been incorporated into the MODULUS 4.0 system. A user's manual to this system is published in TTI Report 1123-4F.

This research is presented in the following four chapters. In Chapter 2 a description is given of each of the enhancements to the system. Chapter 3 covers the field validation procedures. A description is given of the 10 experimental sections, including the measured layer properties from laboratory tests and the field testing program. The

Multidepth Deflectometer validation procedure is also discussed in Chapter 3. The data analysis is covered in Chapter 4 and the conclusions and recommendations are presented in Chapter 5. Detailed subgrade, laboratory test, deflection data, and backcalculation results are given in the appendices.

CHAPTER II

DESCRIPTION OF ENHANCEMENTS TO MODULUS 4.0

2.1 Depth to an Apparent Rigid Layer

Several researchers (Bush, 1980, Uddin, et al. 1986, Lytton, et al. 1990,) have shown that the existence of a rigid layer underlying the subgrade, significantly influences the analysis of deflection data. As stated by Uddin et al. (1986):

Ignorance of rigid bottom considerations may lead to substantial errors in the predicted moduli of a pavement-subgrade system. The subgrade modulus may be significantly overpredicted if a semi-infinite subgrade is falsely assumed, when actual bedrock exists at a shallow depth.

To improve the analysis of deflection data, MODULUS 4.0 incorporates a method to determine the depth to an apparent rigid layer from surface deflections. The approach expands the Ullitz single layer procedure (Ullitz and Stubstad 1985) so that it can be used in a multilayered system. The approach is based on the "line of influence" shown schematically in Figure 1. As the load is applied, it spreads through a portion of the pavement system as represented by the conical zone in the figure. The slope of this stress zone varies from layer to layer and is related to each layer's stiffness. The measured surface deflection is purely a result of the deformation of the material in the stress zone. The measured surface deflection at any offset is therefore a result of the deflection below a certain depth in the pavement. If a stiff layer occurs at some depth, no surface deflection will occur beyond the offset at which the stress zone and the stiff layer intercept. The method to predict the apparent depth to a rigid layer is based on the hypothesis that the position of zero surface deflection should be strongly related to the depth in the pavement at which no deflection occurs (i.e., a stiff layer).

To estimate the depth at which zero deflection occurs, it is necessary to plot measured surface deflection against the inverse of the distance from the center of the applied load ($1/r$). The results of a theoretical study are shown in Figure 2. Deflections for a number of pavement structures calculated using the multilayered, linear elastic

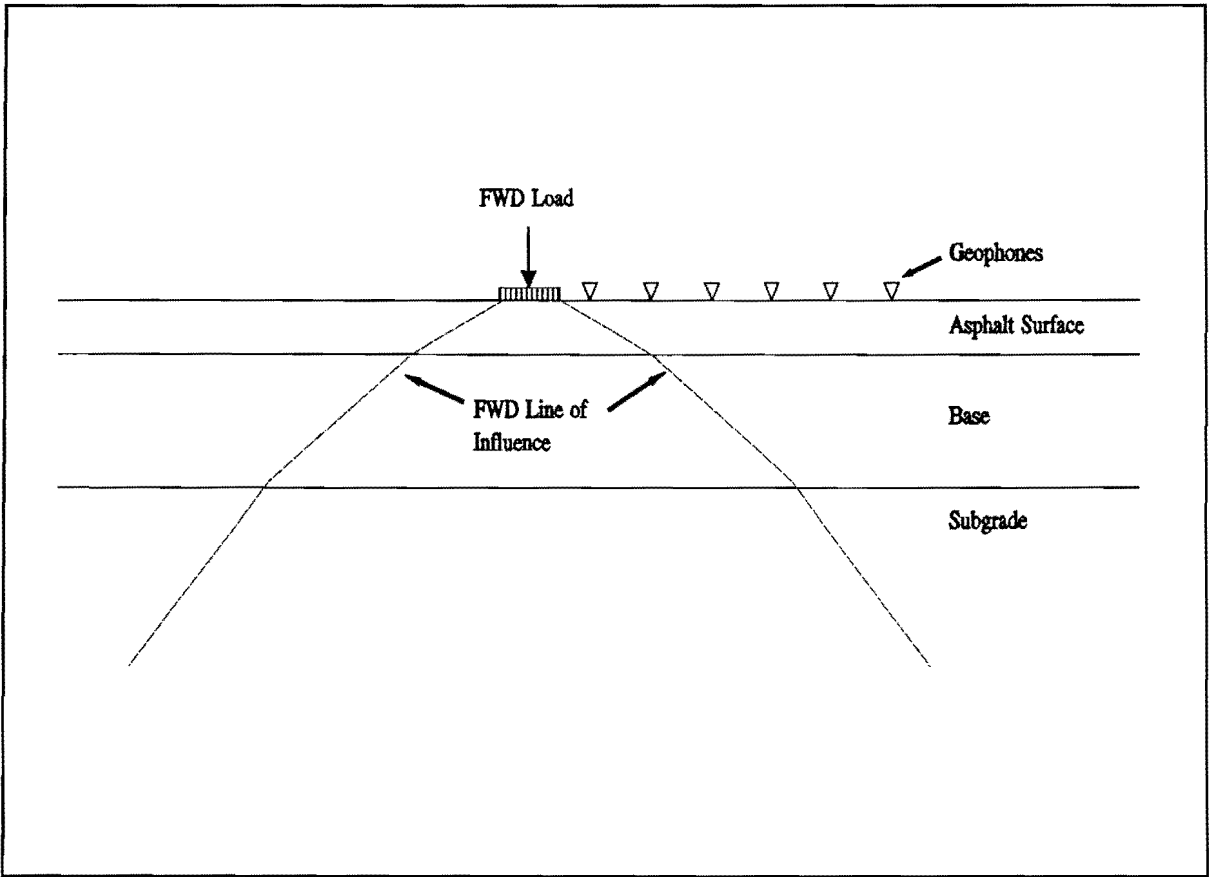


Figure 1. A Schematic of the Stress Distribution Below an FWD Load.

program BISAR have been plotted against the inverse of the offset. The load level, pavement structure, and material properties used are also shown. When the subgrade modulus is changed, the slope of the lines change but the intercept with the $1/r$ axis remains relatively constant. The deeper the rigid layer, the smaller the intercept. This intercept is also influenced by the stiffness, and thickness of the upper layers.

However, in actual pavements the deflection versus $1/r$ plot is only linear over the mid part of the curve, as shown in Figure 3. Non-linearities associated with stiff upper layers and stress-sensitive subgrades tend to curve both the upper and lower portions of the deflection versus $1/r$ plot, as represented by positions A and C in Figure 3. In plots such as these it is necessary to estimate the zero deflection position. This is done by extrapolating the linear portion of the curve at B to the x-axis intercept, position D. In the regression analysis described below the intercept position was calculated by extending the steepest part of the curve.

To develop a relationship between the depth to the rigid layer and the $1/r$ intercept, a regression analysis was completed. Deflection bowls and $1/r$ intercepts were generated for 1008 pavement structures under a 9,000 lb. load equivalent to a FWD load. The structures had the following moduli and thicknesses:

$$\begin{aligned} \frac{E_1}{E_{sg}} &= 10, 30, 100; \\ \frac{E_2}{E_{sg}} &= 0.3, 1.0, 3, 10; \\ \frac{E_{rigid}}{E_{sg}} &= 100; \\ T_1 &= 1, 3, 5, \text{ and } 10 \text{ inches} \\ T_2 &= 6, 10, \text{ and } 15 \text{ inches} \\ B &= 5, 10, 15, 20, 25, 30 \text{ and } 50 \text{ feet} \end{aligned}$$

where

$$\begin{aligned} E_i &= \text{Young's modulus of layer } i; \\ T_i &= \text{Thickness of layer } i; \\ B &= \text{Depth of the rigid layer from the pavement surface in feet.} \end{aligned}$$

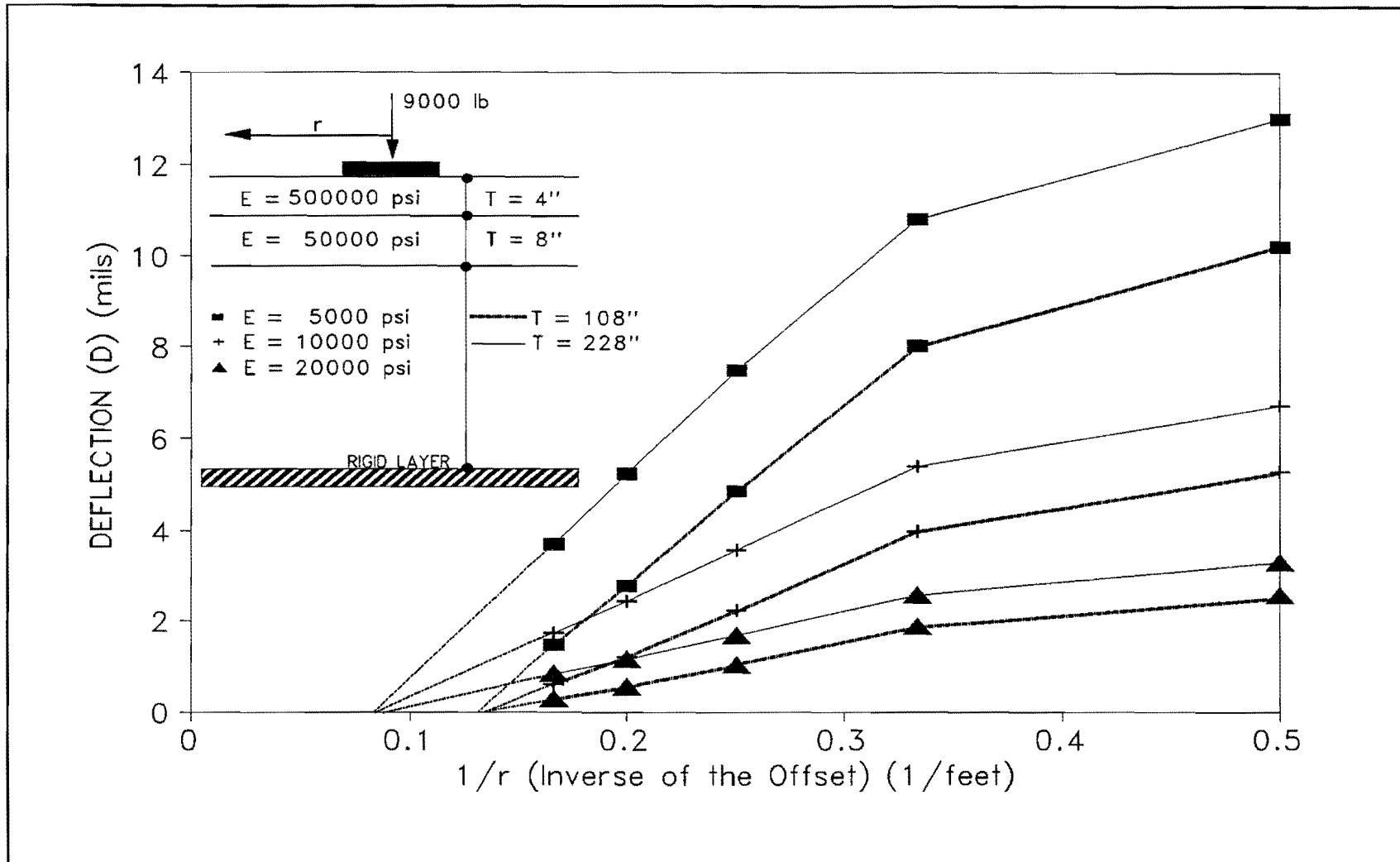


Figure 2. Deflection vs. the Inverse of Offset (1/r) for a Number of Hypothetical Pavement Structures.

In the analysis the relationship between the rigid layer depth and the 1/r intercept was improved by also accounting for the stiffness and thickness of the upper layers. This was done by using the basin shape factors SCI, BCI, and BDI, as defined below. The results were further improved by developing four separate equations based on the asphalt layer thickness.

For pavements with asphalt surface layers less than 2 inches thick ($r^2 = 0.98$):

$$\frac{1}{B} = 0.0362 - 0.3242r_0 + 10.2717r_0^2 - 23.6609r_0^3 - 0.0037BCI \quad (2.1)$$

For pavements with asphalt surfaces between 2 and 4 inches thick ($r^2 = 0.98$):

$$\frac{1}{B} = 0.0065 + 0.1652r_0 + 5.42898r_0^2 - 11.0026r_0^3 - 0.0004BDI \quad (2.2)$$

For pavements with asphalt surfaces between 4 and 6 inches thick ($r^2 = 0.94$):

$$\frac{1}{B} = 0.0413 + 0.9929r_0 - 0.0012SCI + 0.0063BDI - 0.0778\log(BCI) \quad (2.3)$$

For pavements with asphalt surfaces greater than 6 inches thick ($r^2 = 0.97$):

$$\frac{1}{B} = 0.0409 + 0.5669r_0 + 3.0137r_0^2 + 0.0033BDI - 0.0665\log(BCI) \quad (2.4)$$

where:

- r_0 = 1/r intercept by extrapolating the steepest section of the 1/r vs. deflection curve as shown in Fig. 3. (1/ft. units);
- SCI = $D_0 - D_1$ (Surface Curvature Index);
- BDI = $D_1 - D_2$ (Base Damage Index);
- BCI = $D_2 - D_3$ (Base Curvature Index);
- D_i = Surface deflection (inches 10^{-3}) normalized to a 9,000lb. load at an offset i in feet.

These four equations have been implemented within MODULUS 4.0. For each input deflection bowl a depth to rigid layer (B) is calculated.

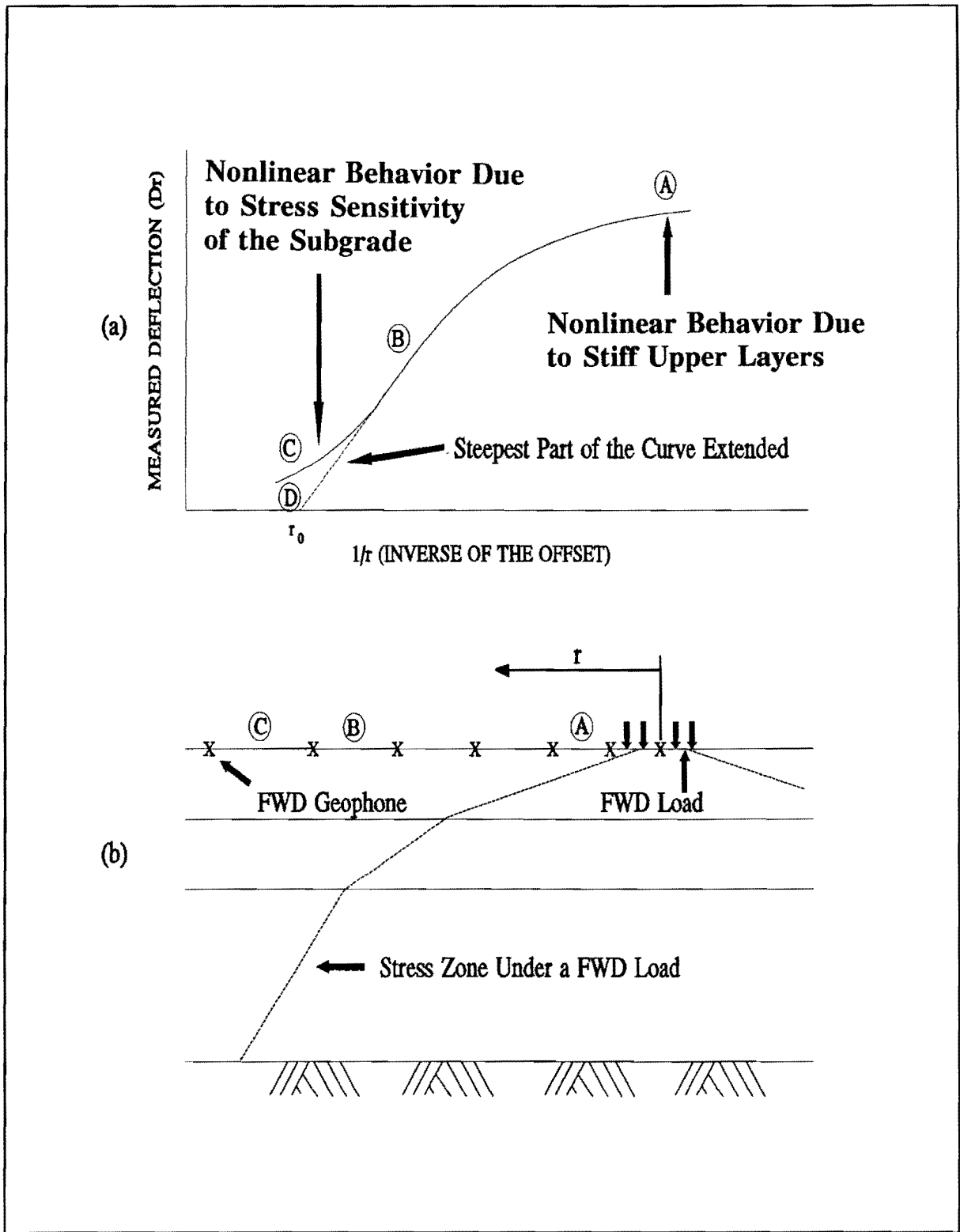


Figure 3. An Illustration of the Method to Determine the Effective Depth to a Rigid Layer.

After determining the apparent rigid layer for each deflection bowl in the FWD file, the average apparent rigid layer depth for the tested section is calculated using the following equation:

$$D = \left[\frac{n}{\sum_{i=1}^n \frac{1}{B_i}} \right] \quad (2.5)$$

where:

- D = Average depth to an apparent rigid layer in ft.;
- B_i = Depth to the apparent rigid layer for the ith deflection bowl.
- n = The number of deflection bowls within one standard deviation of the mean 1/B_i.

The B values for each bowl are output in the summary listing report and also can be plotted using the graphic routine in MODULUS 4.0. The B value is used to calculate the H4 (thickness of subgrade from bottom of base to rigid layer), this was formally a user input typically set at 20 feet. However, it is important to note that the user can overwrite this H4 value if required. The H4, as explained in Research Report 1123-1, is used to generate the deflection data base prior to matching the measured and theoretical deflection bowls. The apparent rigid layer depth calculated might not be a stiff layer underlying the subgrade but can be caused by an apparent increase in subgrade stiffness with depth. The depth of this apparent rigid layer is a function of the nonlinearity of the subgrade. The more rapid the subgrade increase in stiffness with depth, the shallower the determined rigid layer. For uniformly stiff, deep subgrades no rigid layer will be determined. Using these equations the following apparent rigid layer depths are typically calculated.

- Sandy Subgrades: 8 to 12 feet.
- Sandy Clay Subgrades: 12 to 17 feet.
- Clay Subgrades: 17 to 25 feet.

On granular and sandy subgrades the subgrade stiffness increases with depth due to an increase in confining stress and a decrease in the deviatoric stress with depth. The clay subgrades show less of an increase in stiffness with depth and as a result the determined apparent rigid layer depths are deeper than for sandy subgrades. In all cases, the use of the apparent rigid layer in the backcalculation of layer moduli leads to more realistic and accurate subgrade, base, and asphalt moduli. This will be illustrated in Chapter IV when the backcalculated moduli are compared to laboratory results.

In order to evaluate how well these equations predicted actual bedrock depths their predictions were compared to measurements made on 5 sites. Measurements of bedrock were obtained through coring, mini core penetration, and seismic refraction testing, details are given elsewhere (Rohde, 1990). The results of the analysis are given in Table 1. The drillers log is incomplete as drilling typically stopped at 12 feet. Seismic reflection was unsuccessful on site 9, the water table was found at 10.75 feet and the minicone penetrometer failed penetration at a depth of 13 feet. The penetration could have stopped at a single large rock, the stiff layer on site 9 was not confirmed by refraction analysis. It is believed that the clay material continues below the stiff layer.

In general the results in Table 1 show that the predictions of stiff layers obtained using Equations 2.1 through 2.4 are reasonable when compared to measured depths.

2.2 Sensor Weighting Factors

The objective of backcalculation procedures is to minimize the difference between the measured and theoretically calculated deflections. Two approaches are commonly used to evaluate the accuracy of this match; the arithmetic absolute sum of the percent error, and the root mean square of the error (Irwin 1989).

The arithmetic absolute sum of the percent error (AASE) is defined as:

Table 1. Comparing Predicted and Measured Depth to Bedrock.

STATISTICAL DESCRIPTION	SITE 7	SITE 8	SITE 9	SITE 11	SITE 12
<u>Computed</u>					
Average (ft.)	10.75	15.99	17.41	14.49	9.41
Median (ft.)	10.67	15.14	16.61	12.07	8.67
Standard Dev.	1.38	5.70	4.91	13.56	3.20
Lower Quartile	9.74	12.69	14.65	10.48	7.18
Upper Quartile	11.69	17.56	19.28	13.77	10.66
Interquart.	1.95	4.87	4.63	3.29	3.48
Range	360	360	360	360	360
Sample Size					
<u>Measured</u>					
Mini cone	9	20	13.0	17.0	12.0
Drillers Id.	10	-	-	-	12.9
Seismic Refraction	9.5	17	-	14.0	10.0

$$AASE = \sum_{i=1}^n \left| 100 \frac{\delta_{ci} - \delta_{mi}}{\delta_{mi}} \right| \quad (2.6)$$

where:

- δ_{mi} = The Measured Deflection of sensor i ;
- δ_{ci} = The Calculated Deflection of sensor i ;
- n = Number of sensors.

The second approach, the root mean square percent error (RMSE), is independent of the number of sensors used to characterize the deflection basin. This measure of error is defined as:

$$RMSE = \sqrt{\frac{1}{n} \sum_{i=1}^n \left[\frac{\delta_{ci} - \delta_{mi}}{\delta_{mi}} \right]^2} \quad (2.7)$$

In the pattern search technique used in the program MODULUS, the basin matching is reported in terms of the RMSE. During the search for the best matching deflection bowl, the following objective function is minimized:

$$\epsilon = \sqrt{\sum_{i=1}^n \left[\left(\frac{\delta_{mi} - \delta_{ci}}{\delta_{mi}} \right) W_i \right]} \quad (2.8)$$

where:

W_i = Weighting Factor Associated with Sensor i .

Deflection analysis results are normally reported in terms of error per sensor, and most specifications require deflection matching errors of less than 2 percent per sensor. In MODULUS 2.0 the recommended weighting factors, (W_i), during deflection analysis is 1.0 for all sensors. This ensures that the program obtains the deflection bowl resulting in the least possible RMSE. In MODULUS 4.0 the calculated subgrade modulus is a function of the whole deflection bowl, and the use of equal weighing factors for all sensors in the search routine, may not lead to the best results. For example, consider the set of backcalculation results shown in Table 2. If the weighting factors used for this deflection bowl were all equal, each sensor would have a $(1/\delta_{mi})^2$ influence during the search on the absolute difference between the measured and calculated deflection bowls. For example a 0.1 mils difference on the outer sensor between the measured and calculated deflection would have the same effect on the search routine as 1.06 mils difference on the sensor below the loading plate. In terms of absolute difference between the measured and calculated deflections, 31 percent of the search effort is placed on the outer sensor and only 2.9 percent on the inner sensor.

For several reasons it is believed that the closer the sensor to the load, the more its contribution should be in the MODULUS search routine. In general, the closer the sensor to the loadplate, the more information it contains about the upper pavement layers. Unlike many backcalculation techniques where the subgrade is purely a function of the deflections measured at the outer sensors, MODULUS uses all sensors to predict the

Table 2. Typical Deflection Matching Results.

Measured Deflections (δ_{mi})	30.60	21.19	12.25	7.48	5.16	3.61	2.89
Predicted Deflections (δ_{ci})	30.04	21.61	12.45	7.33	4.85	3.64	2.99
RMSE (Error/Sensor) (percent)	1.83	-1.98	-1.63	2.01	6.01	-0.83	-3.46
Absolute Difference ($\delta_{mi} - \delta_{ci}$)	0.56	-0.42	-0.20	0.15	0.31	-0.03	-0.10

subgrade modulus. Due to the stress sensitive behavior of soils, the apparent subgrade stiffness is smaller below the load and increases in stiffness towards the outer sensors. By placing such a large emphasis on matching the outer sensor deflections, the subgrade modulus is generally overpredicted. The measuring accuracy of the geophones involves both a percentage and an absolute possible error. This implies that the smaller the deflection, the bigger the possible error in measurement. An additional reason for reducing the importance of the outer sensors during the deflection analysis is the possibility of dynamic effects at the outer sensors. These dynamic effects are caused by refraction of waves and can lead to attenuation of the measure's deflections (Roesset, 1990). This effect is more likely at the outer sensors. Especially in the presence of rigid layers, this could lead to erroneous deflection measurements.

By setting the weighting factor at each sensor equal to the square of the measured deflection, the minimum absolute difference between measured and calculated deflection bowls can be obtained. This results in a situation where the deflection analysis is dominated by the magnitude of the inner sensors. The deflections at the outer sensors have very little influence on the backcalculation process. To prevent domination by either the inner or outer sensors in the deflection analysis, weighting factors proportionate to the magnitude of the measured deflection should be used. The weighting factors at each sensor are:

$$W_i = \frac{\delta_i}{\delta_1} \quad (2.9)$$

where:

- W_i = The Weighting Factor for Sensor i ;
- δ_i = The Measured Deflection of Sensor i ;
- δ_1 = The Measured Deflection beneath the loadplate.

This has been incorporated in the new MODULUS 4.0, and as shown in Chapter IV, it leads to favorable results.

2.3 Sensor Selection Criteria

A further improvement involves a procedure to select the number of sensors to be used in the deflection analysis. This involves using the sensors close to the load up to and including the first sensor that measures purely deflections in the subgrade. Boussinesq's equation for deflection under a point load is used to determine the surface location at which the measured deflection is purely originating in the subgrade. At each sensor the apparent Young's modulus E_r of the infinite halfspace is calculated:

$$E_r = \frac{P (1 - \mu^2)}{\pi r D_r} \quad (2.10)$$

where:

- D_r = Surface deflection at offset r due to load P ;
- P = Point load;
- μ = Poisson's ratio;
- r = Horizontal offset from the load.

By plotting the E_r at the various sensors, it is possible to determine the approximate offset at which the measured deflection is purely originating in the subgrade. The technique is illustrated in Figure 4. At the inner sensors, near position A, the calculated E_r is high due to the influence of the upper layers. With an increase in offset (point B in Figure 4), the apparent halfspace modulus reduces. The minimum apparent modulus

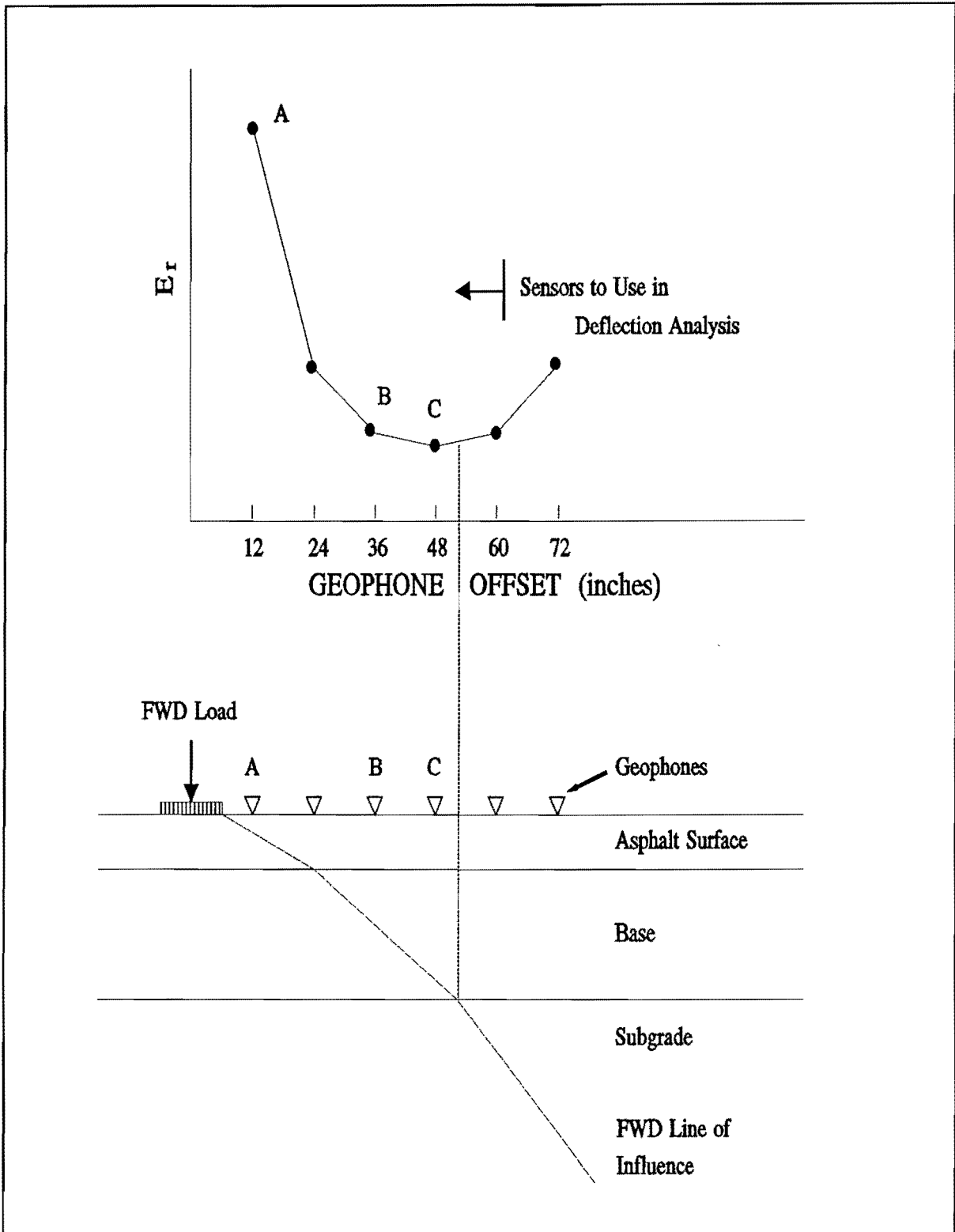


Figure 4. A Schematic Illustrating the Procedure to Select the Number of Sensors to Use During Deflection Analysis.

occurs at position C. It is postulated that position C can be associated with the weakest modulus normally found near the top of the unmodified subgrade. Because most subgrades increase in stiffness with depth and distance from the load, the predicted E_r increases beyond this offset. The curve in Figure 4a is not continuous, and the actual minimum E_r might occur beyond position C. It is therefore suggested that the sensors up to and one beyond position C be used in deflection analysis. The other sensors do not measure the subgrade at its weakest position, and as a result the subgrade modulus is overpredicted. By using only the selected sensors, and an apparent rigid layer to account for the increasing stiffness in the subgrade, the backcalculated subgrade modulus is more representative of the weakest part of the subgrade. As a result, deflection analysis is improved.

This sensor selection procedure has been included into the MODULUS 4.0 system. On thin pavements it may remove the outer sensors from the bowl fitting process, on thick stiff pavements often 6 or all 7 sensors are used. Removing a sensor is achieved by setting its weighting factor equal to zero. The calculated weighting factors used are listed on the detailed section listing. One overriding factor is that the system uses as a minimum, a number of sensors equal to the number of unknown layer moduli plus one.

2.4 Inclusion of the WES5 Layered Elastic Program

The backcalculation scheme within MODULUS is a two step process. First, a linear elastic layer program is run several times and a deflection database is built covering a range of layer moduli. The second stage is a pattern search routine to match measured and theoretical deflection bowls. In selecting a linear elastic program a review was made of the available programs. In a general purpose backcalculation scheme the linear elastic program must give realistic predictions for a range of layer thickness, subgrade thickness and moduli values. Some programs were found to have problems in the case of a rigid layer being placed close to the surface. In this review process it was judged that the BISAR program was the most reliable and it was included in the original MODULUS system (Uzan, 1988).

However, the major problem with BISAR is that the program is copyrighted and its distribution is restricted. This meant that the distribution of MODULUS would be limited. This problem was largely overcome with the release by the U.S. Corp of Engineers of the WESLEA program (Van Cauwelaert, 1989). The current version of the program is called WES5 which handles up to five layers with varying interface conditions and a maximum of 20 loads. The fifth layer is semi-infinite and can be made rigid. The program was evaluated by TTI and found to give identical predictions of deflection for a typical range of pavements and loading conditions found in Texas. A major advantage of the WES5 program is that it runs three to five times faster than BISAR so it greatly improves the efficiency of MODULUS.

CHAPTER III

FIELD VALIDATION PROCEDURES OF MODULUS 4.0

This chapter describes the facilities used to evaluate and validate the MODULUS 4.0 backcalculation program. The validation was done by comparing backcalculation results from MODULUS 4.0 to those obtained in the laboratory. This was done using NDT deflection data collected over a period of one year on ten¹ inservice pavement sections (shown in Figure 5). The program was also validated on two instrumented pavement sections. Measured indepth deflections were compared to those predicted using the backcalculation results. The layout and location of the test sections, the materials, and the various tests conducted are described in this section.

3.1 THE EXPERIMENTAL SECTIONS

3.1.1 Description of the Sections

Ten test pavement sections were used in this study. Five pavement structures were selected in District 8, near Abilene Texas. In this area, stiff layers are often encountered at shallow depths. Another five pavement structures were selected from District 21, near Brownsville Texas. The subgrades in this region are thick, and shallow rigid layers are a less frequent occurrence. Table 3 summarizes the location and pavement structure of the selected test sites.

At each test section, ten positions, ten feet apart, were marked in the outside wheelpath. These ten positions, as shown in Figure 6, were used for the position of the monthly deflection testing. Cores of the asphalt layer at each site were taken from position 05. A testpit was also dug in the middle of each section to obtain base and subgrade samples for laboratory testing. To classify the subgrade, a hole was drilled to a depth of 12 feet, or to the depth at which the water table was reached. On the sections where penetration tests were done, the subgrade was penetrated at positions 00, 05, and 09.

¹ These ten sites are a subset of the 17 sites monitored in this study. They were chosen for detailed analysis as they exhibit all of the characteristics of interest (depth to stiff layer and layer thicknesses).

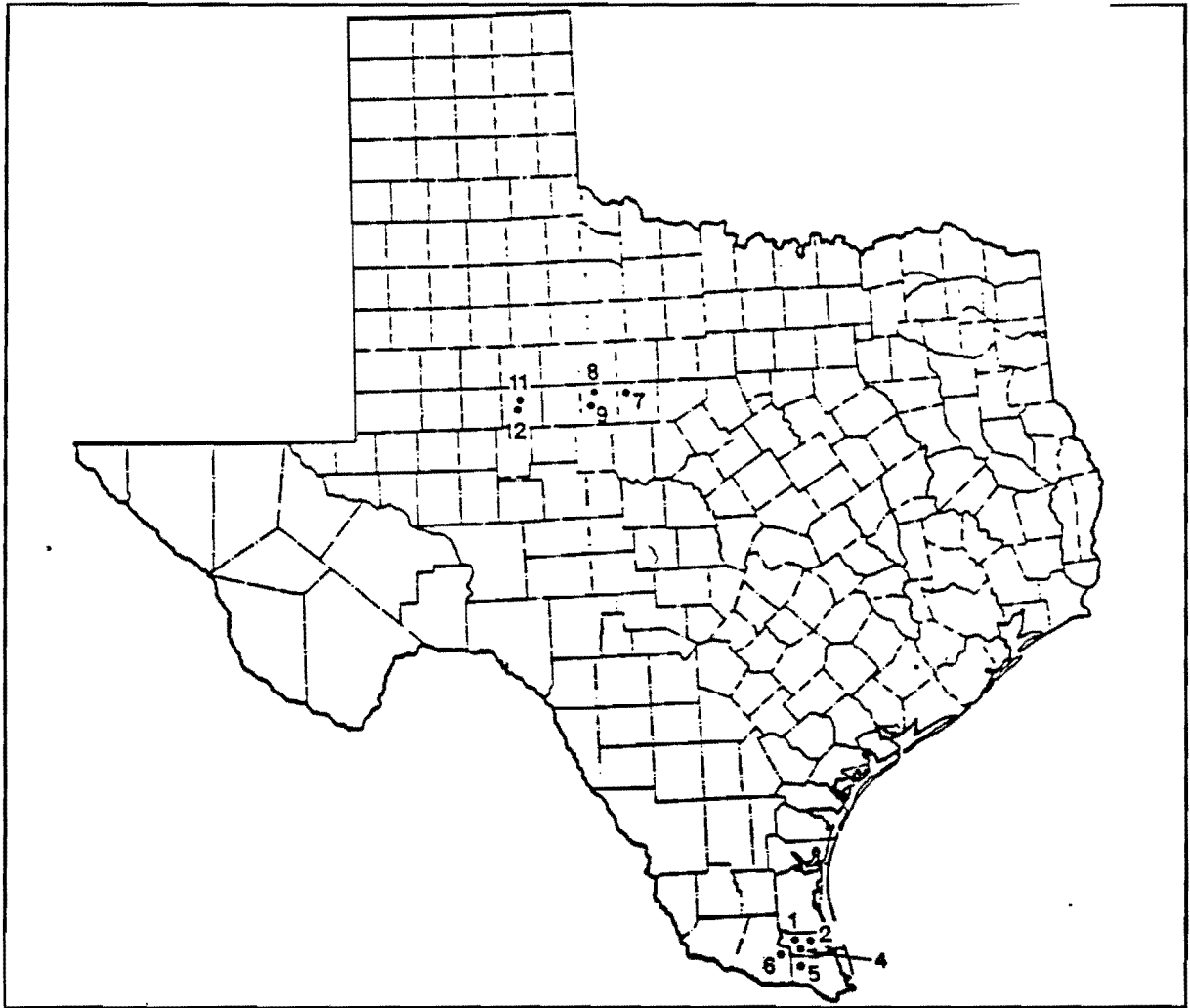


Figure 5. Location of the Test Pavement Sections.

3.1.2 Field Testing

FWD deflection testing was conducted at all test sections over a period of one year. Monthly, a series of deflection tests were conducted in the morning and the afternoon at every site. During these tests, the following FWD configuration was used: an 11.8 inches diameter loadplate, the 440 pounds weight set, and deflection sensors placed at radial distances of 0, 12, 24, 36, 48, 60, and 72 inches. The general testing procedure at each test site was as follows:

Table 3. The Location and Pavement Structure of the 10 Test Sites.

Site	District	County	Route	Pavement Structure and Subgrade*
1	21	Willacy	US 77 MP 4.1	2.25" Asphalt Concrete 4.25" Asphalt Treated 6.0" Base Flex Base Sand Subgrade
2	21	Willacy	SH 186 MP 33.2	1.0" Surface Layer 8.8" Calacie Flex Base Sand Subgrade
4	21	Willacy	FM 1425 MP 5	4.0" Asphalt Concrete 5.0" Lime Treated Calacie Clay Subgrade
5	21	Hidalgo	FM 1425 MP 3	3.0" Asphalt Concrete 3.0" Asphalt Concrete 6.0" Calacie Flex Base Dark Sandy Clay
6	21	Hidalgo	FM 491 MP 6.1	1.2" Surface Layer 7.8" Calacie Flex Base Clay Subgrade
7	8	Callahan	IH 20 MP 293	10.0" Asphalt Concrete 11.0" Limestone Base Clay Subgrade
8	8	Taylor	IH 20 MP 273.6	8.0" Asphalt Concrete 13.0" Limestone Base Clay Subgrade
9	8	Taylor	FM 1235 MP 21	1.0" Seal Coat 8.0" Limestone Base Clay Subgrade
11	8	Mitchell	IH 20 MP 216	5.0" Asphalt Concrete 18.0" Limestone Base Sand Subgrade
12	8	Mitchell	FM 1983 MP 1.0	1.0" Asphalt Concrete 8.0" Limestone Base Sand Subgrade

* Additional Subgrade Information is given in Appendix A.

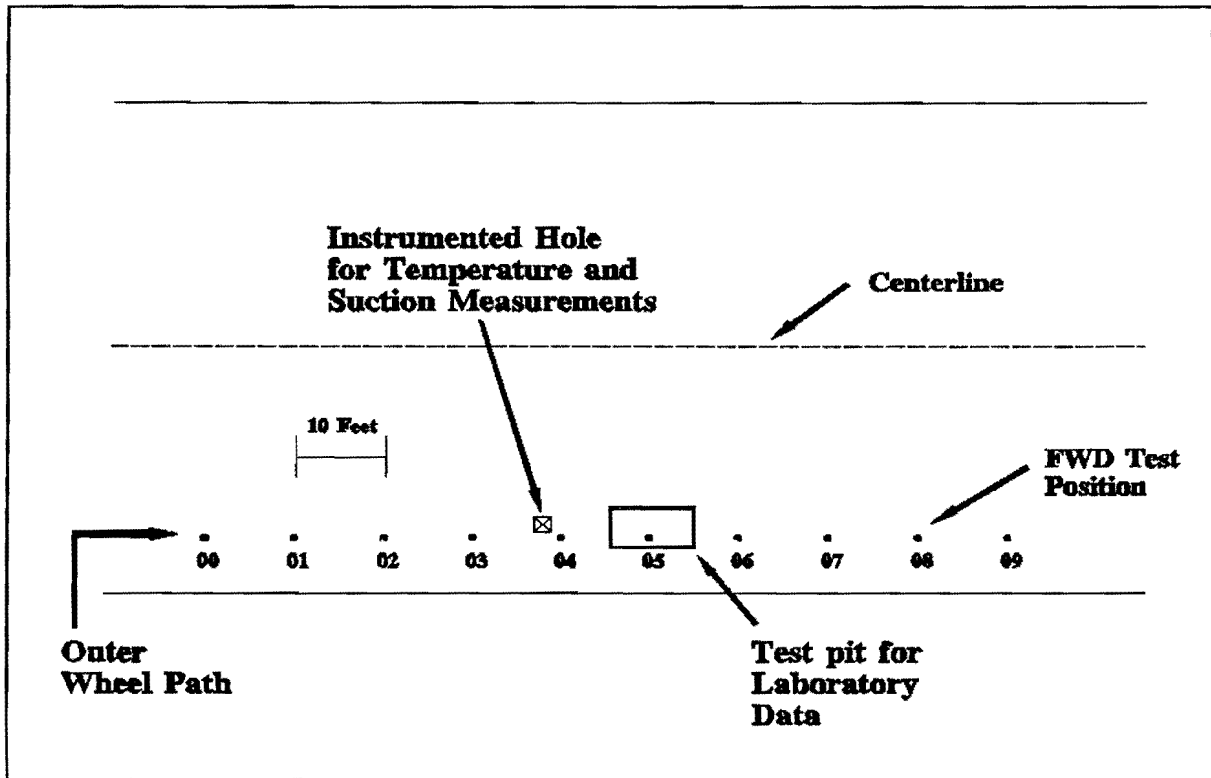


Figure 6. The Layout of a Typical Test Section.

- The FWD operating software was set up to record the load and deflections with the proper gains.
- Starting at position 0, the following drop height sequence was used:
 - 1 seating drop to ensure proper contact,
 - 1 drop with an applied load of 6000 lb. \pm 10%
 - 1 drop with an applied load of 9000 lb. \pm 10%
 - 1 drop with an applied load of 12000 lb. \pm 10%
 - 1 drop with an applied load of 16000 lb. \pm 10%
- The drop sequence was repeated at all positions, positions 4 and 5 were excluded as being too close to the test pit.
- The pavement temperature was recorded from thermocouples placed in the asphalt and the base.
- The air temperature and pavement surface temperature were recorded.
- The data was saved on a floppy diskette for later analysis.

This deflection data was returned to TTI where it has been stored in a database for subsequent analysis. Several access programs were written to sort, average, and normalize the deflection bowls.

3.1.3 Laboratory Testing

Selected samples obtained from the asphalt concrete, the base course, and the subgrade were subjected to standard ASTM and AASHTO test procedures. This testing was required to determine the basic constitutive relationship between stress and deformation of the test site materials. For asphaltic concrete the indirect tension test was chosen, while a repeated load triaxial test was selected for characterization of the base course and subgrade.

To model the behavior of base courses and subgrades, under a cyclic load such as expected under traffic, a repeated load triaxial device was used. In this test a cyclic load can be applied to a test sample while the confining pressure is controlled. The test has two major limitations. The deviatoric stress can only be applied along the principal axis of the specimen, and two of the three principal stresses are equal. The triaxial device can therefore only reproduce a stress state directly under a wheel load or the FWD base plate. As reported by McVay et al. (1985), even at this position a moving wheel load might induce a rotation of the principal axis. Furthermore, the confining stresses expected under a vehicle or FWD load changes in a cyclic nature, while the standard test only applies a constant confining stress. Allen and Thompson (1984) found that the improvements in testing the sample using cyclic confining stresses were not significant enough to be required. To characterize the test site materials, the following procedures were followed.

Asphalt Concrete

On each test site, four inch diameter cores were taken through the asphalt concrete at approximately position 05. On the thicker pavement structures, these cores were retrieved, and sawed to produce two samples (i.e., top and bottom section) for testing. Cores from the thinner asphalt sections were left intact. From these samples, an indirect

tensile test was run at two frequencies, 10 and 20 Hz, and at four different temperatures, 0, 32, 77, and 100 degrees Fahrenheit. These temperatures were selected to provide a representative range of pavement temperatures.

Because an impulse load like the FWD excites a wide range of frequencies, it is not possible to identify a single frequency to simulate during the laboratory testing. By assuming that the FWD load is a harmonic wave, the frequency can be approximated as between 17 and 20 Hz. The results of these indirect tensile tests are listed in Tables B1 through B10 in Appendix B.

Granular Base

Samples from the granular base material were also obtained from all test sections. This material, obtained from a test pit at approximately position 05, was bagged and brought to the laboratory. Before disturbing the material in the test pit, the moisture content and density were obtained using a nuclear density device (AASHTO T238-79). In the laboratory, six inch diameter specimens, twelve inches long, were remolded at approximately the measured field moisture content, and field density. These cylindrical specimens were tested in a repeated load triaxial test according to AASHTO T 274-82. All measurements were made in the 200th cycle. The test sequence used and the confining and deviatoric stresses applied were as specified in the AASHTO test procedure for granular soils. The calculated resilient modulus, and pressures at which the deformations were measured are listed, per test site, in Tables B1 through B10 of Appendix B.

The measured resilient moduli and stress states for each sample were used to develop equations in which the resilient modulus is a function of both the mean principal stress and the octahedral shear. For this purpose a model proposed by Witczak and Uzan (1988) was used:

$$M_R = (k_1 p_a) \left[\frac{\theta}{p_a} \right]^{k_2} \left[\frac{\sigma_d}{p_a} \right]^{k_3} \quad (3.1)$$

where:

- E_R = Resilient modulus of the material;
- k_i = Constants;
- p_a = Atmospheric pressure used in the equation to make the coefficients independent of the units used;
- θ = The bulk stress or first stress invariant ($\sigma_1 + \sigma_2 + \sigma_3$);
- σ_d = The deviatoric stress ($\sigma_1 - \sigma_3$);
- σ_i = Principal stresses.

The laboratory data was analyzed and the results of a least squares curve fitting analysis are shown in Table 4. The coefficient of determination, r^2 , for each set of data is also shown.

Table 4. Base Course Coefficients for Equation 3.1.

SITE	MATERIAL	k_1	k_2	k_3	r^2
1	Caliche	779	0.89	-0.47	0.93
2	Caliche	495	0.83	-0.36	0.75
4	Lime-Treated Caliche	433	0.62	-0.52	0.95
5	Caliche	128	1.49	-1.53	0.96
6	Caliche	645	0.63	-0.22	0.86
9	Limestone	1282	0.32	-0.06	0.91
11	Limestone	307	0.78	-1.39	0.52
12	Limestone	699	0.60	-0.08	0.84

Subgrade

Samples of the subgrade material were obtained from thin-walled sampling tubes, pushed into the subgrade at the position of the test pit. These samples, extruded from the tubes, were wrapped and brought to the laboratory for testing purposes. In the laboratory, the fine-grained samples, as retrieved from the thin-walled sampling tube were trimmed to a diameter of 2.81 inches and used for the resilient modulus testing. The material retrieved from sites with sandy subgrades, were remolded to

the field measured moisture content and density obtained using a nuclear density testing device. The specimens, 2.81 inches in diameter, were subjected to a standard resilient modulus test as described in AASHTO T 274-82. All measurements were made in the 200th cycle. The calculated resilient modulus for every stress state is listed, per test site, in Tables B1 through B10 of Appendix B.

In the analysis of the laboratory data two models were used. In the first model the measured resilient modulus was described as a function of both the mean principal stress and the octahedral shear (Equation 3.1). The results of the curve fitting analysis are shown in Table 5.

Table 5. Subgrade Coefficients for Equation 3.1.

SITE	MATERIAL	k ₁	k ₂	k ₃	r ²
1	Sand	340	0.43	-0.84	0.92
2	Sand	148	0.25	-0.48	0.76
4	Clay	82	0.10	-0.86	0.97
5	Sandy Clay	109	0.17	-0.67	0.92
6	Clay	46	0.25	-1.38	0.95
7	Clay	255	0.11	-0.32	0.93
8	Clay	127	0.16	-0.81	0.87
9	Clay	119	0.09	-0.95	0.87
12	Sand	207	0.51	-0.75	0.97

The clay subgrades were also analyzed using the bilinear model (Thompson and Robnett 1976). As shown in Figure 7 the resilient modulus rapidly decrease with an increase in deviatoric stress until a certain value. Then the soil stiffness gradually increases, stays constant, or shows a slight decrease in stiffness as the deviatoric stress is further increased. The shape of the curve can be described by the following bilinear equation:

$$M_R = K_2 + K_3[K_1 - \sigma_d] \text{ for } K_1 > \sigma_d \quad (3.2a)$$

$$M_R = K_2 + K_4[\sigma_d - K_1] \text{ for } K_1 < \sigma_d \quad (3.2b)$$

where:

M_R = Resilient modulus of the fine-grained soil;

σ_d = The deviatoric stress ($\sigma_1 - \sigma_3$).

The coefficients resulting from a least squares analysis on the clay subgrades are shown in Table 6.

3.2 MULTIDEPH DEFLECTION TESTING

The verification of improvements to backcalculation procedures is often obtained by comparing results from theoretical analysis to those obtained in laboratory testing. Accurate duplication of field conditions in the laboratory is difficult, if not impossible. Scullion et al. (1989) illustrated an alternative, and highly effective method to verify backcalculation procedures. In this study pavement sections instrumented with a multidepth deflection device are used to validate improvements to the linear elastic backcalculation of layer moduli.

Table 6. Subgrade Coefficients for the Bilinear Model (Equation 3.2) on sections with Clay Subgrades.

SITE	MATERIAL	k_1	k_2	k_3	k_4	r^2
4	Clay	5.1	4019	2605	-102	0.98
6	Clay	4.6	6426	7144	-519	0.95
7	Clay	6.3	4864	331	-224	0.80
8	Clay	6.1	5406	2582	124	0.90
9	Clay	5.1	5832	5830	170	0.98

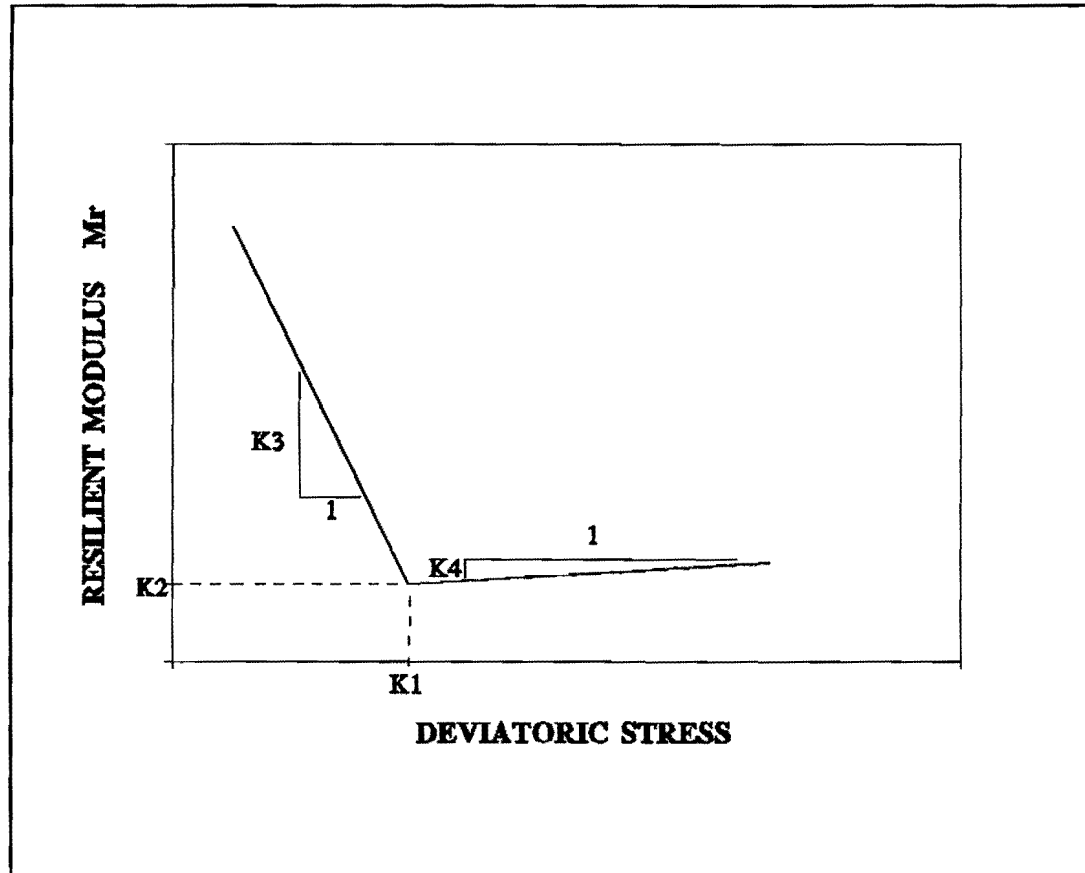


Figure 7. The Arithmetic Model (Bilinear Model) Describing the Nonlinear Resilient Modulus of a Fine-Grained Soil.

The Multidepth Deflectometer² (MDD) consists of series of linear variable differential transformers (LVDTs) clamped into the pavement structure at various depths. Details about the installation, calibration, and use of the MDD have been documented by Scullion et al. (1988). The system is anchored at a depth of 6 to 8 feet as shown in Figure 8. During testing the LVDTs monitor the relative deflection between the anchor and the pavement layers. The LVDT output, in voltage, is recorded for a duration of 60 milliseconds. This data is recorded at a sampling rate of up to 10,000 data points per second. This data is recorded in digital form in a microcomputer.

² The MDD was developed at the National Institute for Transportation and Road Research in South Africa (Basson et al. 1981).

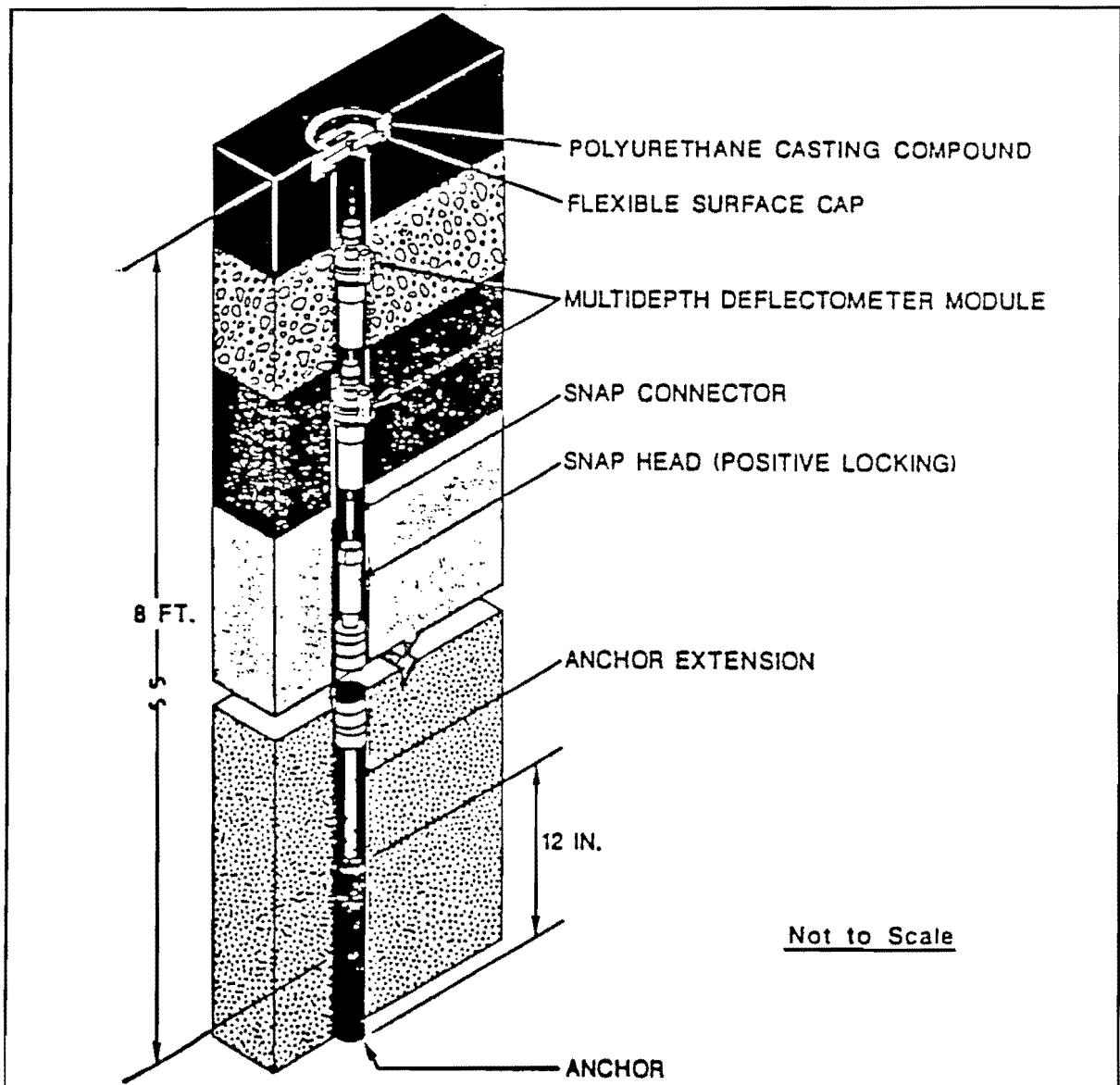


Figure 8. A Schematic of the Multidepth Deflectometer.

Under FWD testing the recorded signal usually contains high frequency noise. This signal is cleaned by performing a Fast Fourier Transform on the signal. The frequency of the noise is determined, removed from the signal, and an inverse Fourier Transform is completed to return the signal to the time domain. A typical response before and after the filtering is shown in Figure 9.

By placing an FWD geophone on the anchor rod, as shown in Figure 10,

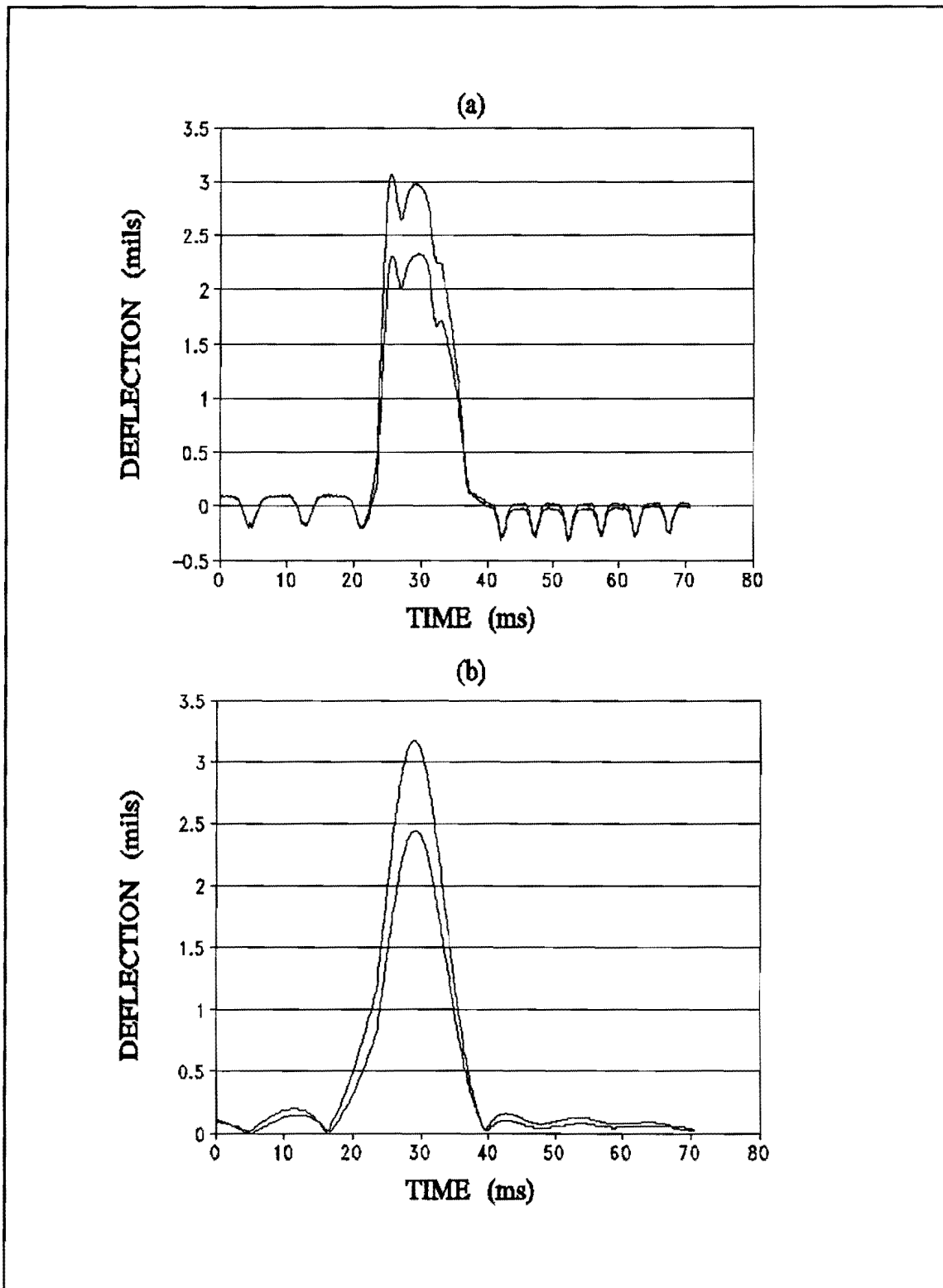


Figure 9. A Typical MDD Signal Under an FWD Load Before and After Noise Filtering.

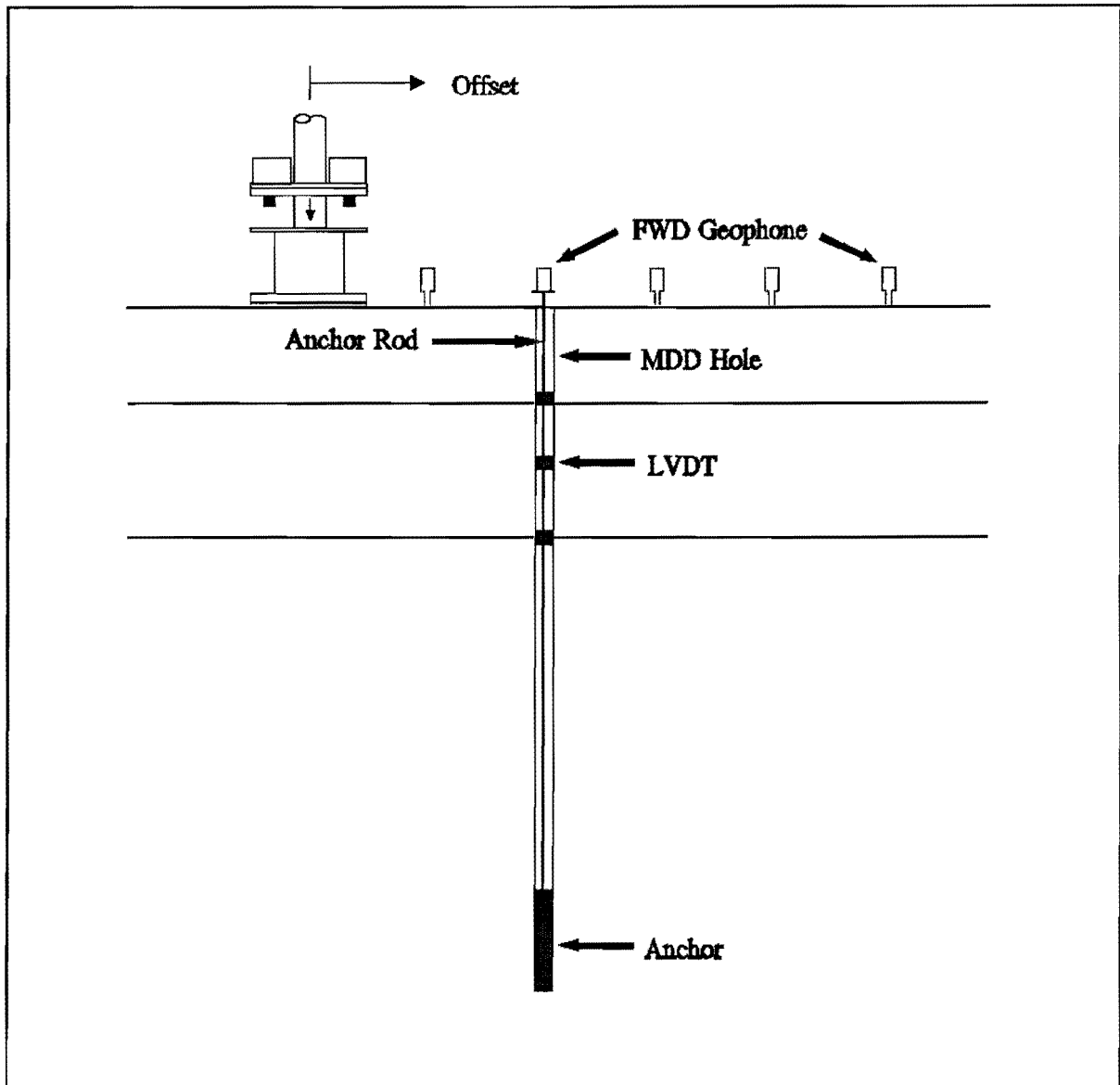


Figure 10. A Schematic Illustrating How One of the FWD Geophones can be Used to Measure the Anchor Deflection of the MDD System.

it is possible to measure the deflections at the surface and in the pavement structure under a FWD load. The absolute deflection at any depth is obtained by adding the measured deflection of the anchor to the relative deflection between the LVDT and the anchor rod. By conducting the FWD test at various offsets away from the MDD hole, it is possible to obtain a range of in-depth pavement deflections.

For the purpose of evaluating improvements to the backcalculation technique, multidepth deflection tests were conducted on two instrumented pavement sections. The first, section A, consisted of a five inch asphalt surface layer on a 24 inch crushed limestone base. This section, test section 12 of the TTI Pavement Testing facility, was selected because it is known that the subgrade is thick with no stiff layers occurring at a shallow depth. This section is equipped with five LVDT's placed at the layer interfaces and at various depths into the subgrade. The results of the FWD and MDD deflection testing on this section are listed in Table 7.

The second section, section B, consists of a 3.5 inch asphalt surface on a 12 inch granular base. This section was selected because the small anchor movements suggested the existence of a shallow rigid layer. Three LVDT's had been installed at the layer interfaces and 7 inches into the subgrade. The results of the FWD and MDD deflection testing for this section is listed in Table 8.

The method of evaluating how well the modulus backcalculation scheme is performing will be described in the next section of this report. It involves using the measured surface deflections to compute the pavement layer moduli, then using these moduli to predict deflections at the MDD positions. A comparison is then made of measured and computed depth deflections.

Table 7. The Measured Surface and In-Depth Deflections Under a FWDD Load for Section A.

Measured MDD and FWD Deflections												
Load	Offset*	FWD Deflections							MDD Deflections			
		0"***	12"	24"	36"	48"	60"	72"	5.1"\$	17.1"	28.9"	36"
9000	8.2	7.52	5.11	3.02	2.08	1.54	1.46	1.07	5.92	4.46	3.59	3.03
9000	8.2	7.74	5.13	3.11	2.06	1.62	1.51	1.02	6.08	4.58	3.68	3.11
9000	8.2	7.82	5.21	3.05	2.07	1.59	1.51	0.99	5.98	4.52	3.67	3.11
9000	8.2	7.79	5.19	3.07	2.01	1.60	1.45	0.99	5.99	4.51	3.62	3.05
	Avg.	7.72	5.16	3.06	2.05	1.59	1.48	1.02	5.99	4.52	3.64	3.07
9000	15.4	7.88	5.26	3.05	2.04	1.47	1.40	1.07	4.53	3.81	3.23	2.80
9000	15.4	8.12	5.33	3.05	2.04	1.46	1.43	1.05	4.54	3.83	3.29	2.85
9000	15.4	8.25	5.39	3.13	2.13	1.55	1.48	1.18	4.57	3.85	3.33	2.89
9000	15.4	8.19	5.44	3.15	2.23	1.67	1.55	1.21	4.71	3.98	3.42	2.96
	Avg.	8.11	5.35	3.10	2.11	1.53	1.46	1.12	4.59	3.87	3.32	2.88
9000	20.0	8.17	5.37	3.07	2.09	1.52	1.37	1.03	3.67	3.27	2.95	2.60
9000	20.0	8.06	5.42	3.09	2.08	1.63	1.35	1.09	3.73	3.30	2.96	2.60
9000	20.0	8.20	5.46	3.11	2.06	1.64	1.36	1.14	3.72	3.29	2.98	2.62
9000	20.0	8.27	5.59	3.24	2.27	1.73	1.49	1.22	3.84	3.40	3.11	2.75
	Avg.	8.17	5.46	3.13	2.12	1.63	1.39	1.12	3.74	3.31	3.00	2.65

* Horizontal distance from the MDD hole to the center of the FWD loadplate.
 ** Horizontal distance from the FWD geophone to the loadplate.
 \$ MDD depth.

Table 7. Continued.

Measured MDD and FWD Deflections												
Load	Offset*	FWD Deflections							MDD Deflections			
		0"***	12"	24"	36"	48"	60"	72"	5.1"\$	17.1"	28.9"	36"
9000	29.5	8.72	5.40	3.00	2.08	1.38	1.27	1.09	2.42	2.35	2.36	2.17
9000	29.5	8.92	5.59	3.16	2.14	1.56	1.37	1.18	2.48	2.43	2.47	2.27
9000	29.5	8.81	5.49	3.03	2.06	1.47	1.24	1.06	2.39	2.34	2.35	2.16
9000	29.5	8.80	5.49	3.07	2.05	1.47	1.28	1.06	2.44	2.37	2.38	2.19
	Avg.	8.82	5.49	3.07	2.08	1.47	1.29	1.10	2.43	2.37	2.39	2.19
9000	42.0	8.79	5.49	3.07	2.08	1.51	1.17	1.11	1.65	1.69	1.84	1.75
9000	42.0	8.81	5.47	3.05	2.06	1.48	1.22	1.12	1.74	1.80	1.90	1.81
9000	42.0	8.96	5.57	3.07	2.03	1.50	1.14	1.13	1.67	1.72	1.83	1.74
9000	42.0	9.00	5.65	3.19	2.20	1.67	1.27	1.29	1.82	1.88	1.96	1.87
	Avg.	8.89	5.54	3.10	2.09	1.54	1.20	1.16	1.72	1.77	1.88	1.79
* Horizontal distance from the MDD hole to the center of the FWD loadplate. ** Horizontal distance from the FWD geophone to the loadplate. \$ MDD depth.												

Table 8. The Measured Surface and In-Depth Deflections Under a FWD Load for Section B.

Measured MDD and FWD Deflections											
Load	Offset*	FWD Deflections							MDD Deflections		
		0"**)	12"	24"	36"	48"	60"	72"	3.8"\$	15.8"	28.5"
9000	3	44.4	26.2	10.9	4.6	2.6	1.5	1.0	42.8	35.7	15
9000	3	43.7	25.9	11.0	4.6	2.5	1.6	1.0	42.4	35.3	17.1
9000	3	43.7	25.9	11.0	4.6	2.5	1.5	1.0	42.7	35.6	14.8
	Avg.								42.66	35.53	15.65
9000	20	44.4	26.3	11.2	4.8	2.5		1.0	15.4	15.8	8.4
9000	20	44.3	26.4	11.2	4.9	2.5		1.1	15.4	15.7	9.3
9000	20	44.4	26.4	11.3	4.8	2.5		1.2	15.4	15.8	9.2
	Avg.								15.42	15.76	8.96
9000	32	44.2	26.0	11.1	4.8	2.6		1.1	6.8	6.8	5.1
9000	32	44.1	26.2	11.4	4.9	2.6		1.1	6.8	6.9	5.2
9000	32	44.1	26.0	11.4	5.1	2.7		1.1	6.8	6.9	5.2
	Avg.								6.81	6.91	5.16
* Horizontal distance from the MDD hole to the center of the FWD loadplate. **) Horizontal distance from the FWD geophone to the loadplate. \$ MDD depth.											

CHAPTER IV DATA ANALYSIS

As discussed in the preceding chapters, the improvements incorporated into the new MODULUS 4.0 were evaluated on a number of test pavement sections throughout the state of Texas. The new backcalculation model using an apparent rigid layer to account for changes in subgrade stiffness with depth in the backcalculation process was used in parallel with existing backcalculation procedures which assumed either a rigid layer at 20 feet or a semi-infinite subgrade. The results are compared and evaluated in terms of the available laboratory data. The technique was also evaluated on two instrumented pavement sections. Deflections were measured in the asphalt, base, and subgrade under a FWD load. These were compared to deflections predicted using layered elastic theory and moduli from the improved backcalculation procedure.

4.1 ANALYSIS OF SURFACE DEFLECTION DATA

To evaluate the use of an apparent rigid layer to model a pavement in which the subgrade stiffness changes with depth, the deflection data collected on ten in-service pavement structures were analyzed. The tests were conducted monthly over the duration of one year as described in Chapter III. In analyzing the deflection data, three backcalculation models were used. The results are compared to that obtained through laboratory testing.

Comparison of Three Backcalculation Models

The analysis of the deflection data was completed using the layered elastic backcalculation program MODULUS. The data were analyzed using three backcalculation models. In the first model, the subgrade was assumed infinitely thick (Model 1). All seven deflection readings were used in the analysis. In the second model a rigid layer was placed at a depth of 20 feet (Model 2), and again all seven deflections were used to determine the layer moduli. In the third model (Model 3) a rigid layer was placed at the depth predicted using the equations 2.1 through 2.4. The geophones used in the deflection analysis were selected and assigned weighing factors as

described in Section 2.3.

For the pavement structures with a thin asphalt surface of less than two inches, the modulus of the surface layer was not backcalculated but assigned a fixed modulus. A pavement layer this thin has little structural value and an arbitrary chosen stiffness of 500,000 psi was used throughout the year. On these sections, only the base and subgrade moduli were backcalculated.

The monthly deflection data for each of the ten sites is shown in Appendix C. These data have been normalized to 9,000 lbs. and averaged over the test section. The monthly backcalculated moduli for each of the ten sections are shown in Figures 11 through 20. These plots show the surface, base, and subgrade moduli of each month for each of the 3 rigid layer conditions specified. The data are also tabulated in Appendix D together with the average surfacing temperature at the time of test and the average error per sensor from the backcalculation scheme. This average temperature represents the average of the temperature measured 1/2" below surface and measured on thermocouples placed at the bottom of the asphalt layer.

On sites 1, 4, 5, 7, 11, and 12 the use of an infinitely thick subgrade (model 1) resulted in an inverse pavement structure (i.e., the backcalculated base modulus is lower than the subgrade modulus) for several months of the year. The cause of the overpredicted subgrade and underpredicted base moduli are twofold. First, the uniformly stiff subgrade was assumed too thick, and in order to match the same surface deflections, the subgrade stiffness were overpredicted. By including an apparent rigid layer to account for any changes in subgrade stiffness with depth, in model 3, the results were significantly improved. The results were also more compatible with the laboratory data as shown in the next section. The six sites mentioned are all sections where an apparent rigid layer was predicted at a depth of less than 15 feet. This suggests either a rigid layer at shallow depth or a subgrade stiffening with depth. The second reason for the overpredicted subgrade is the high weighting factors assigned to the outer sensors in the bowl matching process. In models 1 and 2 weighting factors of 1.0 were applied to each sensor, in model 3 the weighting factors were calculated using the procedure described in section

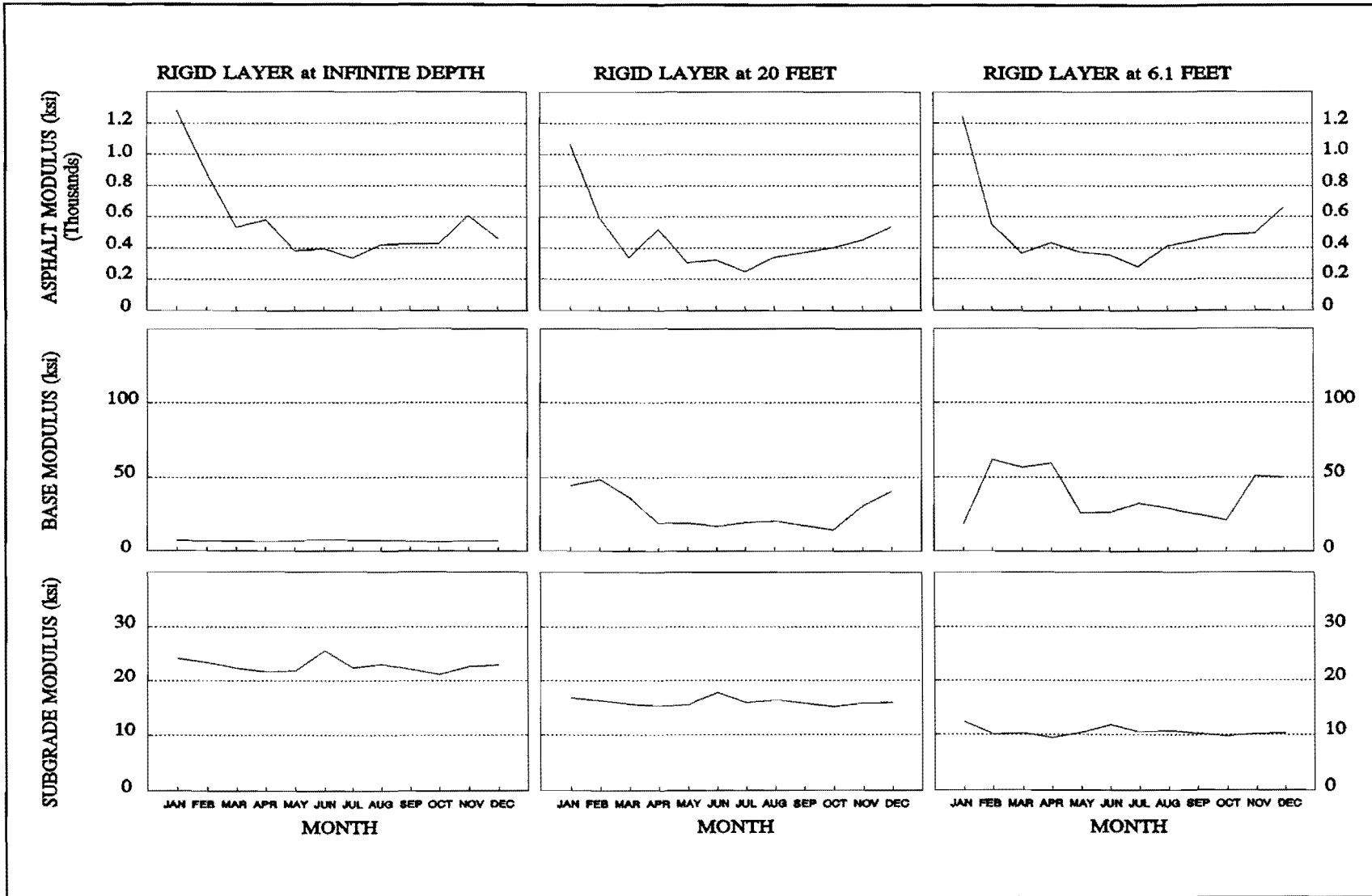


Figure 11. Monthly Backcalculation Results for Site 1.

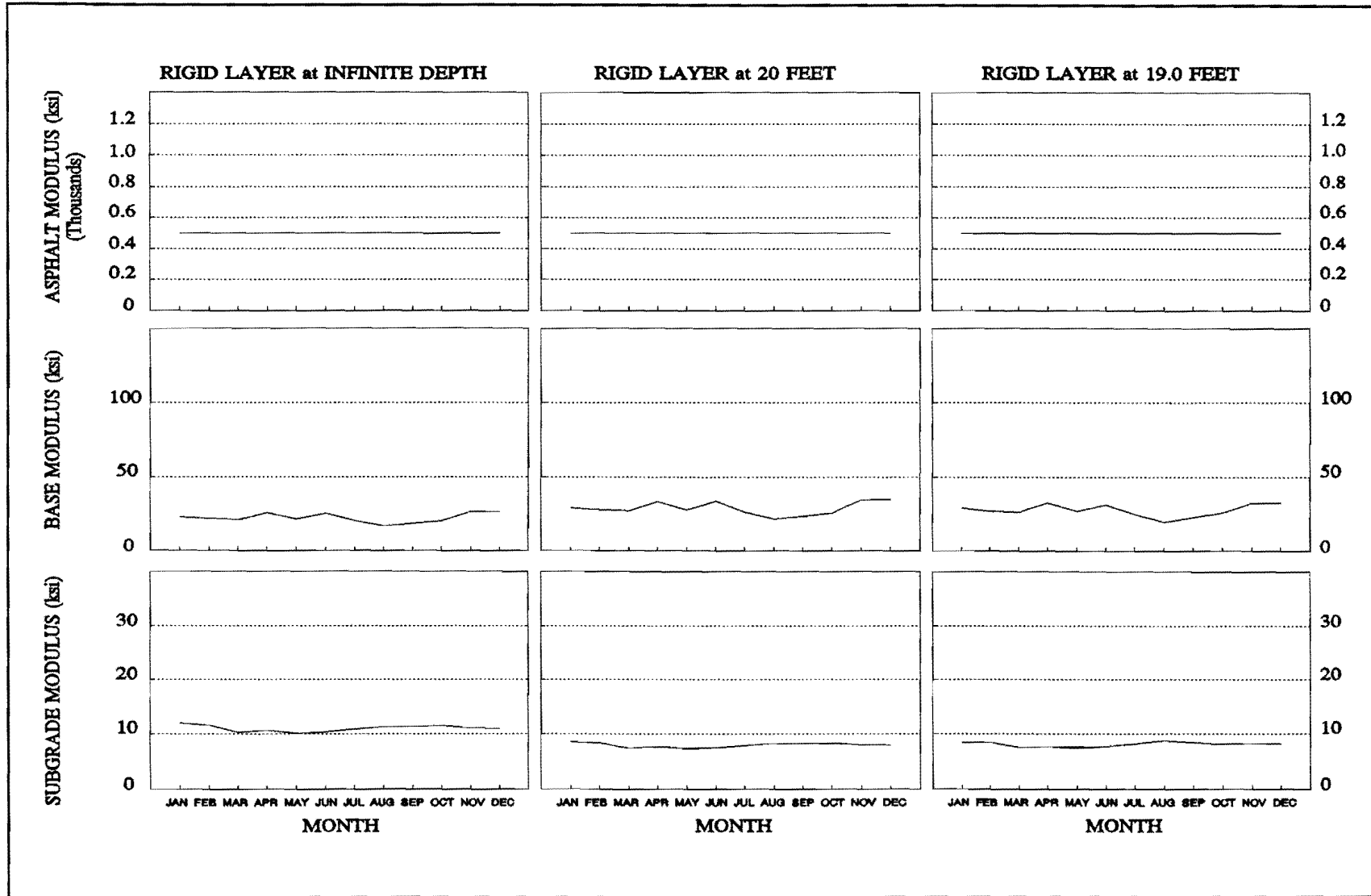


Figure 12. Monthly Backcalculation Results for Site 2.

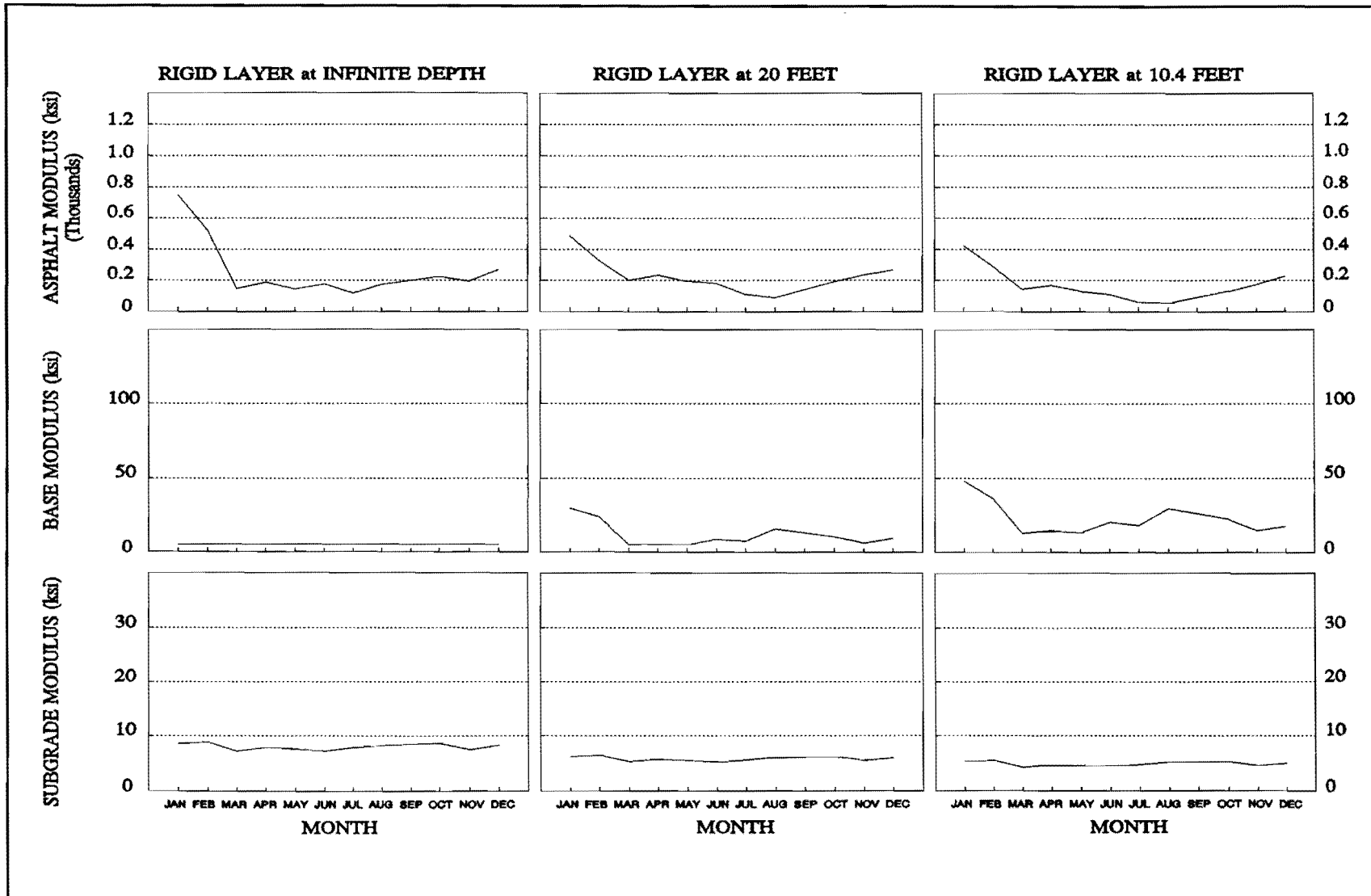


Figure 13. Monthly Backcalculation Results for Site 4.

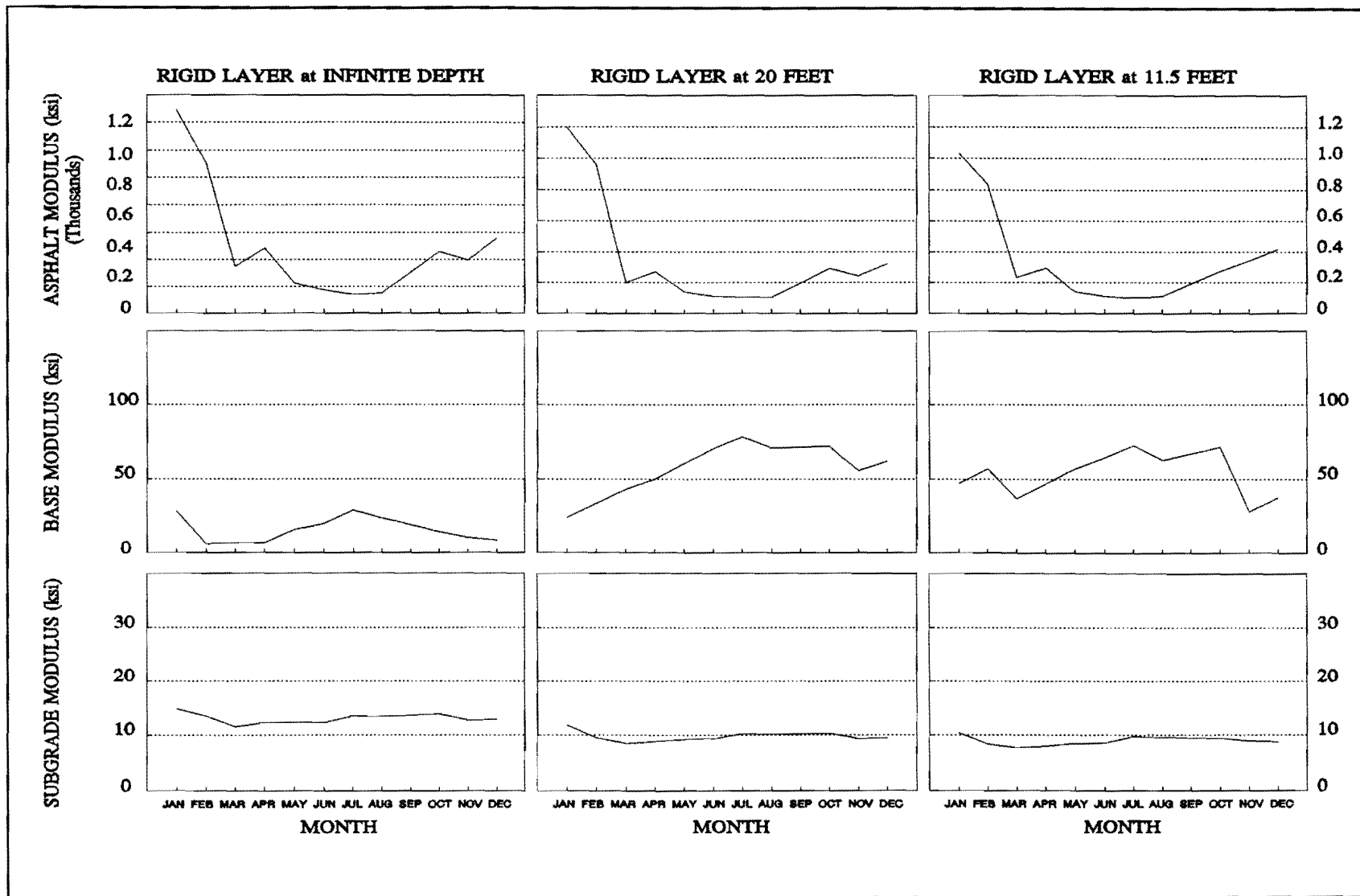


Figure 14. Monthly Backcalculation Results for Site 5.

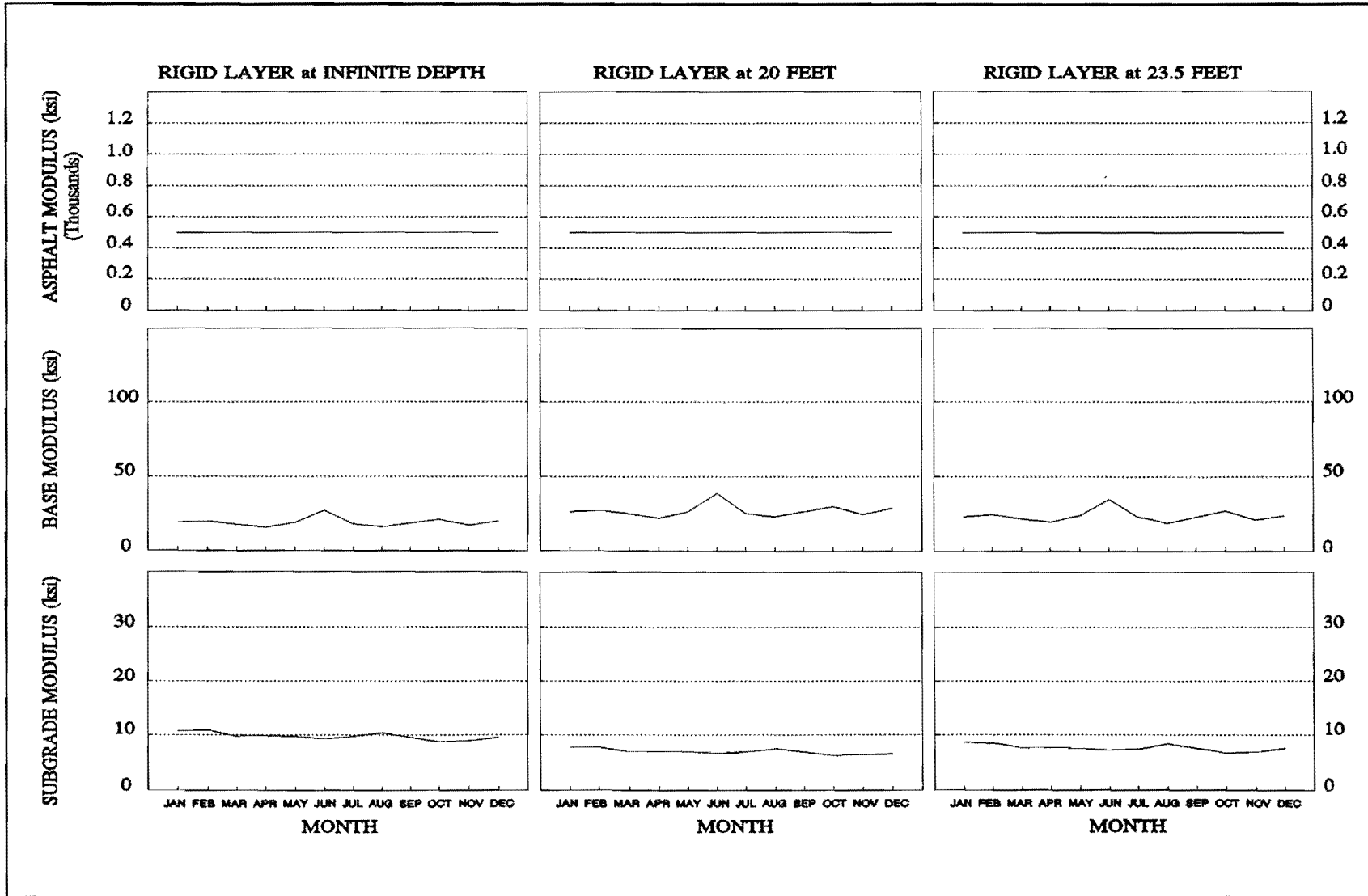


Figure 15. Monthly Backcalculation Results for Site 6.

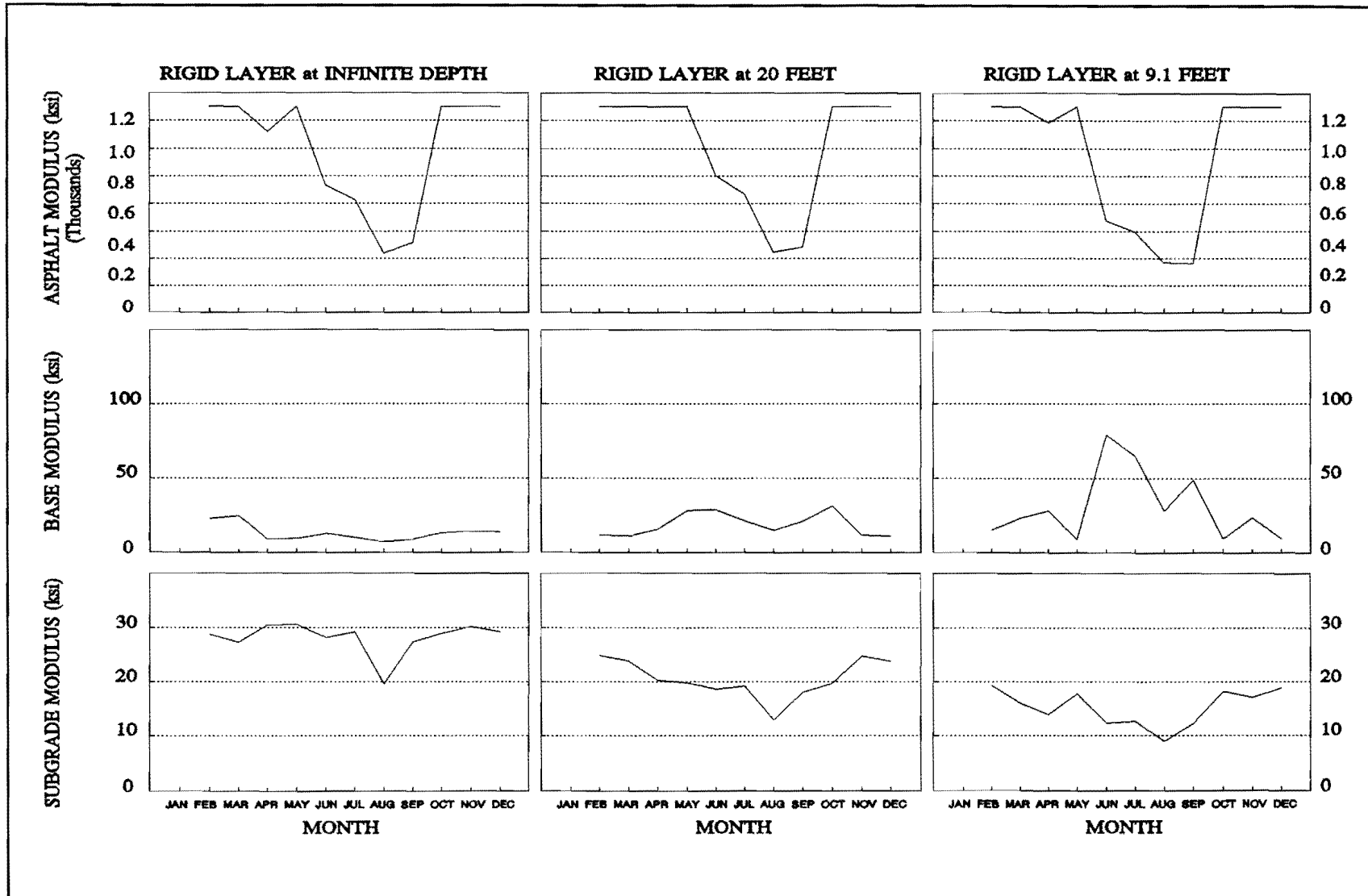


Figure 16. Monthly Backcalculation Results for Site 7.

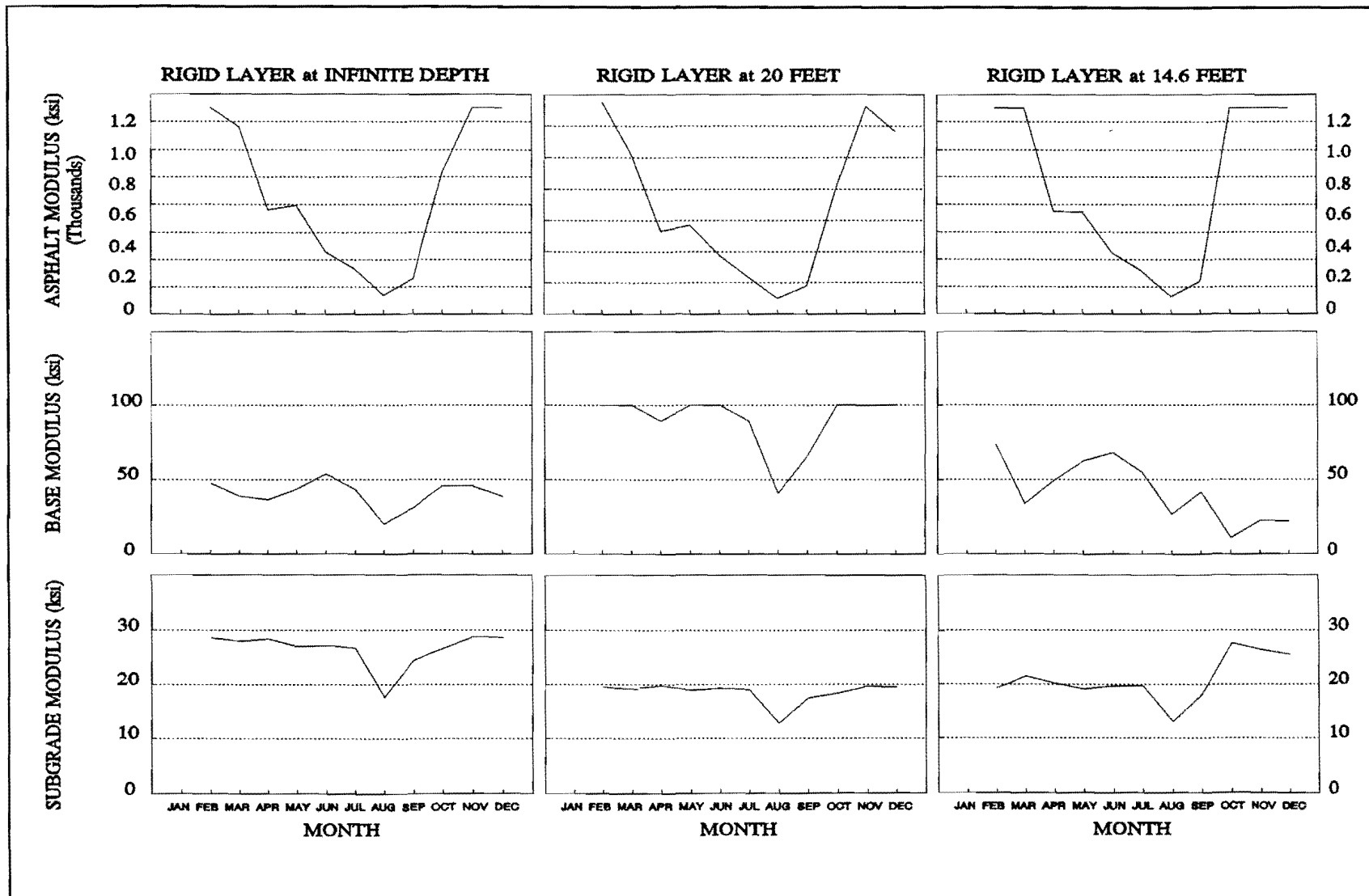


Figure 17. Monthly Backcalculation Results for Site 8.

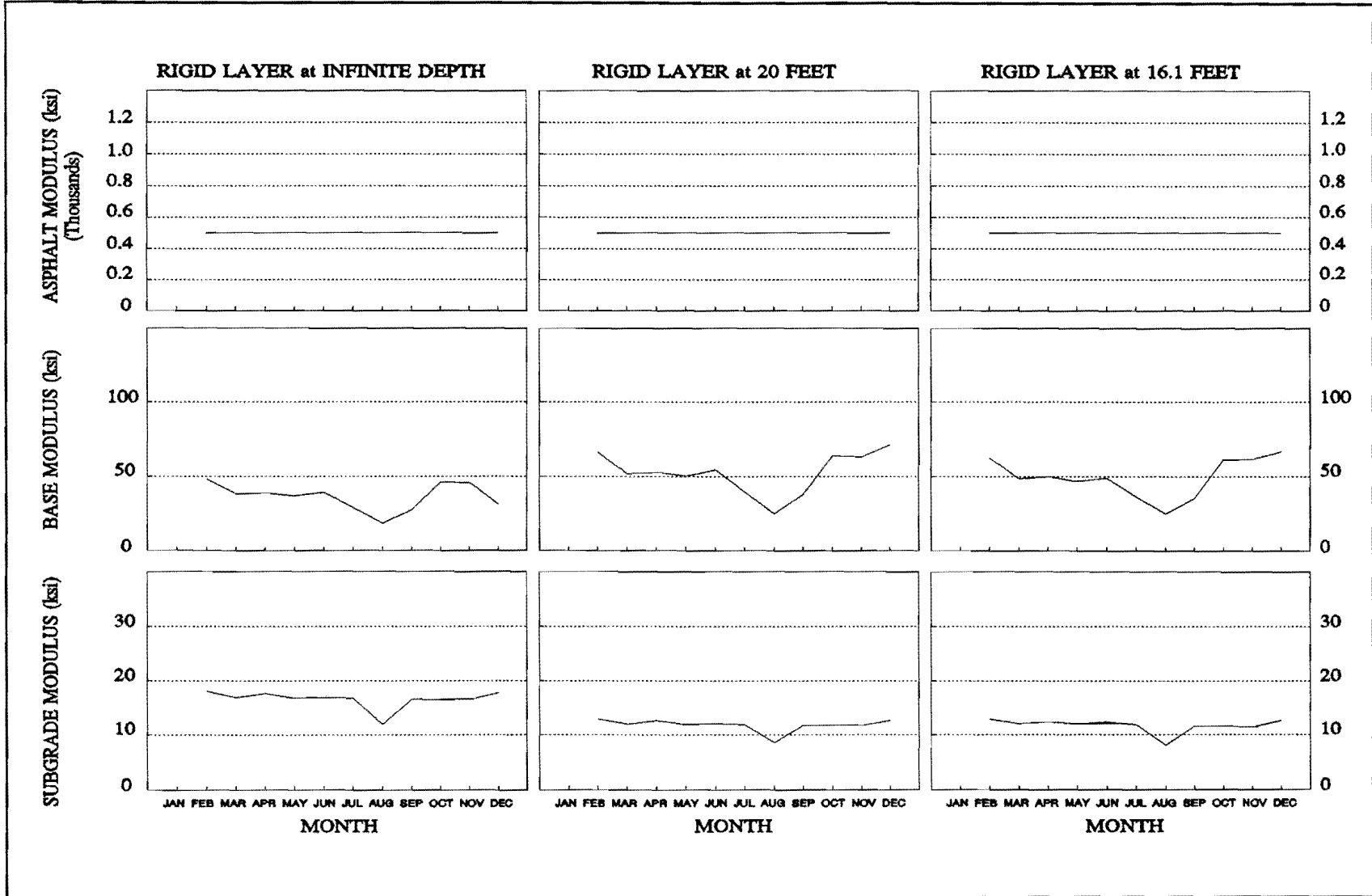


Figure 18. Monthly Backcalculation Results for Site 9.

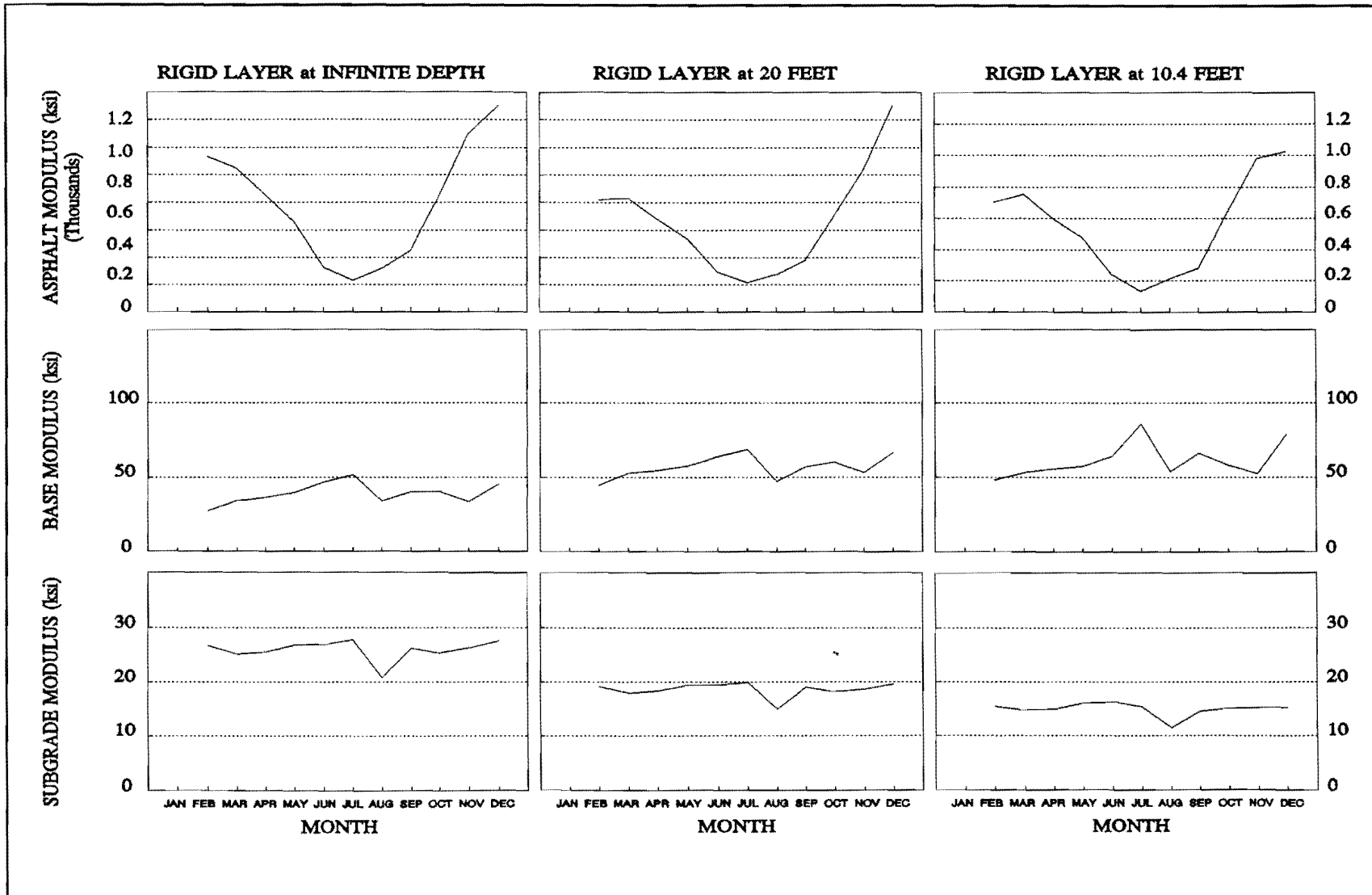


Figure 19. Monthly Backcalculation Results for Site 11.

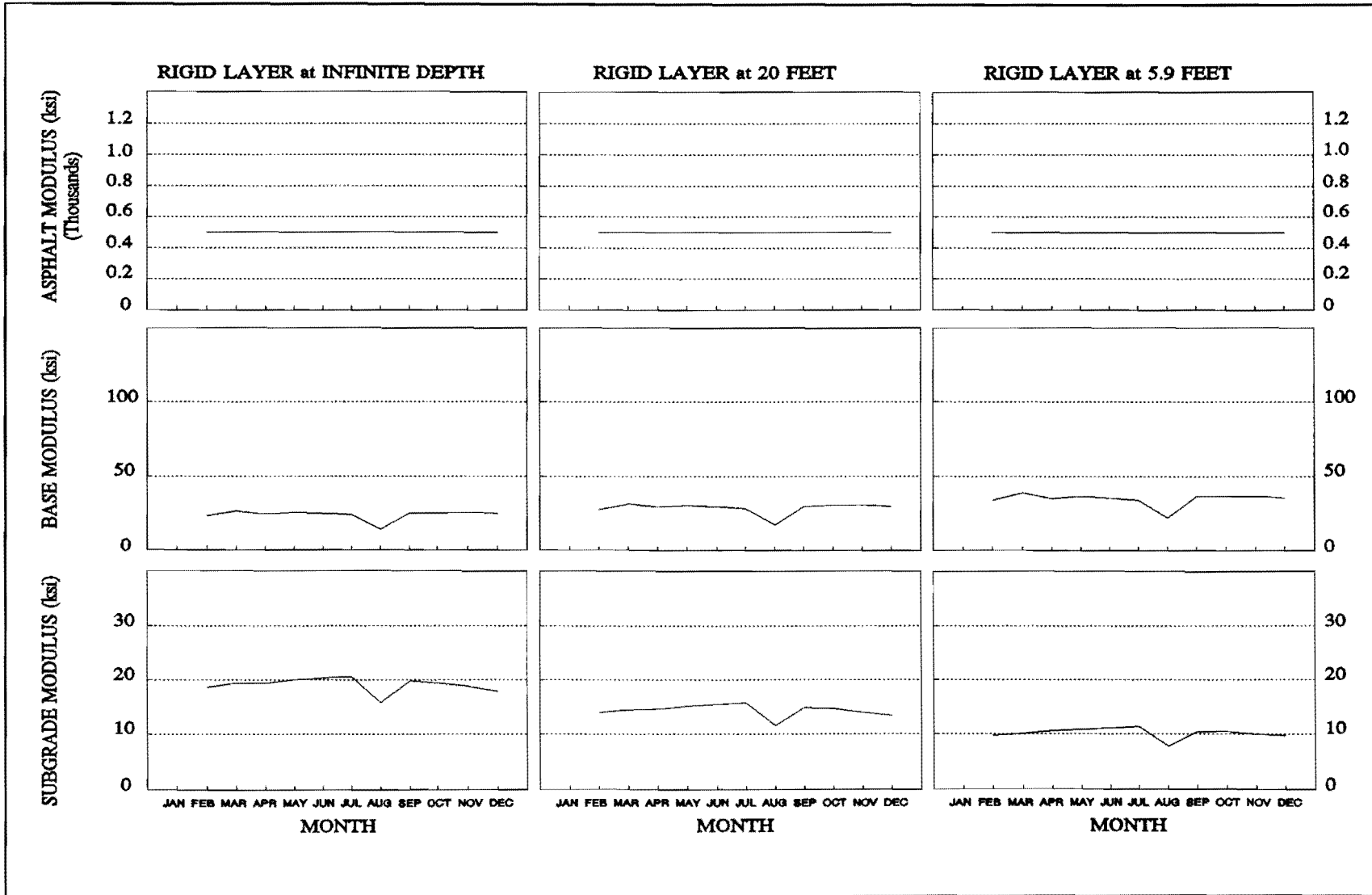


Figure 20. Monthly Backcalculation Results for Site 12.

2.2. The actual subgrade is not linearly elastic, and for both sandy and fine-grained subgrades, the apparent stiffness of the subgrade increases toward the outer sensors. By including all sensors in the analysis, and forcing the calculated deflection bowl through the measured deflection bowl at the outer sensors, an elastic analysis will find a subgrade modulus higher than that occurring beneath the load. This is a problem with all layered elastic procedures, but the influence can be reduced by using only the sensors required to obtain a representative subgrade as described in section 2.3.

On sections 2, 6, 8, and 9, the base moduli values determined using the infinite subgrade were lower than expected. In these sections where the apparent rigid layer predicted was in excess of 15 feet, both models 2 and 3 lead to reasonable results. In all sections the third model which includes a rigid layer at the predicted depth provides reasonable results. (From the monthly deflection data for the 10 sites a total of 40 inverse bowls were calculated for the semi-infinite subgrade, ten for the twenty feet subgrade and 4 for model 3). This observation is substantiated by comparing the backcalculation results to those obtained from laboratory testing.

Comparison of Backcalculation Results to Laboratory Data

The backcalculation results, illustrated in Figures 11 through 20, were further evaluated by comparing them to available laboratory data. As discussed in Chapter III, the laboratory testing consisted of indirect tension tests on asphalt surface cores and resilient modulus tests on samples of the base and subgrade materials. The laboratory and backcalculated moduli are shown in Figures 21 through 30.

When comparing laboratory and backcalculated moduli, no perfect agreement should be expected. The laboratory tests are only simulating stress conditions expected in the pavement under repeated loads. Furthermore, the material samples are disturbed and in some cases even remolded. On the other hand, the results from the backcalculation, are model properties rather than material properties. Using a layered elastic approach a single stiffness per pavement layer is obtained. This is only an apparent stiffness for the whole layer. Actually the stiffness of each

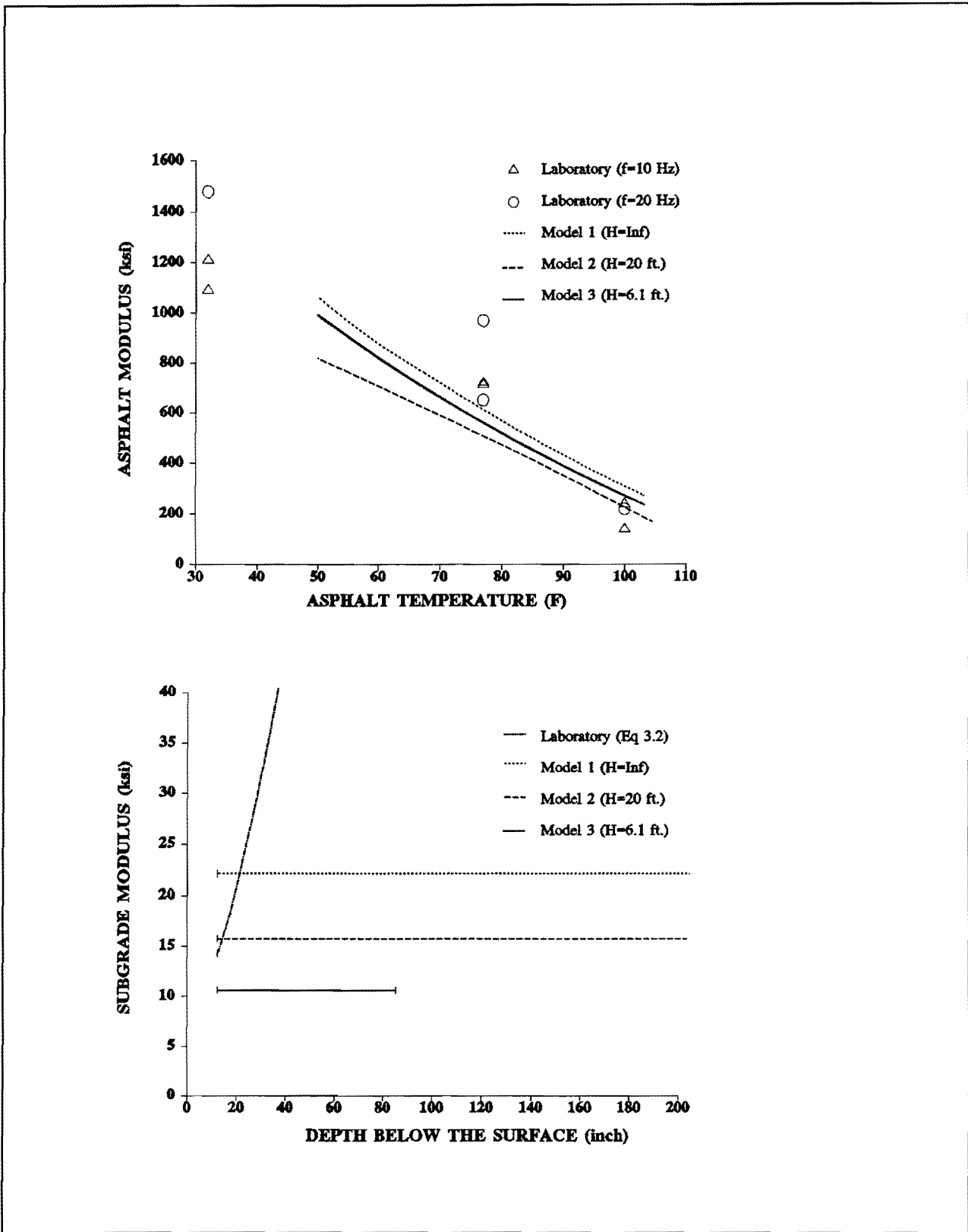


Figure 21. Comparison Between Backcalculation and Laboratory Results for the Asphalt Concrete and Subgrade of Site 1

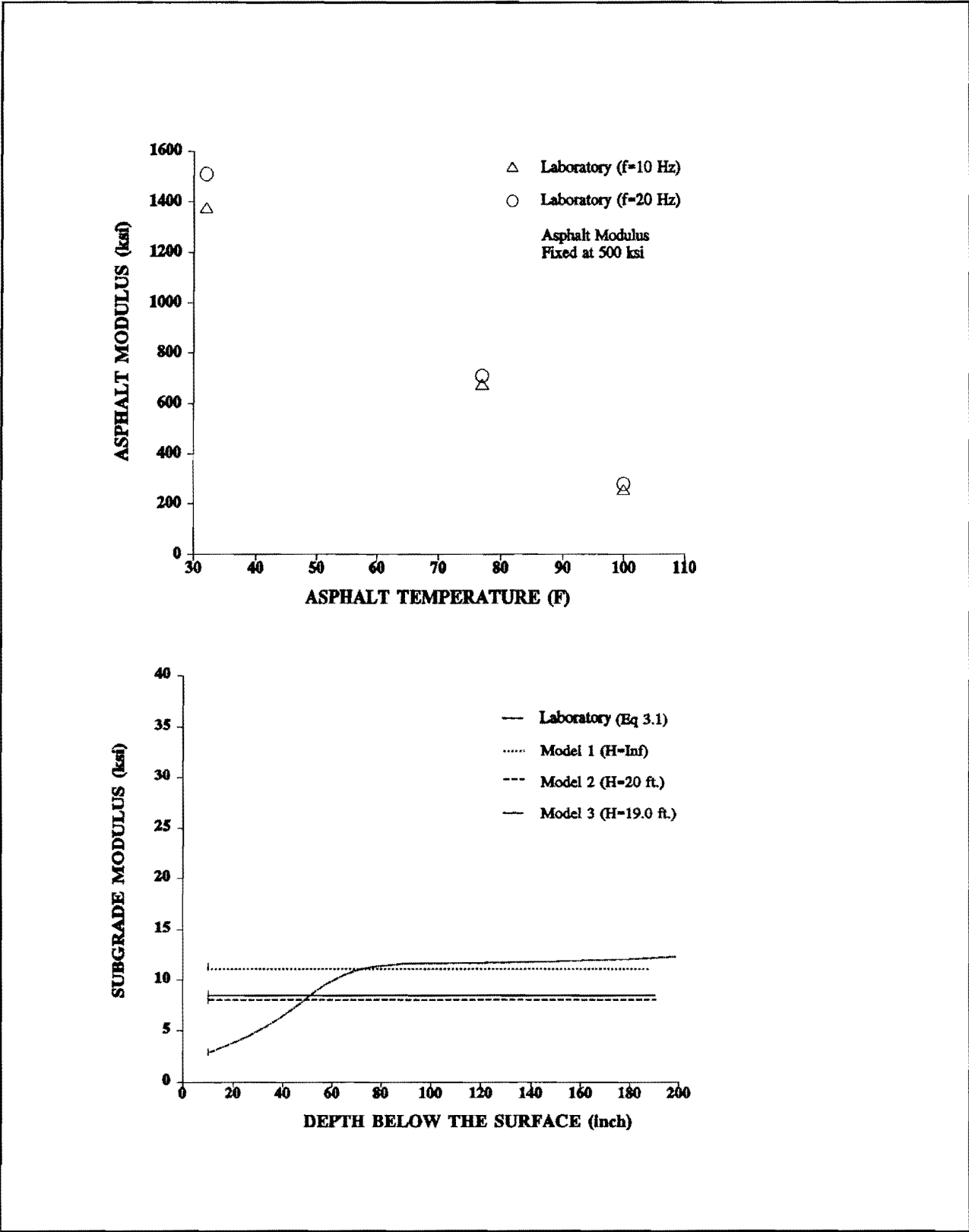


Figure 22. Comparison Between Backcalculation and Laboratory Results for the Asphalt Concrete and Subgrade of Site 2

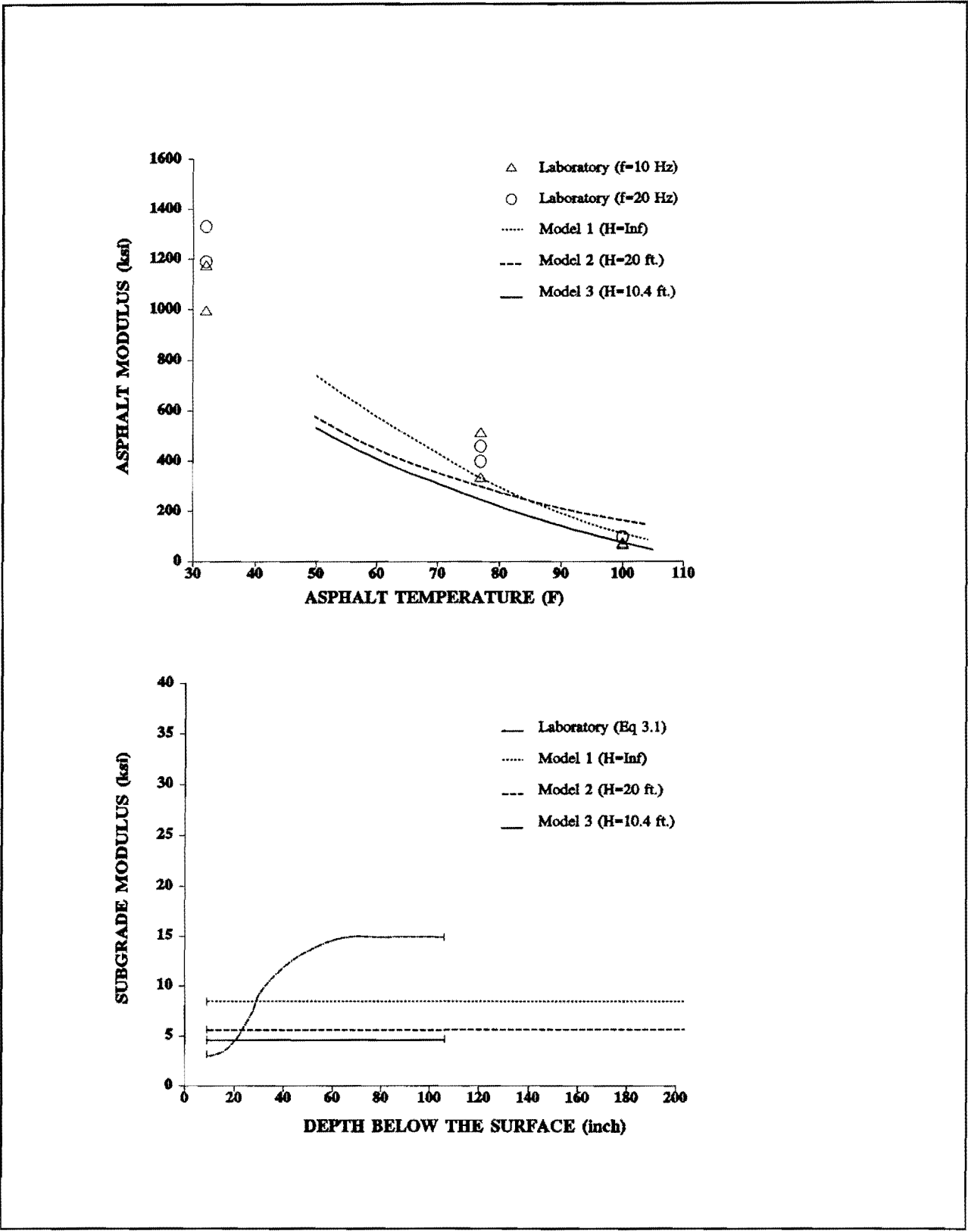


Figure 23. Comparison Between Backcalculation and Laboratory Results for the Asphalt Concrete and Subgrade of Site 4

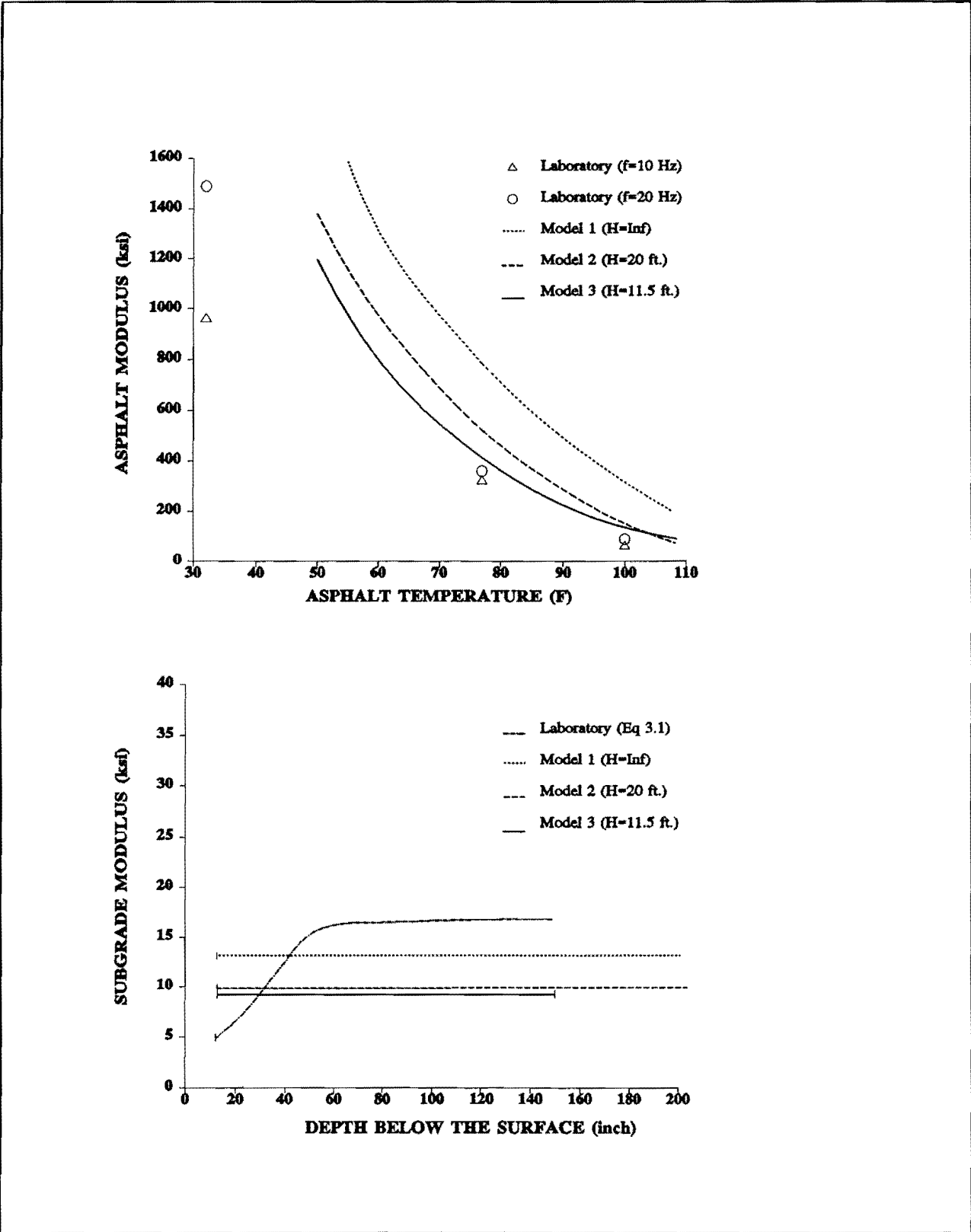


Figure 24. Comparison Between Backcalculation and Laboratory Results for the Asphalt Concrete and Subgrade of Site 5

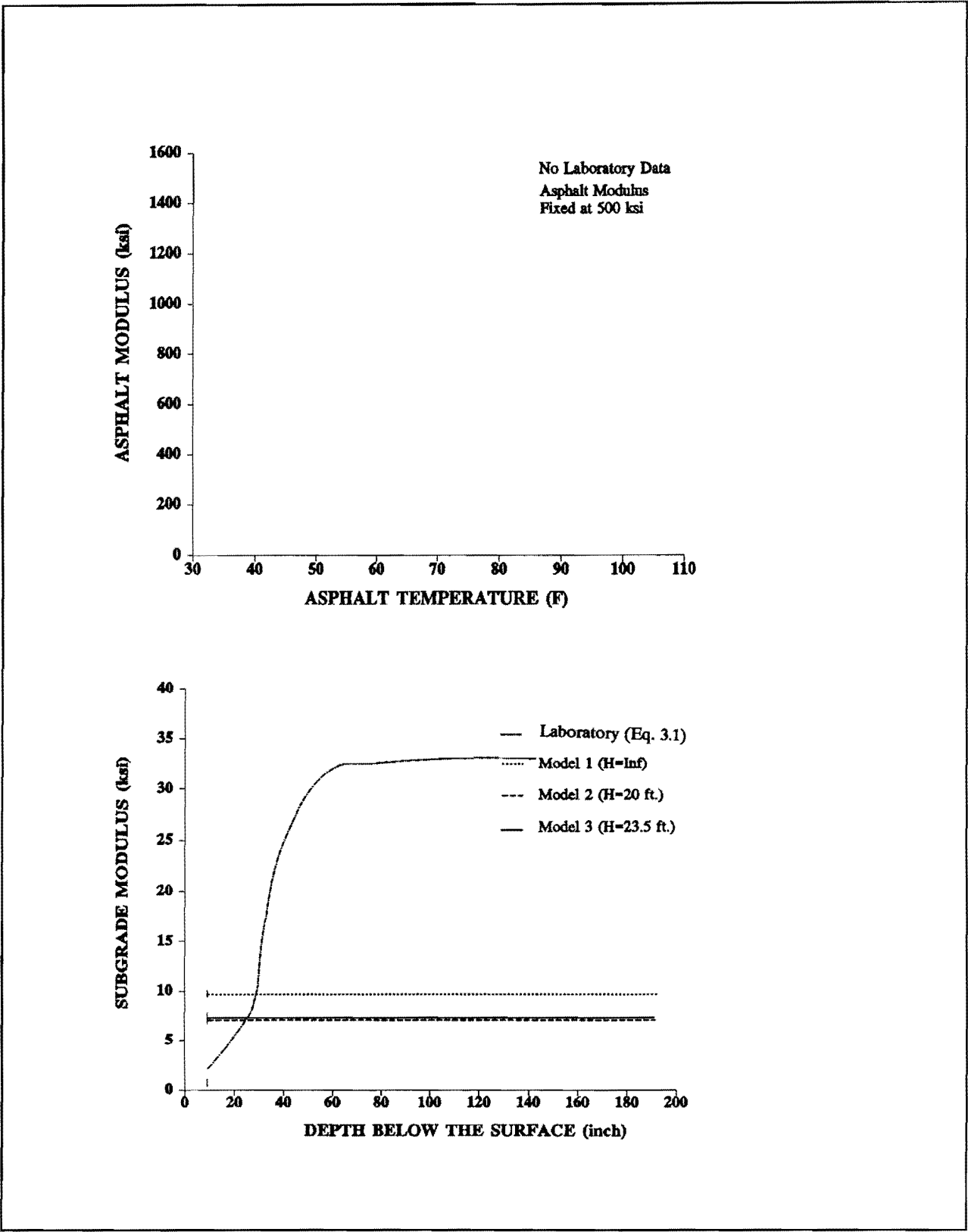


Figure 25. Comparison Between Backcalculation and Laboratory Results for the Asphalt Concrete and Subgrade of Site 6

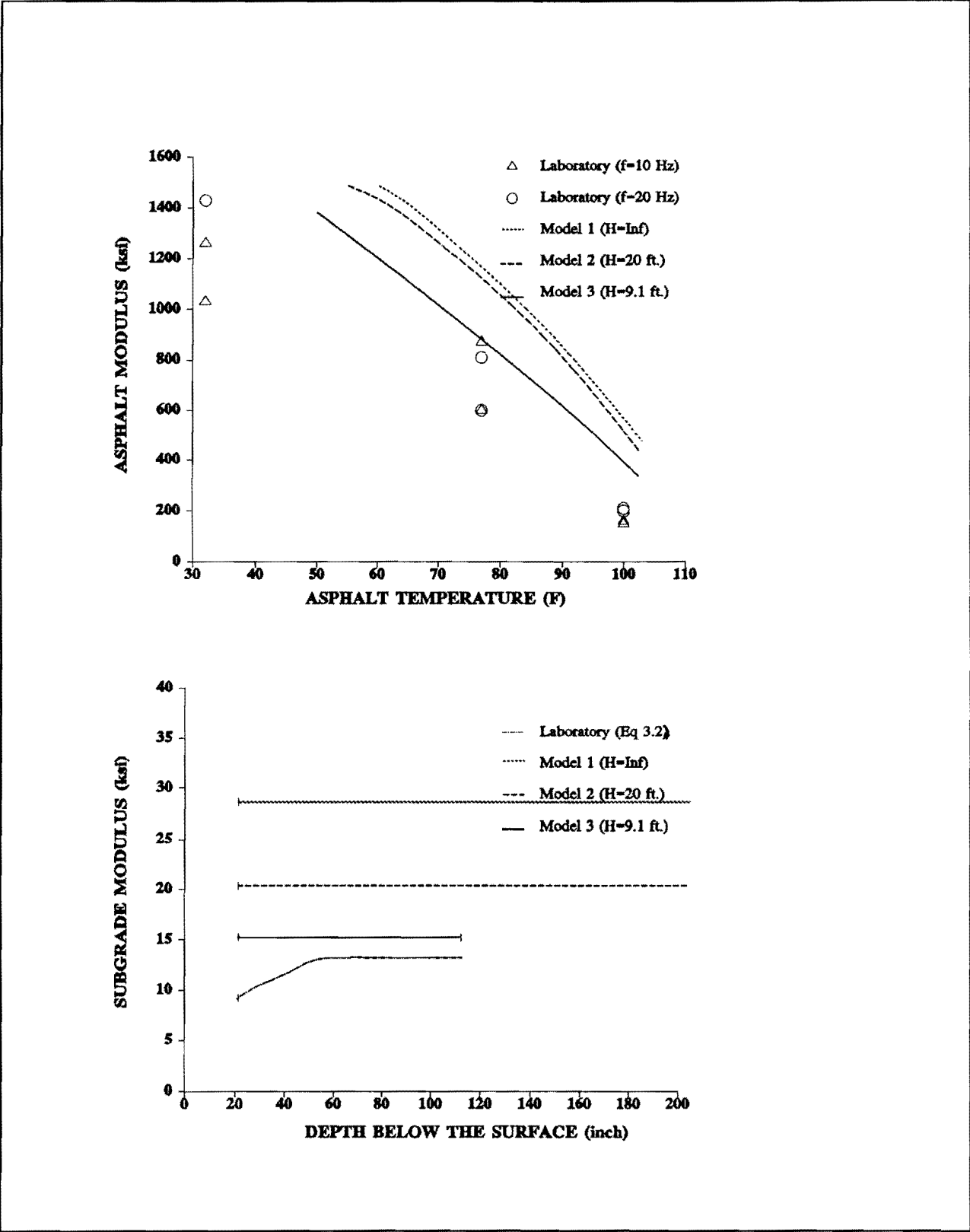


Figure 26. Comparison Between Backcalculation and Laboratory Results for the Asphalt Concrete and Subgrade of Site 7

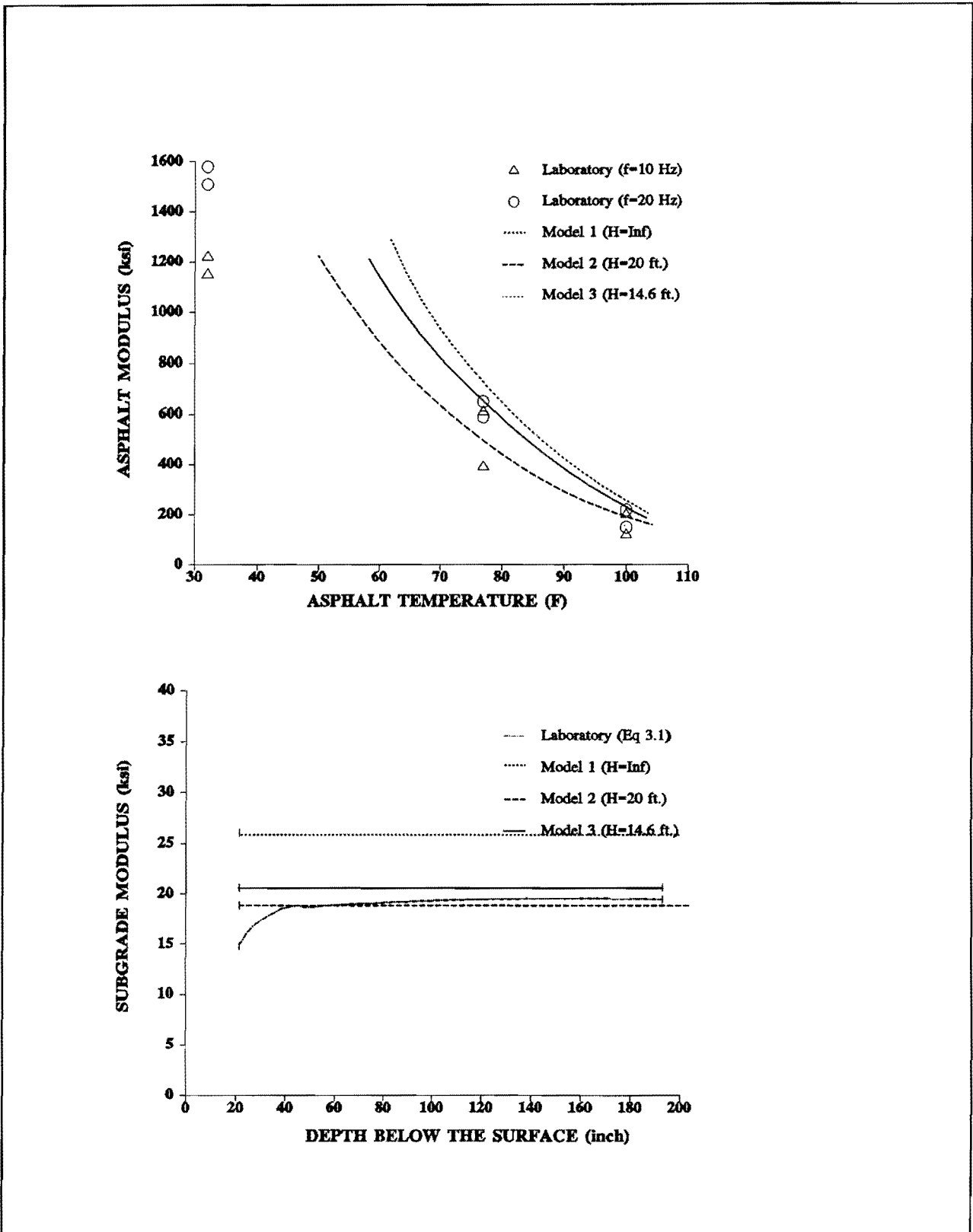


Figure 27. Comparison Between Backcalculation and Laboratory Results for the Asphalt Concrete and Subgrade of Site 8

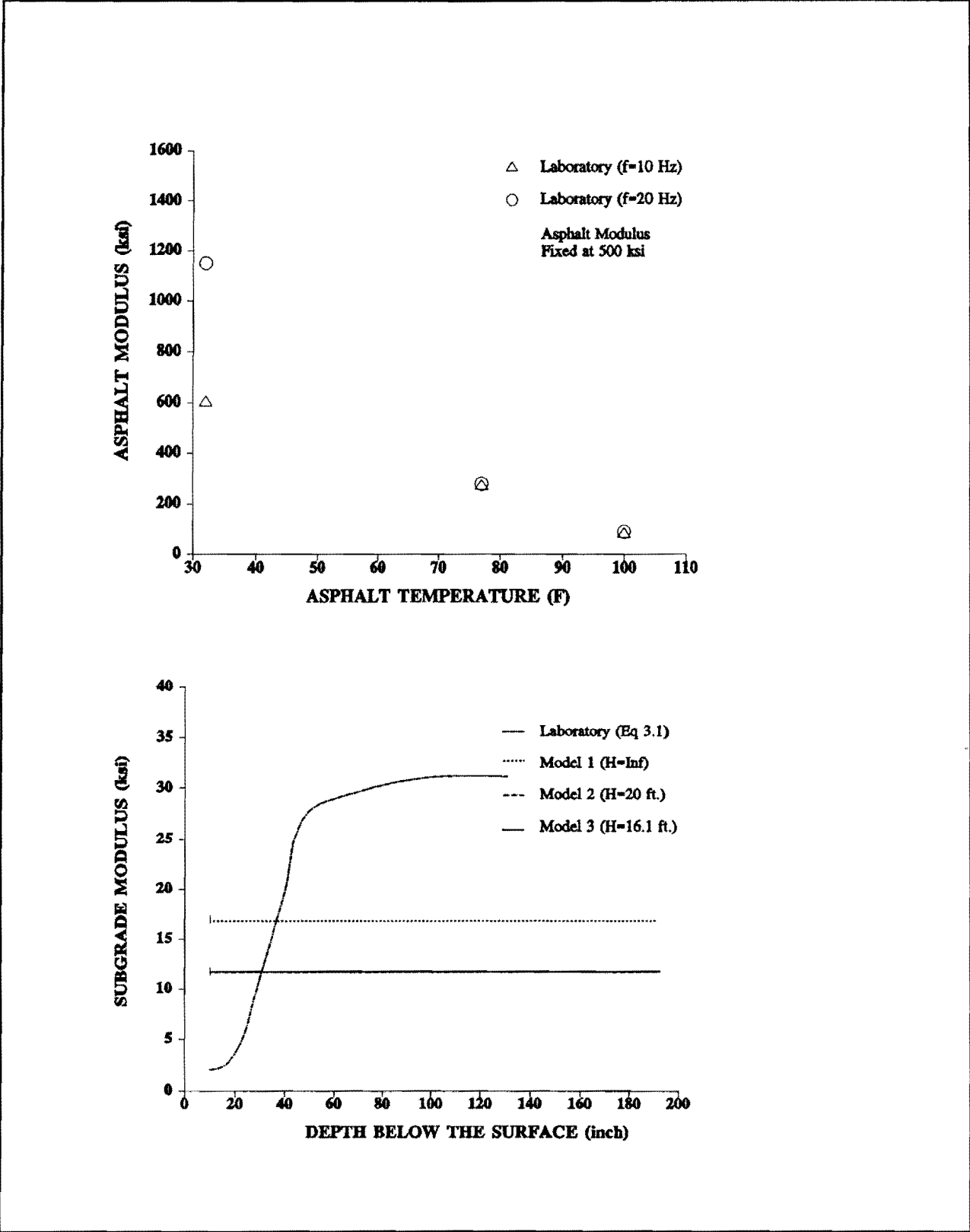


Figure 28. Comparison Between Backcalculation and Laboratory Results for the Asphalt Concrete and Subgrade of Site 9

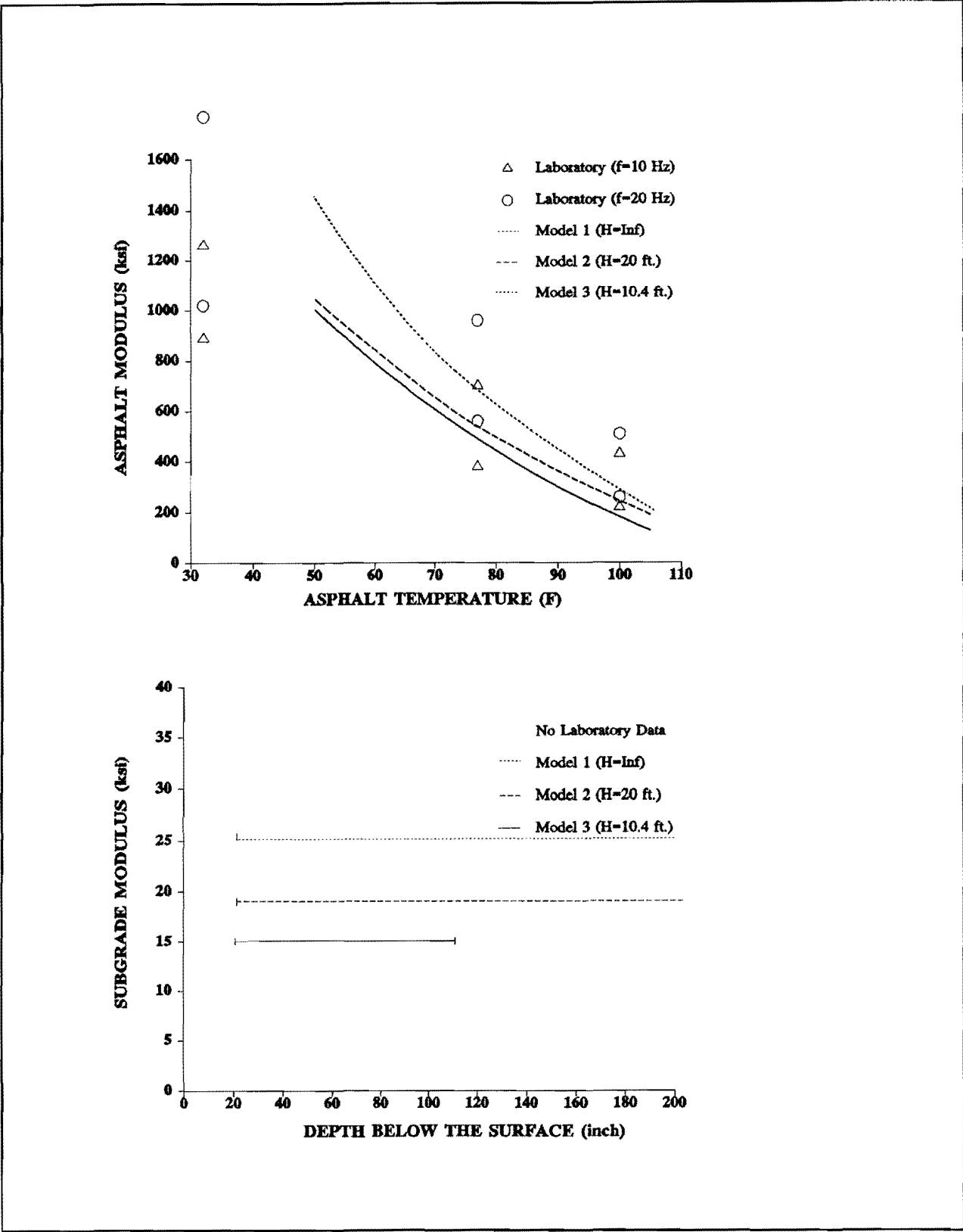


Figure 29. Comparison Between Backcalculation and Laboratory Results for the Asphalt Concrete and Subgrade of Site 11

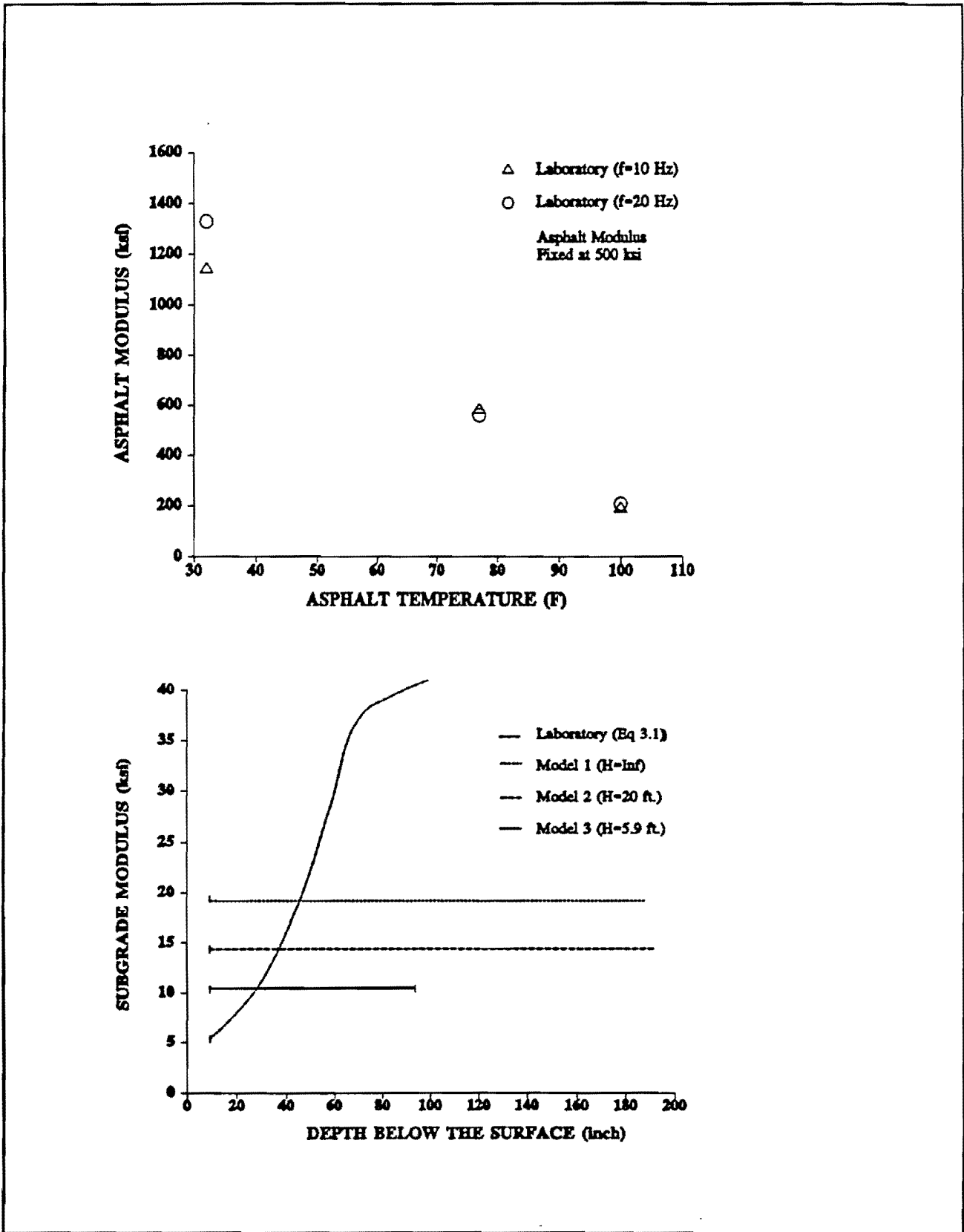


Figure 30. Comparison Between Backcalculation and Laboratory Results for the Asphalt Concrete and Subgrade of Site 12

pavement layer changes vertically and horizontally. As a result, the laboratory data and backcalculated layer moduli should not show a perfect agreement. However, they should show the same trends. For example, the results from both methods should show that asphalt stiffness reduces with an increase in temperature, or subgrade stiffness reduces with increased applied loads. The moduli should also be in the same general range.

The Subgrade

Most subgrades are stress sensitive, and in order to compare the backcalculated and laboratory moduli, the stress state at various depths in the subgrade is required. The stress state is defined by the confining pressure and the deviatoric stress. The confining pressure was calculated using the moisture content, the unit weight of the soil, and the coefficient of lateral earth pressure. The deviatoric stress was determined using the layered elastic program. Because all stresses in the layered elastic programs are load related, the vertical stress in the subgrade directly beneath the FWD load was taken to be the deviatoric stress. Using the stress-stiffness models developed from laboratory results (Tables 4 and 5), the stiffness at various depths in the subgrade was calculated and plotted against depth. In Figures 21 through 30 the backcalculated subgrade moduli, calculated using equation 3.1, are compared to the laboratory data. The backcalculated values for each model are represented by a single horizontal line. The laboratory data is shown as a curve representing its stiffness versus depth.

On all the pavement sections, with the exception of site 1, backcalculation model 3 led to good subgrade stiffness predictions. This stiffness is most representative of the material in the top 18 to 24 inches of the subgrade. The curve representing the laboratory data is a best estimate of the stiffness of the material directly beneath the load where the apparent subgrade stiffness is at its softest. This area is normally the weakest link in the pavement structure. It should therefore be used for design purposes. Toward the outer sensors the subgrade stiffness increases. On the sand sections, there is a significant improvement in results from model 2 to model 3. On the clay sections where little change in stiffness with depth is expected, both models 2 and 3 tend to provide

satisfactory results.

The Base

The characterization of granular materials are extremely complex for several reasons (Witczak and Uzan, 1988). The stress strain-behavior of granular bases depends on the confining stress, shear strain amplitude, compaction history, and the stress path during loading. In addition gradation, particle orientation, suction, and compaction all influence the stiffness of a granular base. These factors are significantly different between the laboratory compacted base samples placed in a repeated load triaxial device and the actual base layer subjected to a FWD impulse load.

By modeling the pavement using a layered elastic or finite element program, tensile stresses are predicted at the bottom of the base layer. It is still an unanswered question whether these stresses actually exist. Possible reasons for the resistance of granular soils to tensile forces are suction, cementation, and aggregate interlock. Heukelom and Klomp (1962) suggested that a granular material might be able to handle tensile bending forces due to interlocking of granules caused by forces perpendicular to the radial bending stress. This behavior of granular soils is not found in triaxial testing. Most granular soils have no strength in the unconfined state (Raad and Figueroa, 1980). To overcome the problem of tensile forces, Raad and Figueroa (1980) developed a procedure to adjust the stress state in the base materials to stay within the Mohr-Coulomb failure envelope. Uzan (1985) suggested that residual stresses that develop due to compaction and loading should be incorporated in granular base modeling. In 1988 Witczak and Uzan added an arbitrary 2 psi residual stress to the base layer before adjusting stresses to comply with the Mohr-Coulomb failure envelope. In 1990, Uzan and Scullion presented a model to include dilation effects when the major to minor principle stress ratio exceeds a given value. This behavior was verified through in-depth deflection testing.

It is obvious that base characterization is extremely complex. Any comparison between laboratory and backcalculated base moduli must include a great deal of correction of stresses and assigning of material properties. Because the results of any of the three models can be supported by

assigning a different set of properties, it is believed that such an exercise does not serve any purpose.

The backcalculated base moduli were also evaluated in terms of the base to subgrade stiffness ratio. Several design procedures, (Izatt et al., 1967; Barker and Brabston, 1977, Uzan et al. 1989) have used a method in which the base stiffness is a function of both the subgrade stiffness and the base thickness. This ratio has been calculated for the deflection bowls analyzed and are shown in Table 9. Several of the ratios found using Model 1 are less than one suggesting a weaker base than subgrade. According to field observations made at these test sites, this is unrealistic. On all sections, the base was in good condition. The ratios obtained using models 2 and 3 are reasonable. According to Barker and Brabston (1977), a ratio of between 1.9 and 4.3 can be expected for a base founded on a subgrade with a stiffness of between 20 and 3 ksi. Seven of the twelve sites fall outside this range of model 1, five for model 2 and two for model 3.

Table 9. Stiffness Ratio of the Average Backcalculated Base Moduli for Sites 1 through 12.

SITE	STIFFNESS RATIO (BASE/SUBGRADE)		
	Model 1	Model 2	Model 3
1	0.30	1.75	3.71
2	2.05	3.72	3.48
4	0.62	2.00	4.71
5	1.18	5.76	5.95
6	1.95	3.87	3.10
7	0.47	0.92	1.97
8	1.52	4.84	2.11
9	2.30	4.44	4.18
11	1.50	3.06	4.08
12	1.25	1.92	3.39

The Asphalt Surface

The stiffness of asphalt concrete is mainly influenced by the temperature and loading frequency. In Figures 21 through 30 the laboratory

results from the indirect tension test are plotted for various temperatures and loading frequencies. The backcalculated moduli were plotted against the asphalt temperature measured in the asphalt layer during the time of testing.

As can be seen from these figures there was a wide range in moduli measured in the laboratory. On thick layers a sample was taken from the top and bottom of the core and tested at two frequencies. For example, on site 7 at 77°F the measured moduli from the same core ranged from 600 to 870 ksi. The laboratory values measured at 32°F are not reliable, this frozen condition is near the measuring accuracy of the test method. This is not a major problem as the minimum field asphalt temperature was 47°F, with the vast majority of the data being collected between 80°F and 110°F.

In reviewing the figures it can be observed that the backcalculated moduli from model 3 are in good agreement with the laboratory data. Also, with the exception of site 4, the model 3 predictions are in better agreement with the laboratory data than models 1 and 2. The good agreement over the higher temperature range is remarkable because the uppermost layer is the pavement system and is the most difficult to backcalculate (Lytton et al., 1990).

4.2 ANALYSIS OF MULTIDDEPTH DEFLECTION DATA

As discussed in the preceding section, it is difficult to validate backcalculation results with laboratory data. The laboratory tests are completed on disturbed samples under simulated stress conditions. At best, they can only give an indication of the material's stiffness. The backcalculated moduli are good indicators of the insitu stiffness under the prevailing stress state, but they are highly model dependent. This is evident from the results of the comparative study presented in the previous section. The first backcalculation model, using an infinitely thick subgrade led to poor deflection analysis results for the majority of test sections. The second backcalculation model, incorporating a rigid layer at 20 feet, provided reasonable results only on the sections founded on a thick clay subgrade. The use of an apparent rigid layer to account for subgrade stiffness changes with depth provided favorable results on nearly all sites.

To further evaluate the use of an apparent rigid layer to model a pavement with the subgrade stiffness increasing with depth, the deflection data collected on two instrumented pavement sections were analyzed. As described in Chapter III, these deflections were measured on the pavement surface and in the pavement structure using Multidepth Deflectometers during FWD load testing. To evaluate and compare various deflection analysis techniques, the following procedure was used:

- The measured surface deflection under a series of FWD loads were analyzed and the layer moduli backcalculated.
- The deflections at the Multidepth Deflectometer positions were forward calculated using the backcalculation model and backcalculated moduli.
- The calculated deflections were then compared to those measured during testing. A close match indicates that the backcalculation model and the obtained moduli are representative of the actual pavement structure under loading.

The Analysis of Section A

Section A consists of a 5 inch asphalt surface layer and a 24 inch granular base founded on a thick sandy clay subgrade. The deflection data collected on this section (Table 7) were analyzed to compare various backcalculation models and to verify that an apparent rigid layer can improve the backcalculation results. In the analysis, two backcalculation models were used. In the first model, a rigid layer was placed at a depth of 20 feet. This model was selected based on the results of a previous deflection analysis of this pavement section. Yazdani (1989) found that a model with a 20 feet deep bedrock led to better deflection matching than a model with an infinitely thick subgrade. The second backcalculation model incorporates an apparent rigid layer. The depth of this layer was determined using the procedures developed in this study. During the deflection analysis of this model, only a selected number of sensors were used to backcalculate the layer moduli.

The results of the first backcalculation model, with a rigid layer at 20 feet, are shown in Table 10. The measured and calculated surface

Table 10. Results of the Deflection Analysis for Section A Using a Backcalculation Model with a Rigid Layer at a Depth of 20 feet.

Surface Deflections					
Offset r (inch)	0.00	12.00	24.00	36.00	48.00
Measured Deflection (mil)	8.34	5.40	3.09	2.09	1.55
Predicted Deflection (mil)	8.37	5.04	3.14	2.24	1.67
Error (percent)	0.40	-6.70	1.60	7.20	7.70
Absolute Error (mil)	0.03	-0.36	0.05	0.15	-0.12
Backcalculated Moduli					
Asphalt Concrete (psi)	588,800				
Granular Base (psi)	70,700				
Subgrade (psi)	20,700				
MDD Deflections					
Offset from Load to MDD Hole	8.20	15.40	20.00	29.00	42.00
LVDT at a Depth of 5.1 inches (Top of the Base)					
Measured Deflection (mil)	5.99	4.59	3.74	2.43	1.72
Predicted Deflection (mil)	6.12	4.34	3.62	2.71	1.93
Error (percent)	2.20	-5.40	-3.20	11.50	12.2
Absolute Error (mil)	0.13	-0.25	-0.12	0.28	0.11
LVDT at a Depth of 17.1 inches (Middle of the Base)					
Measured Deflection (mil)	4.52	3.87	3.31	2.37	1.77
Predicted Deflection (mil)	4.74	3.99	3.50	2.72	1.93
Error (percent)	4.90	3.10	5.70	14.80	9.00
Absolute Error (mil)	0.22	0.12	0.19	0.35	0.16
LVDT at a Depth of 28.8 inches (Bottom of the Base)					
Measured Deflection (mil)	3.64	3.32	3.00	2.39	1.88
Predicted Deflection (mil)	3.88	3.46	3.15	2.56	1.88
Error (percent)	6.60	4.20	5.00	7.10	0.00
Absolute Error (mil)	0.24	0.14	0.15	0.17	0.00
LVDT at a Depth of 36.0 inches (7 inches into the Subgrade)					
Measured Deflection (mil)	3.07	2.88	2.65	2.19	1.79
Predicted Deflection (mil)	3.26	3.00	2.79	2.35	1.79
Error (percent)	6.20	4.20	5.30	7.30	0.00
Absolute Error (mil)	0.19	0.12	0.14	0.16	0.00

deflections as well as the backcalculated layer moduli are listed. These moduli were used to forward calculate the deflections at the MDD positions. The measured and calculated deflections are shown in Figure 31.

In the second backcalculation model, an apparent rigid layer was used to account for changes in subgrade stiffness with depth. Using the procedure summarized in Chapter II, the depth of an apparent rigid layer was determined to be 16 feet. The results of this deflection analysis are listed in Table 11 and graphically illustrated in Figure 32.

From the results it is clear that the second backcalculation model, with an apparent rigid layer at a depth of 16 feet, lead to the best results. For the five surface deflections this model resulted in an average RMSE¹ of 1.8 percent while the model with a 20 feet rigid layer, resulted in a RMSE of 4.71 percent. The predicted in-depth deflections were also better with an average RMSE of 4.08 percent compared to a RMSE of 5.89 percent for the model with a rigid layer at a depth of 20 feet.

In studying the results of the second model (Figure 32), it is obvious that the analysis led to excellent deflection matching at the surface and at a depth of 36 inches, or 7 inches into the subgrade. The deflections in the base, as measured by the first and second MDD, are smaller than the predicted deflections. It can be concluded that the base stiffness was slightly underpredicted while the asphalt stiffness was overpredicted. To distinguish better between the surface and base stiffness, more surface deflection readings close to the load are needed. It is believed that a measured surface deflection at an offset of 8 inches can greatly improve the stiffness characterization of the upper layers. The excellent match at the fourth LVDT, in the subgrade, indicates that the use of the apparent rigid layer effectively models the subgrade with changing stiffness with depth.

¹ RMSE is an abbreviation for the Root Mean Square of the Error (Equation 4.1)

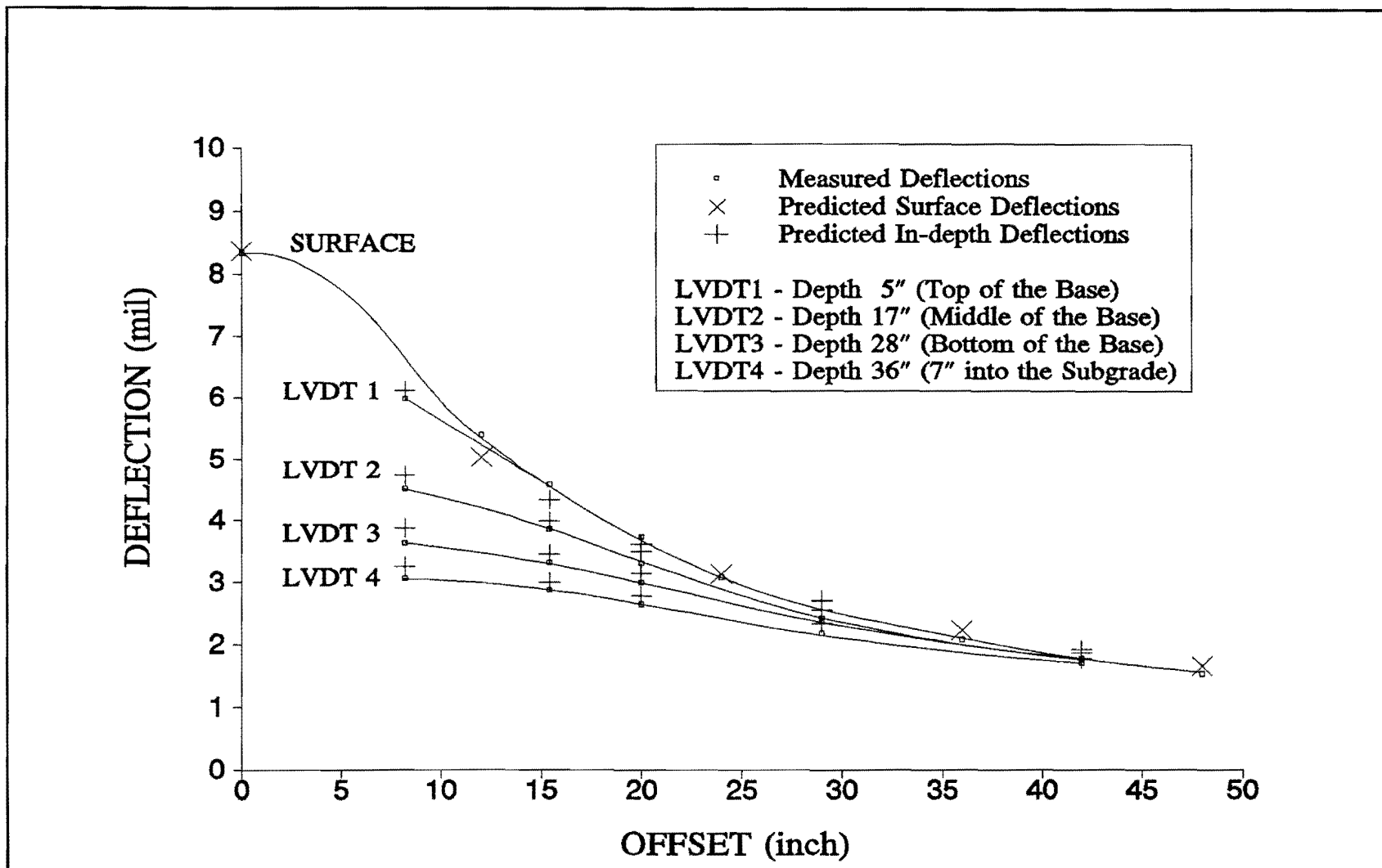


Figure 31. Measured and Predicted Deflections for Section A Based on a Pavement Model with a Rigid Layer at a Depth of 20 feet.

Table 11. Results of the Deflection Analysis for Section A Using a Backcalculation Model with an Apparent Rigid Layer at a Depth of 16 feet.

Surface Deflections					
Offset r (inch)	0.00	12.00	24.00	36.00	48.00
Measured Deflection (mil)	8.34	5.40	3.09	2.09	1.55
Predicted Deflection (mil)	8.37	5.32	3.16	2.11	1.49
Error (percent)	0.40	-1.50	2.30	1.00	-3.90
Absolute Error (mil)	0.03	-0.08	0.05	0.02	-0.06
Backcalculated Moduli					
Asphalt Concrete (psi)	845,500				
Granular Base (psi)	55,500				
Subgrade (psi)	21,000				
MDD Deflections					
Offset from Load to MDD Hole	8.20	15.40	20.00	29.00	42.00
LVDT at a Depth of 5.1 inches (Top of the Base)					
Measured Deflection (mil)	5.99	4.59	3.74	2.43	1.72
Predicted Deflection (mil)	6.39	4.54	3.72	2.65	1.77
Error (percent)	6.70	-1.10	-0.05	9.10	2.90
Absolute Error (mil)	0.40	-0.05	-0.02	0.22	0.05
LVDT at a Depth of 17.1 inches (Middle of the Base)					
Measured Deflection (mil)	4.52	3.87	3.31	2.37	1.77
Predicted Deflection (mil)	4.81	4.02	3.49	2.62	1.77
Error (percent)	6.40	3.90	5.40	10.50	0.00
Absolute Error (mil)	0.29	0.15	0.18	0.25	0.00
LVDT at a Depth of 28.8 inches (Bottom of the Base)					
Measured Deflection (mil)	3.64	3.32	3.00	2.39	1.79
Predicted Deflection (mil)	3.82	3.39	3.06	2.43	1.62
Error (percent)	4.90	2.10	2.00	1.70	-9.50
Absolute Error (mil)	0.18	0.07	0.06	0.04	-0.17
LVDT at a Depth of 36.0 inches (7 inches into the Subgrade)					
Measured Deflection (mil)	3.07	2.88	2.65	2.19	1.79
Predicted Deflection (mil)	3.17	2.89	2.67	2.21	1.62
Error (percent)	3.30	0.30	0.80	0.90	-9.50
Absolute Error (mil)	0.10	0.01	0.02	0.02	-0.10

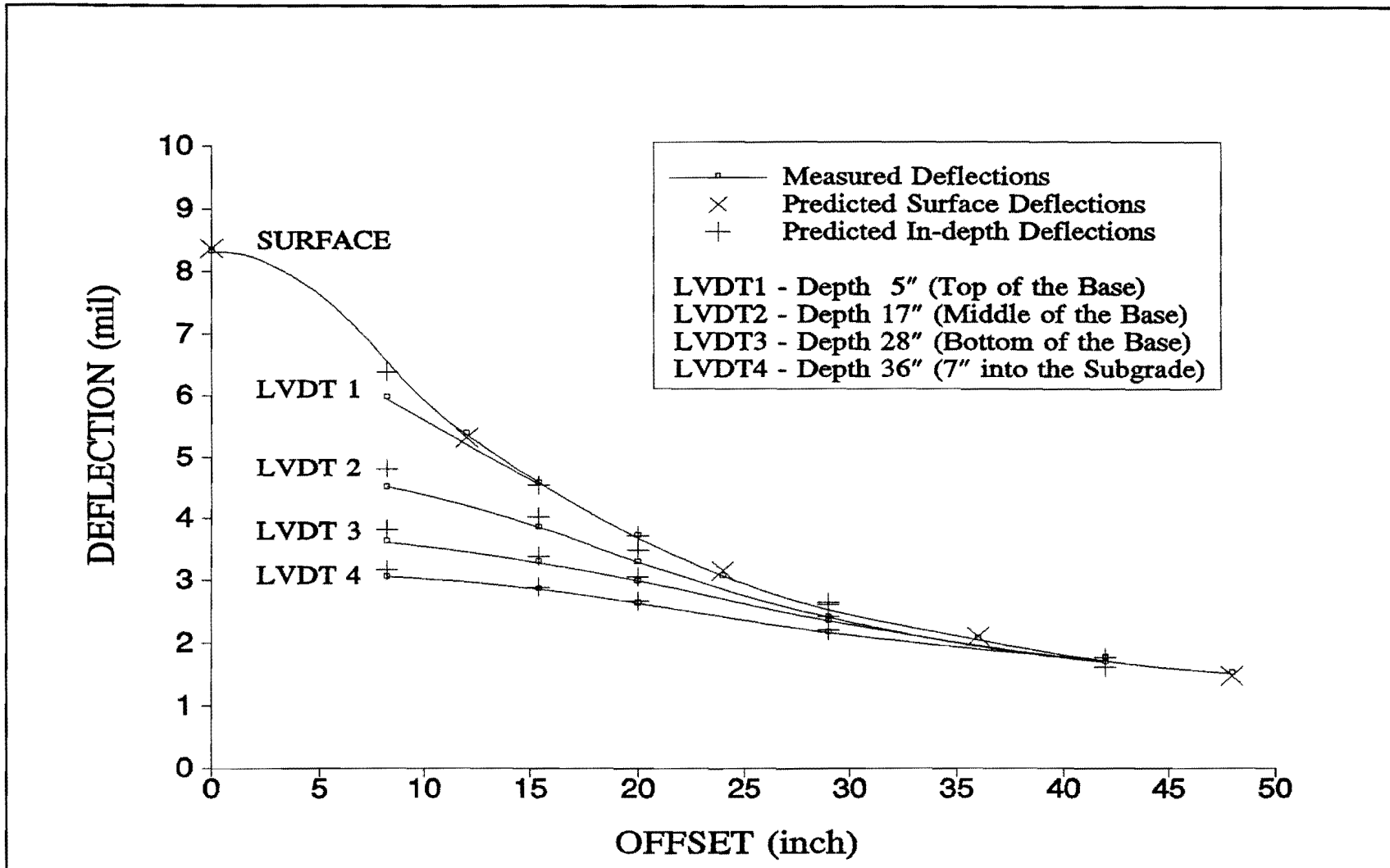


Figure 32. Measured and Predicted Deflections for Section A Based on a Pavement Model with an Apparent Rigid Layer at a Depth of 16 feet.

The Analysis of Section B

Section B consists of a 3.5 inch asphalt surface and 12 inch granular base founded on a weathered limestone subgrade containing boulders. This section was selected for analysis because the small anchor movements (only 0.8 mils at a depth of 72 inches) suggested a stiff subgrade material at a shallow depth. The deflection data collected on this section (Table 8) were analyzed similarly to that of section A. The first model used to analyze the surface deflection data was a three layer linear elastic model with a rigid layer at a depth of 20 feet. This resulted in an inverse pavement structure with a backcalculated subgrade stiffness of 12,000 psi and a base stiffness of 5,000 psi, which was the lower limit set on the base modulus. These results led to a poor match of the measured in-depth deflections as listed in Table 12 and do not agree with the observations made by the technical personnel during installation of the MDD system. They reported that the base was in sound condition and noticeably stiffer than the subgrade.

The second model used to analyze the surface deflection data is a three layer linear elastic model with an apparent rigid layer at a calculated depth of 5.5 feet using the procedure summarized in Chapter II. The results of this analysis are listed in Table 13 and are graphically shown in Figure 33. Although the surface deflections are closely matched, the deflections predicted within the pavement structure only match those measured with an average RMSE of 17.1 percent. From the deflection plots in Figure 33 it is possible to draw conclusions about the backcalculated layer moduli. For example, the three predicted deflections at the bottom of the base are all underpredicted, while those 13 inches into the subgrade closely match the measured deflections. This indicates that the stiffness of the subgrade material in the top 13 inches was overpredicted. To still obtain the same surface deflections a stiffer base would be required. It can therefore be concluded that the stiffness of the first 13 inches of the subgrade was overpredicted while the base was underpredicted.

As mentioned before, the prediction of an apparent rigid layer at such a shallow depth might be indicating a shallow rigid layer or a

Table 12. Results of the Deflection Analysis for Section B Using a Backcalculation Model with a Rigid Layer at a Depth of 20 feet.

Surface Deflections					
Offset r (inch)	0.00	12.00	24.00	36.00	48.00
Measured Deflection (mil)	44.16	26.10	11.10	4.80	2.57
Predicted Deflection (mil)	37.61	22.12	8.98	4.00	2.40
Error (percent)	-	-	-18.63	-16.50	- 8.52
Absolute Error (mil)	14.70	15.30	-2.12	-0.80	-0.17
	-6.55	-3.98			
Backcalculated Moduli					
Asphalt Concrete (psi)	566,000				
Granular Base (psi)	5,000 (Lower Limit)				
Subgrade (psi)	12,000				
MDD Deflections					
Offset from Load to MDD Hole	3.00	20.00	32.00		
LVDT at a Depth of 3.8 inches (Top of the Base)					
Measured Deflection (mil)	42.66	15.42	6.81		
Predicted Deflection (mil)	35.71	12.23	5.10		
Error (percent)	-16.45	-20.24	-24.9		
Absolute Error (mil)	-6.95	-3.19	-1.71		
LVDT at a Depth of 15.8 inches (Bottom of the Base)					
Measured Deflection (mil)	35.53	15.76	6.91		
Predicted Deflection (mil)	15.60	9.18	5.24		
Error (percent)	-56.12	-41.77	-24.50		
Absolute Error (mil)	-19.93	-6.58	-1.67		
LVDT at a Depth of 28.5 inches (13 inches into the Subgrade)					
Measured Deflection (mil)	15.65	8.96	5.16		
Predicted Deflection (mil)	13.23	8.63	5.14		
Error (percent)	-15.43	-4.68	-0.41		
Absolute Error (mil)	2.45	-0.33	-0.02		

Table 13. Results of the Deflection Analysis for Section B Using a Backcalculation Model with an Apparent Rigid Layer at a Depth of 5.5 feet.

Surface Deflections					
Offset r (inch)	0.00	12.00	24.00	36.00	48.00
Measured Deflection (mil)	44.16	26.10	11.10	4.80	2.57
Predicted Deflection (mil)	44.17	26.11	11.10	4.23	1.19
Error (percent)	0.02	0.04	-0.03	-11.85	-53.75
Absolute Error (mil)	0.01	0.01	0.00	-0.57	-1.38
Backcalculated Moduli					
Asphalt Concrete (psi)	421,000				
Granular Base (psi)	9,000				
Subgrade (psi)	5,000				
MDD Deflections					
Offset from Load to MDD Hole	3.00	20.00	32.00		
LVDT at a Depth of 3.8 inches (Top of the Base)					
Measured Deflection (mil)	42.66	15.42	6.81		
Predicted Deflection (mil)	41.17	14.22	5.33		
Error (percent)	-3.50	-7.80	-21.8		
Absolute Error (mil)	-1.49	-1.20	-1.48		
LVDT at a Depth of 15.8 inches (Bottom of the Base)					
Measured Deflection (mil)	35.53	15.76	6.91		
Predicted Deflection (mil)	24.12	11.96	5.15		
Error (percent)	-32.10	-24.10	-25.50		
Absolute Error (mil)	-11.41	-3.80	-1.76		
LVDT at a Depth of 28.5 inches (13 inches into the Subgrade)					
Measured Deflection (mil)	15.65	8.96	5.16		
Predicted Deflection (mil)	18.97	10.46	4.82		
Error (percent)	21.20	16.70	-6.50		
Absolute Error (mil)	3.32	1.50	-0.34		

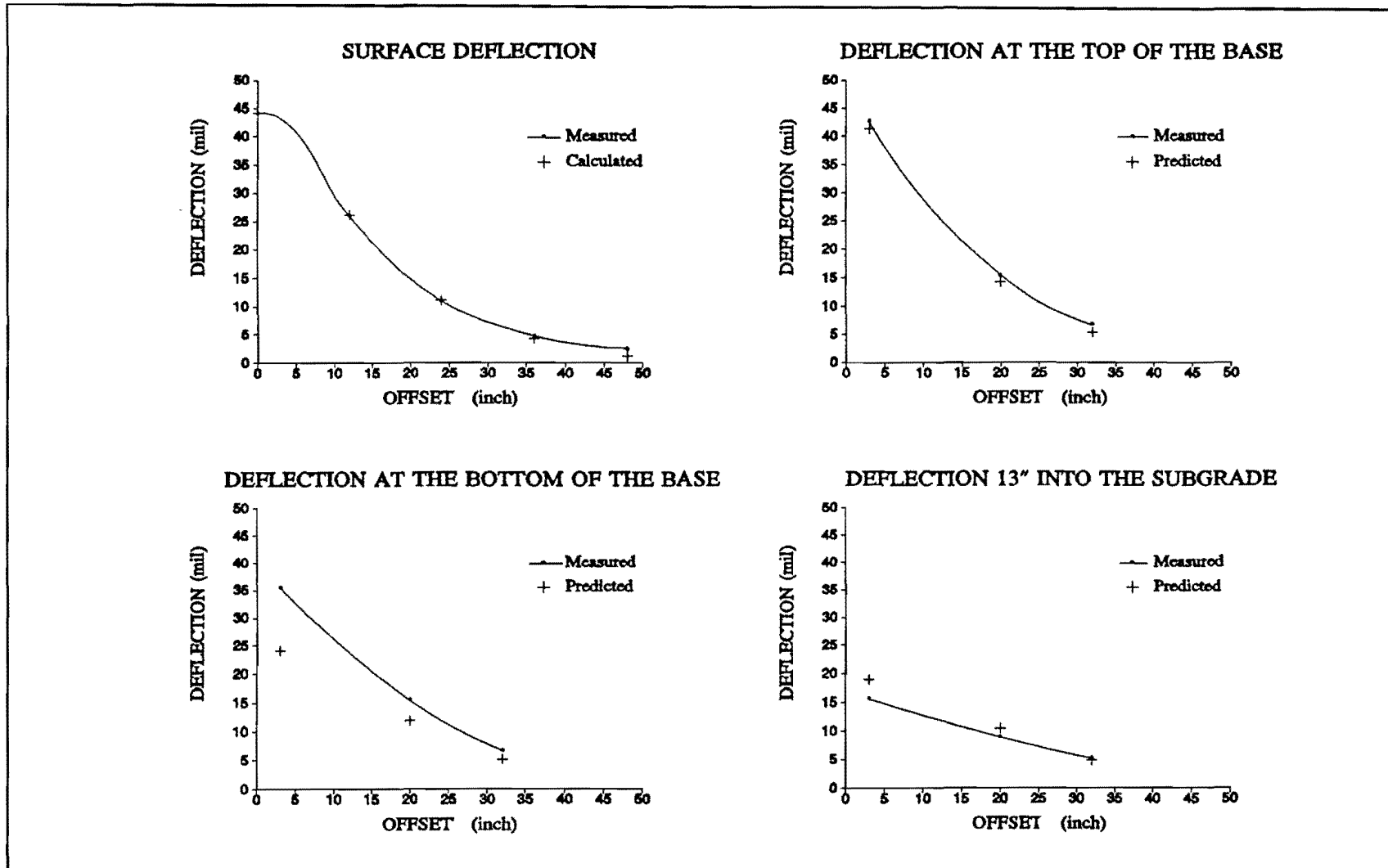


Figure 33. Measured and Predicted Deflections for Section B Based on a Pavement Model with an Apparent Rigid Layer at a Depth of 5.5 feet.

subgrade rapidly increasing in stiffness with depth. The fact that there were deflections measured at the anchor (72 inches deep) rejects the possibility of a shallow rigid layer and indicates a subgrade stiffening with depth. These indications led to the use of a third backcalculation model in which the first 24 inches of the subgrade was modeled as an independent layer. This led to a considerable improvement in the deflection matching as listed in Table 14. The average RMSE for the deflections within the pavement structure was reduced to 7.21 percent. Similar to the results from the second model, the base stiffness is still underpredicted while the deflections predicted at 13 inches into the subgrade are considerably better than before. The RMSE calculated for the deflections at this depth reduced from 14.8 percent to 6.96. percent

To further evaluate the deflections measured in section B, the surface deflections were also analyzed using a nonlinear backcalculation procedure as described elsewhere (Rohde, 1990). The pavement was modeled as a four layer system with the bottom boundary of the finite element mesh at a depth of 5.5 feet. The asphalt layer was assumed linear elastic while the base, and two layers in the subgrade were modeled as nonlinear elastic materials, using the universal model (equation 3.1). The material properties used in this analysis are listed in Table 15 and the results of the analysis in Table 16. As illustrated in Figure 35 the analysis led to a good match of the predicted and measured surface, and in-depth deflections. The average RMSE for the deflections within the pavement structure reduced to 5.36 percent. Figure 36 illustrates how the stiffness in the pavement structure changes horizontally as well as vertically. Although the stiffness in each layer changes with depth and distance from the load, they are remarkably close to those backcalculated using the four layer linear elastic model (Table 15). These moduli were:

Asphalt Concrete	:	141,200 psi
Granular Base	:	15,400 psi
24" Subgrade 1	:	3,900 psi
Subgrade 2	:	4,900 psi

Table 14. Results of the Deflection Analysis for Section B Using a Backcalculation Model with an Apparent Rigid Layer at a Depth of 5.5 feet and a Subgrade Divided into Two Layers.

Surface Deflections					
Offset r (inch)	0.00	12.00	24.00	36.00	48.00
Measured Deflection (mil)	44.14	26.15	11.15	4.80	2.57
Predicted Deflection (mil)	47.82	24.92	11.77	5.51	2.18
Error (percent)	8.33	-4.69	5.57	14.69	-15.27
Absolute Error (mil)	3.68	-1.23	0.62	0.71	-0.39
Backcalculated Moduli					
Asphalt Concrete (psi)	141,200				
Granular Base (psi)	15,400				
Top 24 " of Subgrade (psi)	3,900				
Subgrade (psi)	4,900				
MDD Deflections					
Offset from Load to MDD Hole	3.00	20.00	32.00		
LVDT at a Depth of 3.8 inches (Top of the Base)					
Measured Deflection (mil)	42.66	15.42	6.81		
Predicted Deflection (mil)	43.87	15.04	7.16		
Error (percent)	2.83	-2.45	5.10		
Absolute Error (mil)	1.21	-0.38	0.35		
LVDT at a Depth of 15.8 inches (Middle of the Base)					
Measured Deflection (mil)	35.53	15.76	6.91		
Predicted Deflection (mil)	27.86	13.92	6.94		
Error (percent)	-21.60	-11.66	0.39		
Absolute Error (mil)	-7.673	-1.84	0.03		
LVDT at a Depth of 28.5 inches (Bottom of the Base)					
Measured Deflection (mil)	15.65	8.96	5.16		
Predicted Deflection (mil)	14.42	9.50	5.52		
Error (percent)	-7.88	6.05	6.96		
Absolute Error (mil)	-1.23	0.54	0.36		

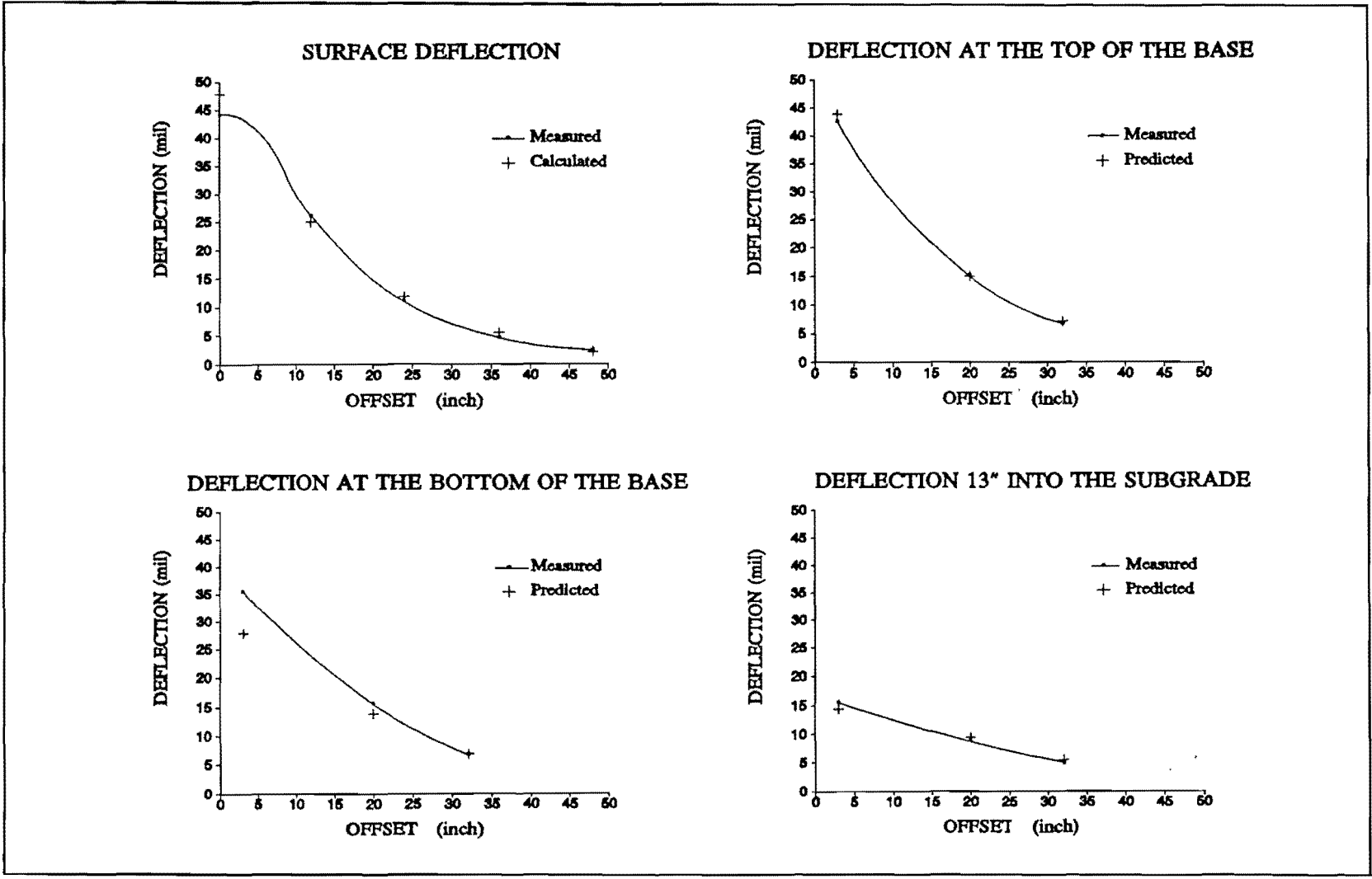


Figure 34. Measured and Predicted Deflections for Section B Based on a Pavement Model with a Rigid Layer at a Depth of 5.5 feet and a Subgrade Divided into Two Layers.

Table 15. Material Properties Used in the Finite Element Model for Section B.

Material Properties used to Model Section B				
Material Property	Asphalt	Base	Subgrade 1	Subgrade 2
Thickness (inch)	3.5	12.0	13.0	31.5
Poisson's Ratio	0.35	0.40	0.45	0.45
Density (pcf)	150	132	110	108
Stiffness Model	Linear*	Equation	Equation 2.5	Equation
K_1	12000	2.5	**	2.5
K_2	--	**	0.0	**
K_3	--	0.8	-0.3	0.0
Friction Angle (ϕ)	45	-0.3	20	-0.3
Cohesion (c)	1000	38	4.5	20
K_0	0.7	2	0.8	4.5
		0.8		0.8
<p>* The Stiffness of the Asphalt Surface Layer was determined through Iteration</p> <p>** Parameter varied in the database and determined through backcalculation</p>				

Table 16. Results of the Nonlinear Deflection Analysis for Section B.

Surface Deflections					
Offset r (inch)	0.00	12.00	24.00	36.00	48.00
Measured Deflection (mil)	44.14	26.15	11.15	4.80	2.57
Predicted Deflection (mil)	46.91	26.29	11.51	4.92	1.86
Error (percent)	6.28	0.52	3.25	2.47	-27.47
Absolute Error (mil)	2.77	0.75	0.36	0.12	-0.71
Backcalculated Moduli					
Asphalt Concrete (psi)	287,000				
Granular Base (psi)	$3474 p_a \left(\frac{\theta}{p_a}\right)^{0.8} \left(\frac{\tau_{oct}}{p_a}\right)^{-0.3}$				
Subgrade 1 (psi)	$54 p_a \left(\frac{\theta}{p_a}\right)^{0.45} \left(\frac{\tau_{oct}}{p_a}\right)^{-0.8}$				
Subgrade 2 (psi)	$54 p_a \left(\frac{\theta}{p_a}\right)^{0.45} \left(\frac{\tau_{oct}}{p_a}\right)^{-0.8}$				
MDD Deflections					
Offset from Load to MDD Hole	3.00	20.00	32.00		
LVDT at a Depth of 3.8 inches (Top of the Base)					
Measured Deflection (mil)	42.66	15.42	6.81		
Predicted Deflection (mil)	44.02	15.14	6.75		
Error (percent)	3.19	-1.82	-3.60		
Absolute Error (mil)	1.36	-0.28	-0.06		
LVDT at a Depth of 15.8 inches (Middle of the Base)					
Measured Deflection (mil)	35.53	15.76	6.91		
Predicted Deflection (mil)	31.37	15.56	6.75		
Error (percent)	-10.68	-1.26	-3.60		
Absolute Error (mil)	-4.16	-0.20	-0.06		
LVDT at a Depth of 28.5 inches (Bottom of the Base)					
Measured Deflection (mil)	15.65	8.96	5.16		
Predicted Deflection (mil)	13.42	9.30	5.48		
Error (percent)	-14.22	3.77	6.18		
Absolute Error (mil)	-2.23	0.34	0.32		

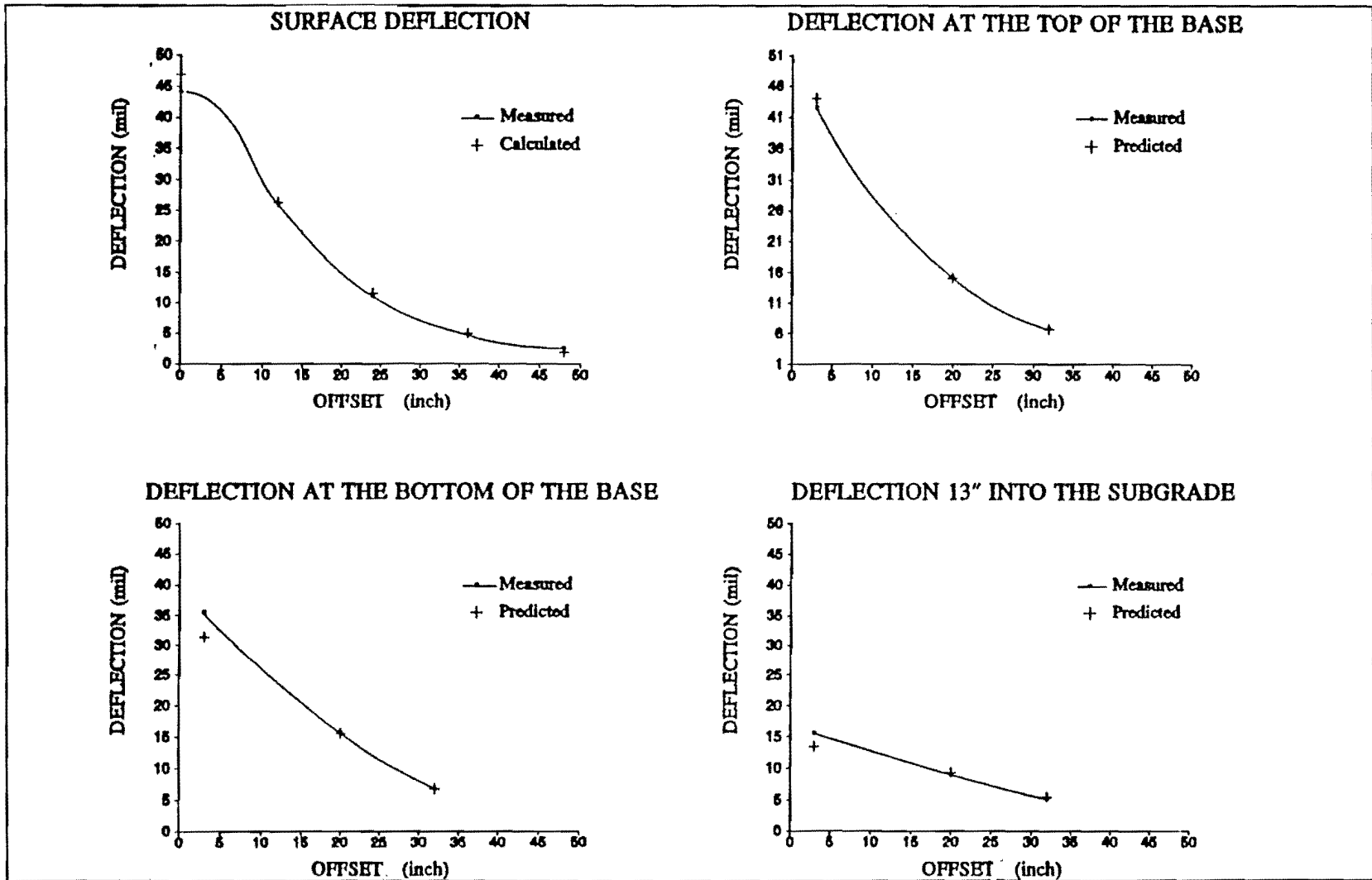


Figure 35. Measured and Predicted Deflections for Section B Based on a Nonlinear Elastic Pavement Model.

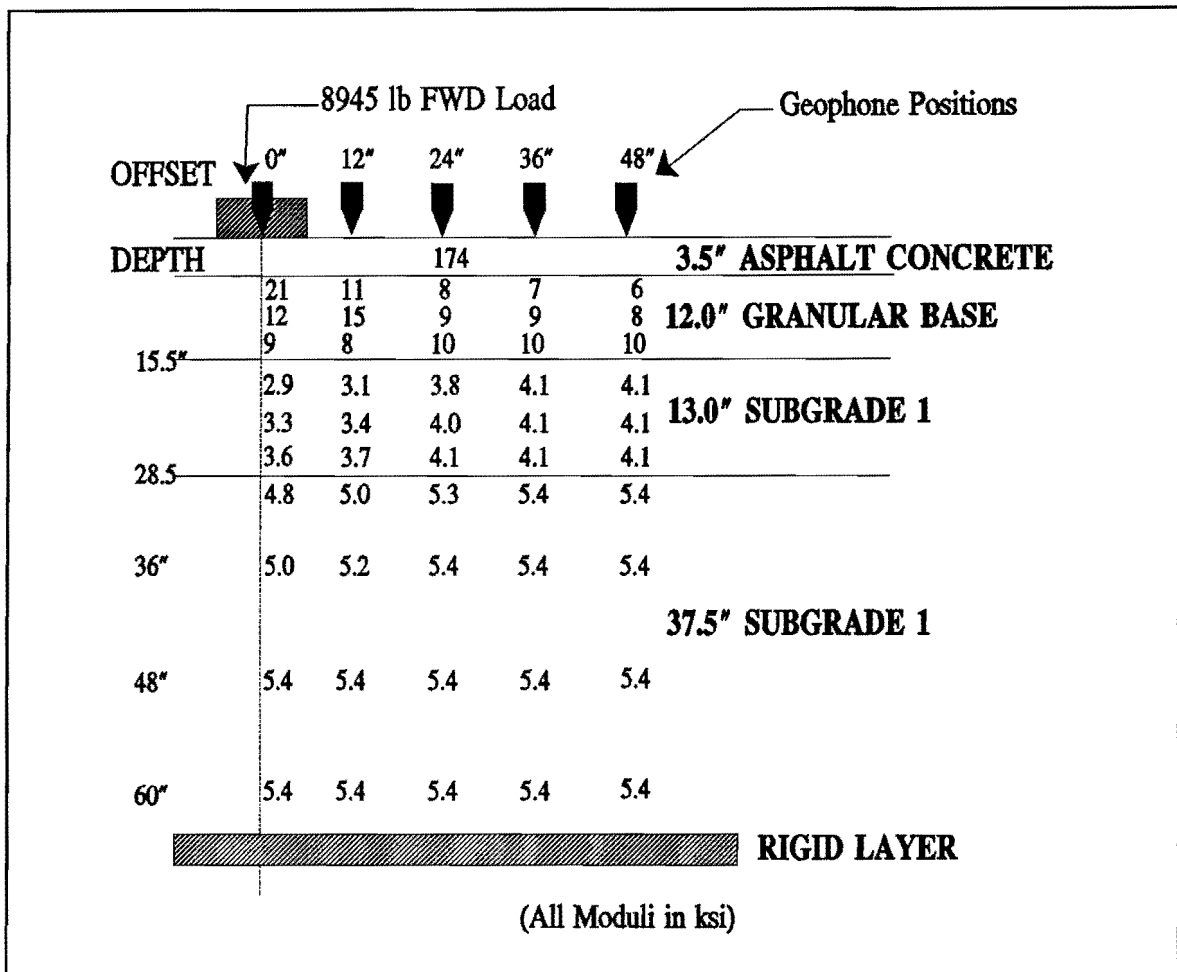


Figure 36. The Backcalculated Moduli for Section B Based on a Nonlinear Elastic Pavement Model.

The pavement structure of section B was best modeled by using a nonlinear elastic pavement model. However, this model is too tedious and time consuming for the general use of analyzing deflection data. From the linear elastic models, the three layer model with an apparent rigid layer at a depth of 5.5 feet led to results considerably better than that using a 20 feet deep rigid layer. The four layer model that treated the top 24 inches of the subgrade as a separate layer provided acceptable results. It is believed that whenever a rigid layer is predicted at a shallow depth, a divided subgrade can improve the deflection analysis. This additional layer can account for the rapid

increase in subgrade stiffness indicated by the shallow rigid layer estimate.

SUMMARY

In this chapter FWD deflection data collected on ten in-service pavement structures were analyzed using various backcalculation models. The results were compared and evaluated in terms of available laboratory data. Three backcalculation models were used in the comparison. The first two are existing methods of analyzing deflection data while the third model incorporates an apparent rigid layer to account for subgrade stiffness changes with depth.

The first backcalculation model, a three layer linear elastic system with an infinitely thick subgrade, led to poor results on the majority of pavement sections analyzed. The second backcalculation model, incorporating a rigid layer at a depth of 20 feet, resulted in favorable moduli only on the thick clay sections. The use of an apparent rigid layer, as proposed in this study, led to reasonable results on nearly all pavement sections.

As expected, the backcalculated moduli did not match the laboratory data. The laboratory tests are conducted on disturbed samples under simulated stress conditions. Although the backcalculated moduli can give an indication of the material stiffness under actual load conditions, the backcalculated moduli are model dependant. No perfect agreement between the laboratory data and backcalculation results should therefore be expected. It was found that the backcalculation model, incorporating an apparent rigid layer, led to subgrade moduli representative of the subgrade stiffness in the top 18 to 24 inches of the subgrade. The backcalculated subgrade stiffness for the other models was stiffer. The backcalculated stiffness for the asphalt concrete compared remarkably well with that found in the laboratory.

The deflections collected on the two instrumented pavement sections were also analyzed. The backcalculation results were evaluated by comparing measured in-depth deflections with those calculated using the backcalculated moduli and backcalculation model. On the first

section the use of an apparent rigid layer led to excellent structural characterization of the pavement system. Both on the surface and within the pavement structure, this model led to better deflection matching than the traditional model with a rigid layer at a 20 feet depth.

The second instrumented pavement structure was founded on a subgrade consisting of boulders in a clay matrix. Due to a rapid increase in stiffness with depth an apparent rigid layer was predicted at a shallow depth. Although the use of the apparent rigid layer improved the backcalculation results and led to more realistic moduli than traditional models, the in-depth deflections were poorly matched. By modeling the top 24 inches of the subgrade as an individual layer, the analysis was considerably improved. It was concluded that when a rigid layer is predicted at a shallow depth, the top part of the subgrade should be modeled as an individual layer.

CHAPTER V CONCLUSIONS AND RECOMMENDATIONS

Enhancements have been made to the MODULUS backcalculation system. These include a procedure to estimate the depth of a stiff layer and the optimum number of sensors to use in the backcalculation procedure. These changes are aimed at providing the user with better procedures for handling non-linear subgrades within the linear elastic framework. The analysis performed on the ten in-service sites and the two instrumented pavements demonstrated that MODULUS 4.0 predicts realistic layer moduli for a range of pavement types under widely varying environmental conditions. It is recommended that this system (MODULUS 4.0) be implemented in the State's pavement analysis and design systems.

Preliminary results from a finite element based backcalculation procedure showed that it can be used to more accurately match measured deflections within the pavement. The procedure is cumbersome and takes about 12 hours to run on a 386 type microcomputer. Although it is not recommended for implementation, research efforts should continue in developing a finite element based backcalculation system.

In the further development of MODULUS 4.0 system attention should be given to including it as the heart of an expert system. Often users do not have accurate base thickness data and frequently composite pavements are found where an old stiff layer (asphalt or concrete) is buried beneath the new base. An expert system would not only assist with the input to the system but also provide an analysis of the backcalculated layer moduli. If the moduli appear suspect or the bowl fitting produces large errors then the expert system could recommend changes to the pavement layer model.

REFERENCES

- AASHTO guide for design of pavement structures.* (1986). American Association of State Highway and Transportation Officials, Washington, D.C.
- Allen, J.S., and Thompson, M.R. (1984). "Significance of variable confined triaxial testing." *J. Transp. Engrg.*, ASCE, 100(4), 827-843.
- ASTM. *Annual book of ASTM standards.* (1987). American Society of Testing Materials, Philadelphia, PA, Vol. 04.03. Road and Paving Materials, D4694 & D4695.
- Barker, W.R., and Brabston, W.N. (1975). "Development of a structural design procedure for flexible airport pavements." *TR S-75-17*, US Army Engineering WES, Vicksburg, M.S.
- Bush, A.J. (1980). "Nondestructive testing for light aircraft pavements; phase II, development of the nondestructive evaluation methodology." Report FAA-RD-80-9-11, U.S. Department of Transportation, Washington, D.C.
- Irwin, L.H. (1983). *User's guide to MODCOMP2*, Version 2.1. Local Roads Program, Cornell University, Ithaca, N.Y.
- Izatt, J.O., Lettier, J.A., and Taylor, C.A. (1967). "The shell group methods for thickness design of asphalt pavements," paper presented at the annual meeting of the National Asphalt Paving Association, San Juan, Puerto Rico.
- Lytton, R.L., Germann, F., and Chou, Y.J. (1990). "Determination of asphaltic concrete pavement structural properties by nondestructive testing," *NCHRP Report 10-27-Phase II*, National Cooperative Highway Res. Program, Transp. Res. Board, Washington, D.C.
- McVay, M., and Taesiri, Y. (1985). "Cyclic behavior of pavement base materials," *J. of Geotechnical Engrg.*, ASCE, 3(1), 1-17.
- Raad, L., and Figueroa, J.L. (1980). "Load response of transportation support system," *J. of Transp. Engrg.*, ASCE, 106, 111-128.
- Roesset, J.M. (1990). "Development of dynamic analysis techniques for Falling Weight Deflectometer data." Summary report for project 2/3-18-88-1175 presented at the SDHPT area II research committee meeting, Victoria, TX.

REFERENCES (Continued)

- Rohde, G.T. (1990). *The mechanistic analysis of pavement deflections on subgrades varying in stiffness with depth*, Ph D. Dissertation, Texas A&M University, College Station, TX.
- Rohde, G.T., Yang, W., and Smith, R.E. (1990). "Inclusion of depth to a rigid layer in determining pavement layer properties," *Proc. Third Int. Conf. on Bearing Capacity of Roads and Airfields*, Trondheim, Norway, 475-486.
- Scullion, T., Uzan, J., Yazdani, J.I., and Chan, P. (1988). *Field evaluation of the multi-depth deflectometers. Res. Report 1123-2*. Texas Transp. Institute, College Station, TX.
- Thompson, M.R., and Robnett, Q.L. (1976). "Resilient response of subgrade soils." *Civil Engrg. Studies Series No. 160*, University of Illinois, Urbana-Champaign, I.L.
- Uddin, W., Meyer, A.H., and Hudson, W.R. (1986). "Rigid bottom considerations for nondestructive evaluation of pavements." *Transp. Res. Record 1070*, Transp. Res. Board, Washington, D.C., 21-29.
- Uzan, J. (1985). "Characterization of granular materials." *Transp. Res. Record 1022*, Transp. Res. Board, Washington, D.C., 52-59.
- Uzan, J., Scullion, T., Michalek, C.H., Parades, M., and Lytton, R.L. (1988). "A microcomputer based procedure to backcalculate layer moduli from FWD data," *Res. Report 2-18-87-1123-1*, Texas Transp. Institute, College Station, TX.
- Van Cauwelaert, F.J., Alexander, D.R., White, T.D., and Barker, W.R., "Multilayer elastic program for backcalculating layer moduli in pavement evaluation," STP 1026, NDT of Pavements and Backcalculation of Moduli, ASTM 1989.
- Witczak, M.W., and Uzan, J. (1988). *The universal airport pavement design system, report I of IV : granular material characterization*, Dept. of Civil Engrg., University of Maryland, College Park, M.D.
- Yazdani, J.I. (1989). *Using the multi-depth deflectometer to study pavement response*. MSc Thesis, Texas A&M University, College Station, TX.

APPENDIX A
SUBGRADE INFORMATION

Table A1. Subgrade Information for Site 1.

SUBGRADE INFORMATION FROM THE DRILLERS LOG			
Depth from Surface (feet)	Material Description	Moisture Content (%)	Density (pcf)
2.30 - 5.30	Sandy Subgrade	14.9	104.7
		14.9	108.0
5.30 - 8.30	Sandy Clay Subgrade	-	-
8.30 -12.00	Sandy Subgrade	-	-
SUBGRADE INFORMATION FROM SOIL SURVEY SERIES*			
Soil Name and Symbol Description	Nueces (Nu) Fine Sand (Top ±22 inches) Sandy Clay Loam (±22 - 76 inches)		
Unified Soil Classification	SP-SM, SM, SM-SC, SC		
AASHTO Soil Classification	A-2-4, A-3, A-2-6, A2-4		
* Map Sheet 11 of the <i>Soil Survey of Willacy County Texas</i> as published by the US Department of Agriculture's Soil Conservation Service (December 1982)			

Table A2. Subgrade Information for Site 2.

SUBGRADE INFORMATION FROM THE DRILLERS LOG			
Depth from Surface (feet)	Material Description	Moisture Content (%)	Density (pcf)
0.83 - 3.83	Sandy Subgrade	13.4	100.0
		13.2	103.2
3.83 - 6.83	Sandy Subgrade	-	-
6.83 -	Sandy Subgrade	-	-
SUBGRADE INFORMATION FROM SOIL SURVEY SERIES*			
Soil Name and Symbol Description	Latia (Le) Sandy Clay Loam (Top ±04 inches) Sandy Clay Loam (±04 - 60 inches)		
Unified Soil Classification	CL		
AASHTO Soil Classification	A-4, A-6, A-7-6		
* Map Sheet 14 of the <i>Soil Survey of Willacy County Texas</i> as published by the US Department of Agriculture's Soil Conservation Service (December 1982)			

Table A3. Subgrade Information for Site 4.

SUBGRADE INFORMATION FROM THE DRILLERS LOG			
Depth from Surface (feet)	Material Description	Moisture Content (%)	Density (pcf)
0.75 - 3.75	Clay Subgrade	24.5	88.4
		24.6	93.4
3.75 - 9.75	Clay Subgrade	-	-
9.75 - 15.0	Clay Subgrade	-	-
SUBGRADE INFORMATION FROM SOIL SURVEY SERIES*			
Soil Name and Symbol Description		Hildago (HoA) Sandy Clay Loam (Top ±42 inches) Clay Loam (±42 - 60 inches)	
Unified Soil Classification		SC, CL	
AASHTO Soil Classification		A-6, A-7-6	
* Map Sheet 23 of the <i>Soil Survey of Willacy County Texas</i> as published by the US Department of Agriculture's Soil Conservation Service (December 1982)			

Table A4. Subgrade Information for Site 5.

SUBGRADE INFORMATION FROM THE DRILLERS LOG			
Depth from Surface (feet)	Material Description	Moisture Content (%)	Density (pcf)
1.00 - 4.00	Sandy Clay Subgrade	16.3	101.0
		15.7	10.34
4.00 - 8.00	Sandy Clay Subgrade (more clayey)	-	-
SUBGRADE INFORMATION FROM SOIL SURVEY SERIES*			
Soil Name and Symbol Description		Racombes (48) Sandy Clay Loam (Top ±13 inches) Sandy Clay Loam (±13 - 49 inches) Sandy Clay Loam (±49 - 72 inches)	
Unified Soil Classification		CL, SC	
AASHTO Soil Classification		A-4, A-6, A-7	
* Map Sheet 78 of the <i>Soil Survey of Hidalgo County Texas</i> as published by the US Department of Agriculture's Soil Conservation Service (June 1981)			

Table A5. Subgrade Information for Site 6.

SUBGRADE INFORMATION FROM THE DRILLERS LOG			
Depth from Surface (feet)	Material Description	Moisture Content (%)	Density (pcf)
0.75 - 3.75	Clay Subgrade	16.4	92.8
		20.0	102.2
		20.5	102.5
3.75 - 11.75	Clay Subgrade	-	-
SUBGRADE INFORMATION FROM SOIL SURVEY SERIES*			
Soil Name and Symbol Description		Hidalgo (28) Sandy Clay Loam (Top ±28 inches) Clay Loam (±28 - 80 inches)	
Unified Soil Classification		SC, CL	
AASHTO Soil Classification		A-6, A-7-6	
* Map Sheet 68 of the <i>Soil Survey of Hidalgo County Texas</i> as published by the US Department of Agriculture's Soil Conservation Service (June 1981)			

Table A6. Subgrade Information for Site 7.

SUBGRADE INFORMATION FROM THE DRILLERS LOG			
Depth from Surface (feet)	Material Description	Moisture Content (%)	Density (pcf)
1.75 - 4.75	Clay Subgrade	9.7	130.9
		21.1	107.5
		21.8	100.8
4.75 - 6.75	Clay Subgrade	-	-
6.75 - 9.75	Sandy Clay Subgrade	-	-
SUBGRADE INFORMATION FROM SOIL SURVEY SERIES*			
Soil Name and Symbol Description		Leeray (21) Clay (Top ±43 inches) Clay, Silty Clay (±43 - 65 inches)	
Unified Soil Classification		CH, CL	
AASHTO Soil Classification		A-7-6, A-6	
* Map Sheet 7 of the <i>Soil Survey of Callahan County Texas</i> as published by the US Department of Agriculture's Soil Conservation Service (August 1981)			

Table A7. Subgrade Information for Site 8.

SUBGRADE INFORMATION FROM THE DRILLERS LOG			
Depth from Surface (feet)	Material Description	Moisture Content (%)	Density (pcf)
1.75 - 4.75	Clay Subgrade	17.8	118.9
		18.2	118.7
4.75 - 7.75	Clay Subgrade	-	-
7.75 - 12.5	Sandy Clay Subgrade	-	-
SUBGRADE INFORMATION FROM SOIL SURVEY SERIES*			
Soil Name and Symbol Description		Mangum (Ma) Silt Loam (Top ±09 inches) Silty Clay (±09 - 54 inches) Clay (±54 - 81 inches)	
Unified Soil Classification		CH, CL	
AASHTO Soil Classification		A-7-6, A-6, A-7	
* Map Sheet 10 of the <i>Soil Survey of Taylor County Texas</i> as published by the US Department of Agriculture's Soil Conservation Service (December 1976)			

Table A8. Subgrade Information for Site 9.

SUBGRADE INFORMATION FROM THE DRILLERS LOG			
Depth from Surface (feet)	Material Description	Moisture Content (%)	Density (pcf)
0.75 - 3.75	Clay Subgrade	7.7	133.2
		8.5	127.1
3.75 -10.75	Clay Subgrade	-	-
SUBGRADE INFORMATION FROM SOIL SURVEY SERIES*			
Soil Name and Symbol Description		Sagerton (SaA) Clay Loam (Top ±11 inches) Clay (±11 - 33 inches) Clay Loam (±33 - 80 inches)	
Unified Soil Classification		CL	
AASHTO Soil Classification		A-6, A-4, A-7	
* Map Sheet 25 of the <i>Soil Survey of Taylor County Texas</i> as published by the US Department of Agriculture's Soil Conservation Service (December 1976)			

Table A9. Subgrade Information for Site 11.

SUBGRADE INFORMATION FROM THE DRILLERS LOG			
Depth from Surface (feet)	Material Description	Moisture Content (%)	Density (pcf)
1.92 - 4.92	Sand Subgrade	20.4	94.5
4.92 - 6.5	Sand Subgrade	19.5	95.2
SUBGRADE INFORMATION FROM SOIL SURVEY SERIES*			
Soil Name and Symbol Description		Tivoli (Tf) Fine Sand (± 00 - 90 inches)	
Unified Soil Classification AASHTO Soil Classification		SP-SM A-3	
* Map Sheet 17 of the <i>Soil Survey of Mitchell County Texas</i> as published by the US Department of Agriculture's Soil Conservation Service (April 1969)			

Table A10. Subgrade Information for Site 12.

SUBGRADE INFORMATION FROM THE DRILLERS LOG			
Depth from Surface (feet)	Material Description	Moisture Content (%)	Density (pcf)
0.75 - 3.75	Sand Subgrade	15.7	90.7
3.75 - 6.75	Sand Subgrade	14.6	96.8
6.75 - 9.75	White Sandy Subgrade	-	-
9.75 - 12.0	White Sandy Subgrade	-	-
SUBGRADE INFORMATION FROM SOIL SURVEY SERIES*			
Soil Name and Symbol Description		Cobb (CmB) Fine Sandy Loam (Top ± 08 inches) Sandy Clay Loam (± 08 - 30 inches)	
Unified Soil Classification AASHTO Soil Classification		Sandstone (weakly cemented) SM, SC, C1 A-4, A-2, A-6	
* Map Sheet 25 of the <i>Soil Survey of Mitchell County Texas</i> as published by the US Department of Agriculture's Soil Conservation Service (April 1969)			

APPENDIX B
LABORATORY RESULTS

Table B1. The Laboratory Results for Site 1.

LABORATORY RESULTS FOR SITE 1

ASPHALT			BASE			SUBGRADE		
Freq (Hz)	Temp (°F)	M _R (ksi)	σ ₃ (psi)	σ _d (psi)	M _R (ksi)	σ ₃ (psi)	σ _d (psi)	M _R (ksi)
TOP			1	5.0	18.5	0	2.05	19.1
10	0	1770	5	5.0	46.1	3	2.21	42.2
10	32	1090	1	9.8	16.5	0	3.90	16.8
10	77	710	5	9.9	27.7	3	3.80	23.2
10	100	140	10	9.9	44.8	6	3.90	29.1
20	0	1890	15	9.7	64.6	0	7.80	12.3
20	32	1480	25	9.9	104.2	3	7.80	17.5
20	77	650	1	14.8	18.3	6	7.89	16.1
20	100	220	5	14.7	27.6	0	10.13	12.9
BOTTOM			10	14.6	38.3	3	10.07	15.4
10	0	1790	15	14.7	52.9	6	10.00	17.5
10	32	1210	25	14.5	64.4			
10	77	720	10	24.6	37.0			
10	100	240	15	25.2	46.8			
20	0	1990	25	25.5	67.0			
20	32	1890	15	39.3	52.6			
20	77	970	25	37.9	75.8			
20	100	*	25	48.8	78.4			

* Test not Successful

Table B2. The Laboratory Results for Site 2.

LABORATORY RESULTS FOR SITE 2								
ASPHALT			BASE			SUBGRADE		
Freq (Hz)	Temp (°F)	M _R (ksi)	σ ₃ (psi)	σ _d (psi)	M _R (ksi)	σ ₃ (psi)	σ _d (psi)	M _R (ksi)
TOP			1	9.8	14.8	0	1.86	5.3
10	0	2240	5	10.2	18.4	3	1.86	7.0
10	32	1370	10	10.3	28.8	6	1.71	9.3
10	77	670	20	10.2	41.4	0	3.74	4.5
10	100	250	30	10.8	47.4	3	3.74	5.8
20	0	2160	5	16.6	7.6	6	3.81	7.6
20	32	1510	10	20.7	23.6	3	7.56	3.3
20	77	710	20	21.0	36.7	6	7.96	6.0
20	100	280	30	21.0	44.0			
BOTTOM			20	36.5	32.5			
10	0		30	36.6	39.5			
10	32		20	46.7	36.5			
10	77		30	47.0	43.6			
10	100		20	62.6	34.9			
20	0		30	63.3	44.6			
20	32							
20	77							
20	100							

Table B3. The Laboratory Results for Site 4.

LABORATORY RESULTS FOR SITE 4								
ASPHALT			BASE			SUBGRADE		
Freq (Hz)	Temp (°F)	M _R (ksi)	σ ₃ (psi)	σ _d (psi)	M _R (ksi)	σ ₃ (psi)	σ _d (psi)	M _R (ksi)
TOP			1	4.9	13.4	0	1.95	11.4
10	0	2010	5	5.1	22.1	3	2.04	12.4
10	32	1170	10	4.9	31.4	6	1.98	12.4
10	77	510	15	5.1	35.1	0	3.86	6.7
10	100	70	20	5.1	39.3	3	3.92	7.3
20	0	1900	1	10.0	10.4	6	3.83	7.4
20	32	1330	5	10.0	15.6	0	7.79	3.3
20	77	460	10	10.0	21.1	3	7.86	3.5
20	100	90	15	19.9	27.1	6	7.63	4.5
BOTTOM			20	9.9	36.1	0	9.68	2.9
10	0	1580	1	14.7	9.2	3	9.74	3.6
10	32	990	5	14.7	14.5	6	9.90	2.1
10	77	330	10	14.8	19.2			
10	100	60	15	14.8	25.0			
20	0	1560	20	14.8	31.5			
20	32	1190	10	25.0	15.9			
20	77	400	15	24.8	17.9			
20	100	100	25	24.8	26.0			
			15	39.7	16.9			
			25	40.3	19.6			
			25	49.6	22.5			

Table B4. The Laboratory Results for Site 5.

LABORATORY RESULTS FOR SITE 5								
ASPHALT			BASE			SUBGRADE		
Freq (Hz)	Temp (°F)	M _R (ksi)	σ ₃ (psi)	σ _d (psi)	M _R (ksi)	σ ₃ (psi)	σ _d (psi)	M _R (ksi)
TOP			1	4.9	12.9	0	1.99	7.5
10	0	2040	5	4.8	69.9	3	2.06	8.6
10	32	960	1	9.6	8.7	6	1.96	9.6
10	77	320	5	9.6	23.3	0	3.73	5.7
10	100	60	10	9.8	54.0	3	3.86	7.1
20	0	2220	15	9.8	84.3	6	3.86	7.9
20	32	1490	1	14.9	8.3	0	7.60	3.7
20	77	360	5	14.6	13.9	3	7.63	4.4
20	100	90	10	14.7	26.1	6	7.82	5.0
BOTTOM			15	14.8	45.0	0	9.61	2.7
10	0		25	14.9	77.6	3	9.84	3.2
10	32		10	24.4	19.2	6	9.97	4.2
10	77		15	24.6	26.9			
10	100		25	24.6	41.4			
20	0		15	39.2	21.6			
20	32		25	39.2	30.3			
20	77		25	47.8	28.4			
20	100							

Table B5. The Laboratory Results for Site 6.

LABORATORY RESULTS FOR SITE 6								
ASPHALT			BASE			SUBGRADE		
Freq (Hz)	Temp (°F)	M _R (ksi)	σ_3 (psi)	σ_d (psi)	M _R (ksi)	σ_3 (psi)	σ_d (psi)	M _R (ksi)
TOP			1	10.2	13.8	0	2.14	21.2
10	0		5	10.1	20.3	3	2.11	22.7
10	32		10	10.3	22.0	6	2.07	28.3
10	77		20	10.7	32.6	0	3.89	9.9
10	100		30	10.8	40.4	3	3.83	10.7
20	0		5	20.2	14.6	6	4.09	12.3
20	32		10	21.0	20.8	0	7.82	2.7
20	77		20	21.4	29.5	3	8.05	5.4
20	100		30	21.5	36.7	6	8.44	6.3
BOTTOM			10	35.6	17.9	0	9.83	2.5
10	0		20	36.8	27.8	3	9.90	3.3
10	32		30	37.1	39.0	6	9.77	4.6
10	77		20	47.3	32.6			
10	100		30	47.9	42.7			
20	0		30	63.9	42.0			
20	32							
20	77							
20	100							

Table B6. The Laboratory Results for Site 7.

LABORATORY RESULTS FOR SITE 7								
ASPHALT			BASE			SUBGRADE		
Freq (Hz)	Temp (°F)	M _R (ksi)	σ ₃ (psi)	σ _d (psi)	M _R (ksi)	σ ₃ (psi)	σ _d (psi)	M _R (ksi)
TOP			1	5.2	45.1	0	2.1	5.3
10	0	1710	5	5.3	91.6	3	2.0	6.3
10	32	1260	1	10.0	23.3	6	1.9	7.0
10	77	870	5	10.1	24.9	0	4.1	5.2
10	100	150	10	10.0	100.4	3	4.0	5.7
20	0	1970	1	15.0	21.7	6	3.9	5.8
20	32	1430	5	15.0	25.5	0	8.2	4.0
20	77	810	10	14.9	111.4	3	8.2	4.5
20	100	200	10	24.9	44.4	6	8.5	4.8
BOTTOM			15	24.7	84.2	0	10.3	3.5
10	0	1700	25	24.7	163.7	3	10.4	4.0
10	32	1030	15	39.6	51.9	6	10.3	4.2
10	77	600	25	40.0	154.0			
10	100	160	25	48.8	79.0			
20	0	1860						
20	32	-*						
20	77	600						
20	100	210						

* Test not Successful

Table B7. The Laboratory Results for Site 8.

LABORATORY RESULTS FOR SITE 8								
ASPHALT			BASE			SUBGRADE		
Freq (Hz)	Temp (°F)	M _R (ksi)	σ ₃ (psi)	σ _d (psi)	M _R (ksi)	σ ₃ (psi)	σ _d (psi)	M _R (ksi)
TOP						0	1.9	13.9
10	0	1850				3	1.9	14.9
10	32	1220				6	1.9	19.3
10	77	610				0	3.9	9.9
10	100	200				3	4.0	11.0
20	0	2000				6	4.0	11.8
20	32	1580				0	6.4	4.7
20	77	650				3	6.3	5.5
20	100	220				6	6.3	6.1
BOTTOM						0	9.6	4.4
10	0	2010				3	9.4	5.7
10	32	1150				6	9.6	7.5
10	77	390						
10	100	120						
20	0	2330						
20	32	1510						
20	77	590						
20	100	150						

Table B8. The Laboratory Results for Site 9.

LABORATORY RESULTS FOR SITE 9								
ASPHALT			BASE			SUBGRADE		
Freq (Hz)	Temp (°F)	M _R (ksi)	σ ₃ (psi)	σ _d (psi)	M _R (ksi)	σ ₃ (psi)	σ _d (psi)	M _R (ksi)
TOP						0	1.9	25.5
10	0	1340				3	2.0	22.4
10	32	600				6	2.1	23.1
10	77	270				0	3.9	11.7
10	100	80				3	3.9	13.0
20	0	1780				6	3.9	13.9
20	32	1150				0	6.1	5.1
20	77	280				3	6.2	6.1
20	100	90				6	6.2	6.7
BOTTOM						0	9.7	5.3
10	0					3	9.7	6.7
10	32					6	9.7	7.8
10	77							
10	100							
20	0							
20	32							
20	77							
20	100							

Table B9. The Laboratory Results for Site 11.

LABORATORY RESULTS FOR SITE 11								
ASPHALT			BASE			SUBGRADE		
Freq (Hz)	Temp (°F)	M _R (ksi)	σ ₃ (psi)	σ _d (psi)	M _R (ksi)	σ ₃ (psi)	σ _d (psi)	M _R (ksi)
TOP			1	9.9	15.6			
10	0	1760	5	10.0	19.8			
10	32	890	1	14.9	13.0			
10	77	380	5	14.9	14.0			
10	100	220	10	14.8	17.6			
20	0	1750	15	14.9	21.5			
20	32	1020	25	14.9	74.2			
20	77	560	10	24.8	12.7			
20	100	260	15	24.8	14.7			
BOTTOM			25	24.7	31.2			
10	0	2220	15	39.8	19.9			
10	32	1260	25	39.5	22.8			
10	77	700	25	48.4	22.8			
10	100	430						
20	0	2110						
20	32	1770						
20	77	960						
20	100	510						

Table B10. The Laboratory Results for Site 12.

LABORATORY RESULTS FOR SITE 12								
ASPHALT			BASE			SUBGRADE		
Freq (Hz)	Temp (°F)	M _R (ksi)	σ ₃ (psi)	σ _d (psi)	M _R (ksi)	σ ₃ (psi)	σ _d (psi)	M _R (ksi)
TOP			1	9.8	24.7	1	2.1	35.9
10	0	2030	5	9.8	27.4	1	5.3	22.9
10	32	1140	5	18.5	17.4	1	8.1	19.3
10	77	580	10	10.3	48.7	1	11.6	16.3
10	100	190	10	21.1	31.7	4	5.2	29.7
20	0	2010	20	21.1	45.6	4	8.2	25.4
20	32	1330	20	35.5	51.7	4	11.8	21.9
20	77	560				8	5.2	46.3
20	100	210				8	8.2	31.0
BOTTOM						8	11.8	26.8
10	0							
10	32							
10	77							
10	100							
20	0							
20	32							
20	77							
20	100							

APPENDIX C
MONTHLY DEFLECTION DATA

Table C1. Average Normalized Monthly Deflection Data for Site 1.

TTI MODULUS ANALYSIS SYSTEM SUMMARY REPORT

District: 21 County: Willacy Highway/Road: US 77 Site 1		Thickness(in)							MODULI RANGE (psi)				
		Pavement: 6.50							Minimum	Maximum			
		Base: 6.00							50,000	1,500,000			
		Subbase: 0.00							5,000	100,000			
		Subgrade: 73.20							0	0			
									15,000				
Date	Load (lbs)	Measured Deflection (mils):							Calculated Moduli Values (psi):				ERROR/SENSOR %
		R1	R2	R3	R4	R5	R6	R7	SURFACE	BASE	SUBBASE	SUBGRADE	
		0	12"	24"	36"	48"	60"	72"	(E1)	(E2)	(E3)	(E4)	
JAN AM	9,000	9.90	7.89	5.44	3.54	2.41	1.73	1.32	1243,000	18,600	0	12,400	5.30
FEB AM	9,000	11.96	8.75	5.67	3.63	2.44	1.72	1.33	549,000	62,000	0	10,100	0.90
MAR AM	9,000	14.86	10.23	6.04	3.57	2.40	1.75	1.35	366,000	56,600	0	10,300	0.90
APR AM	9,000	14.52	10.39	6.51	3.84	2.53	1.78	1.36	433,000	59,700	0	9,500	0.10
MAY AM	9,000	16.84	11.50	6.39	3.53	2.32	1.71	1.36	372,000	25,900	0	10,400	0.90
JUN AM	9,000	15.86	10.80	5.39	3.19	2.28	1.52	1.01	355,000	26,300	0	11,900	4.10
JUL AM	9,000	17.74	11.60	6.23	3.45	2.23	1.68	1.34	277,000	32,400	0	10,500	1.40
AUG AM	9,000	15.61	10.84	6.04	3.43	2.09	1.68	1.32	414,000	29,300	0	10,800	1.40
OCT AM	9,000	16.27	11.66	6.78	3.80	2.43	1.76	1.35	487,000	21,200	0	9,800	0.60
NOV AM	9,000	13.92	9.97	6.08	3.61	2.39	1.74	1.35	492,000	50,900	0	10,200	0.70
DEC AM	9,000	12.66	9.40	5.88	3.58	2.41	1.76	1.39	659,000	50,000	0	10,300	0.60

Table C2. Average Normalized Monthly Deflection Data for Site 2.

TTI MODULUS ANALYSIS SYSTEM SUMMARY REPORT

District: 21 County: Willacy Highway/Road: FM 186 Site: 2		Thickness(in)							MODULI RANGE (psi)				
		Pavement: 1.00							Minimum	Maximum			
		Base: 8.80							499,950	500,050			
		Subbase: 0.00							5,000	100,000			
		Subgrade: 228.00							0	0			
									15,000				
Date	Load (lbs)	Measured Deflection (mils):							Calculated Moduli Values (psi):				ERROR/SENSOR %
		R1	R2	R3	R4	R5	R6	R7	SURFACE	BASE	SUBBASE	SUBGRADE	
		0	12"	24"	36"	48"	60"	72"	(E1)	(E2)	(E3)	(E4)	
JAN AM	9,000	42.25	21.30	10.13	5.99	4.15	3.22	2.51	500,000	29,400	0	8,500	5.40
FEB AM	9,000	44.35	21.01	10.32	6.20	4.32	3.33	2.61	500,000	27,200	0	8,500	3.40
MAR AM	9,000	47.43	23.22	11.64	7.03	4.95	3.68	2.98	500,000	26,500	0	7,500	3.30
APR AM	9,000	41.90	21.69	11.25	6.81	4.74	3.55	2.80	500,000	32,700	0	7,700	3.20
MAY AM	9,000	47.30	23.20	11.92	7.20	5.00	3.75	2.96	500,000	27,100	0	7,400	2.60
JUN AM	9,000	42.90	21.70	11.13	7.17	4.99	3.67	2.85	500,000	31,600	0	7,700	2.20
JUL AM	9,000	47.37	21.42	10.93	6.61	4.69	3.51	2.76	500,000	25,000	0	8,200	1.50
AUG AM	9,000	52.40	20.24	10.41	6.35	4.52	3.39	2.70	500,000	19,700	0	8,800	1.40
OCT AM	9,000	45.84	22.41	10.72	6.24	4.37	3.29	2.56	500,000	26,200	0	8,100	5.10
NOV AM	9,000	40.96	20.33	10.59	6.49	4.61	3.46	2.77	500,000	32,400	0	8,300	2.20
DEC AM	9,000	40.84	20.54	10.70	6.54	4.60	3.47	2.76	500,000	32,900	0	8,200	2.40

Table C3. Average Normalized Monthly Deflection Data for Site 4.

TTI MODULUS ANALYSIS SYSTEM SUMMARY REPORT

District: 21										MODULI RANGE (psi)			
County: Willacy										Minimum	Maximum		
Highway/Road: FM 1425										50,000	1,500,000		
Site 4										5,000	100,000		
E										0	0		
										15,000			
Date	Load (lbs)	Measured Deflection (mils):							Calculated Moduli Values (psi):				ERROR/SENSOR %
		R1 0	R2 12"	R3 24"	R4 36"	R5 48"	R6 60"	R7 72"	SURFACE (E1)	BASE (E2)	SUBBASE (E3)	SUBGRADE (E4)	
NOV AM	9,000	57.44	35.43	17.96	9.92	6.52	4.70	3.65	423,000	48,100	0	5,300	0.30
DEC PM	9,000	49.37	31.19	16.32	8.99	5.87	4.32	3.49	292,000	36,800	0	5,500	0.60
JAN AM	9,000	34.70	24.84	15.04	9.01	6.02	4.31	3.36	142,000	13,100	0	4,200	0.60
FEB AM	9,000	38.37	25.82	14.60	8.52	5.67	4.12	3.34	167,000	14,600	0	4,700	0.60
MAR AM	9,000	64.18	38.58	19.21	10.51	6.69	4.80	3.80	131,000	13,300	0	4,500	3.00
APR AM	9,000	57.15	34.54	17.33	9.49	6.16	4.46	3.53	110,000	20,800	0	4,300	1.10
MAY AM	9,000	63.09	37.08	17.88	9.93	6.46	4.63	3.64	59,000	18,200	0	4,700	1.80
JUN AM	9,000	60.76	36.52	18.02	11.05	7.06	4.84	3.71	52,000	29,500	0	5,200	0.80
JUL AM	9,000	66.73	35.18	16.81	9.33	6.18	4.49	3.51	129,000	22,400	0	5,200	0.80
AUG AM	9,000	57.18	30.46	15.20	8.74	5.94	4.33	3.43	175,000	14,900	0	4,500	0.70
OCT AM	9,000	51.81	30.46	15.42	8.63	5.70	4.15	3.25	229,000	17,500	0	5,000	0.10

Table C4. Average Normalized Monthly Deflection Data for Site 5.

TTI MODULUS ANALYSIS SYSTEM SUMMARY REPORT

District: 21										MODULI RANGE (psi)			
County: Willacy										Minimum	Maximum		
Highway/Road: FM 1425										50,000	1,500,000		
Site 5										5,000	100,000		
										0	0		
										15,000			
Date	Load (lbs)	Measured Deflection (mils):							Calculated Moduli Values (psi):				ERROR/SENSOR %
		R1 0	R2 12"	R3 24"	R4 36"	R5 48"	R6 60"	R7 72"	SURFACE (E1)	BASE (E2)	SUBBASE (E3)	SUBGRADE (E4)	
JAN AM	9,000	11.56	9.57	7.13	5.10	3.77	2.86	2.25	1,036,000	47,100	0	10,400	8.60
FEB AM	9,000	15.85	12.57	8.81	5.97	4.24	3.15	2.51	836,000	57,200	0	8,400	1.40
MAR AM	9,000	24.91	17.36	10.28	6.36	4.51	3.44	2.78	234,000	37,000	0	7,700	3.30
APR AM	9,000	22.03	15.82	9.77	6.18	4.35	3.30	2.62	294,000	46,800	0	8,000	2.70
MAY AM	9,000	24.46	15.80	8.96	5.70	4.15	3.22	2.62	140,000	57,100	0	8,600	4.50
JUN AM	9,000	25.27	15.89	8.51	5.88	4.36	3.22	2.49	111,000	64,600	0	8,600	6.20
JUL AM	9,000	23.92	14.17	7.75	5.14	3.87	3.07	2.48	97,000	72,800	0	9,700	5.90
AUG AM	9,000	24.14	14.65	7.95	5.13	3.88	3.05	2.45	108,000	62,900	0	9,600	5.10
OCT AM	9,000	18.88	13.27	8.17	5.25	3.78	2.93	2.35	275,000	71,500	0	9,400	3.20
NOV AM	9,000	21.56	15.19	9.08	5.72	4.09	3.17	2.56	341,000	28,400	0	9,000	0.90
DEC AM	9,000	19.67	14.34	9.04	5.80	4.12	3.16	2.50	417,000	37,500	0	8,800	0.50

Table C5. Average Normalized Monthly Deflection Data for Site 6.

TTI MODULUS ANALYSIS SYSTEM SUMMARY REPORT

District: 21 County: Hidalgo Highway/Road: FM 491 Site 6										Thickness(in)				MODULI RANGE (psi)	
										Pavement:	1.20	Minimum	499,950	Maximum	500,050
										Base:	7.80	5,000	100,000		
										Subbase:	0.00	0	0		
										Subgrade:	282.00	15,000			
Date	Load (lbs)	Measured Deflection (mils):							Calculated Moduli Values (psi):				ERROR/SENSOR %		
		R1 0	R2 12"	R3 24"	R4 36"	R5 48"	R6 60"	R7 72"	SURFACE (E1)	BASE (E2)	SUBBASE (E3)	SUBGRADE (E4)			
JAN AM	9,000	48.31	21.22	10.42	6.75	4.81	3.58	2.76	500,000	23,200	0	8,700	1.70		
FEB PM	9,000	47.33	21.09	10.81	6.83	4.73	3.48	2.69	500,000	24,700	0	8,500	0.80		
MAR AM	9,000	53.60	22.85	12.54	7.99	5.39	3.85	2.84	500,000	21,800	0	7,600	3.10		
APR PM	9,000	55.58	23.11	12.04	7.74	5.29	3.79	2.88	500,000	19,500	0	7,800	2.30		
MAY AM	9,000	51.06	23.42	12.37	7.81	5.38	3.88	2.87	500,000	24,100	0	7,500	0.90		
JUN AM	9,000	44.04	23.02	12.38	8.34	5.69	3.95	3.15	500,000	35,100	0	7,200	2.30		
JUL AM	9,000	52.58	23.35	12.72	8.08	5.40	3.67	2.92	500,000	23,300	0	7,400	2.00		
AUG AM	9,000	54.42	21.01	11.14	7.28	5.16	3.65	2.74	500,000	19,100	0	8,400	5.00		
OCT AM	9,000	51.15	24.57	13.70	8.68	5.93	4.29	3.18	500,000	27,000	0	6,800	1.43		
NOV AM	9,000	56.16	24.53	13.53	8.62	5.92	4.18	3.11	500,000	21,300	0	7,000	2.90		
DEC AM	9,000	50.92	22.29	12.42	7.97	5.54	4.01	2.99	500,000	24,100	0	7,600	3.20		

Table C6. Average Normalized Monthly Deflection Data for Site 7.

TTI MODULUS ANALYSIS SYSTEM SUMMARY REPORT

District: 8 County: Callahan Highway/Road: IH 20 Site: 7										Thickness(in)				MODULI RANGE (psi)	
										Pavement:	10.20	Minimum	50,000	Maximum	1,500,000
										Base:	11.00	5,000	100,000		
										Subbase:	0.00	0	0		
										Subgrade:	109.20	15,000			
Date	Load (lbs)	Measured Deflection (mils):							Calculated Moduli Values (psi):				ERROR/SENSOR %		
		R1 0	R2 12"	R3 24"	R4 36"	R5 48"	R6 60"	R7 72"	SURFACE (E1)	BASE (E2)	SUBBASE (E3)	SUBGRADE (E4)			
FEB AM	9,000	4.54	4.11	3.36	2.71	2.13	1.66	1.29	1,500,000	15,400	0	19,300	13.60		
MAR AM	9,000	5.01	4.41	3.56	2.81	2.14	1.64	1.28	1,500,000	23,400	0	16,000	7.60		
APR AM	9,000	5.95	4.99	3.87	2.95	2.18	1.60	1.25	1,387,000	28,100	0	13,900	1.20		
MAY AM	9,000	5.53	4.77	3.72	2.87	2.12	1.59	1.26	1,500,000	9,000	0	17,800	5.30		
JUN AM	9,000	6.91	5.44	4.05	3.03	2.22	1.65	1.28	681,000	79,100	0	12,400	1.20		
JUL AM	9,000	7.47	5.73	4.30	3.04	2.24	1.61	1.23	596,000	65,000	0	12,700	1.10		
AUG AM	9,000	12.08	9.53	6.34	4.72	3.21	2.32	1.80	367,000	28,300	0	9,000	2.70		
SEP PM	9,000	9.71	7.02	4.91	3.33	2.37	1.68	1.24	358,000	48,900	0	12,300	1.70		
OCT AM	9,000	6.02	4.99	3.84	2.88	2.18	1.64	1.25	1,500,000	9,700	0	18,200	7.20		
NOV AM	9,000	4.69	4.18	3.42	2.72	2.09	1.63	1.27	1,500,000	23,800	0	17,100	10.20		
DEC AM	9,000	4.88	4.32	3.55	2.83	2.16	1.69	1.31	1,500,000	9,700	0	18,800	11.50		

Table C7. Average Normalized Monthly Deflection Data for Site 8.

TTI MODULUS ANALYSIS SYSTEM SUMMARY REPORT

District: 8										MODULI RANGE (psi)			
County: Taylor										Minimum	Maximum		
Highway/Road: IH 20										Pavement: 8.00	50,000	1,500,050	
Site: 8										Base: 13.00	5,000	100,000	
										Subbase: 0.00	0	0	
										Subgrade: 175.20	15,000		
Date	Load (lbs)	Measured Deflection (mils):							Calculated SURFACE (E1)	Moduli Values (psi):			ERROR/SENSOR %
		R1 0	R2 12"	R3 24"	R4 36"	R5 48"	R6 60"	R7 72"		BASE (E2)	SUBBASE (E3)	SUBGRADE (E4)	
FEB AM	9,000	5.56	4.61	3.40	2.55	1.89	1.46	1.19	1,500,000	73,600	0	19,300	0.90
MAR AM	9,000	6.05	4.92	3.51	2.58	1.91	1.48	1.23	500,000	34,100	0	21,500	2.60
APR AM	9,000	7.39	5.60	3.66	2.57	1.87	1.42	1.19	752,000	49,400	0	20,200	2.00
MAY AM	9,000	7.23	5.42	3.73	2.65	1.94	1.50	1.26	748,000	62,300	0	19,100	1.00
JUN AM	9,000	8.18	5.65	3.66	2.56	1.91	1.49	1.25	448,000	68,000	0	19,700	2.00
JUL AM	9,000	9.64	6.21	3.91	2.58	1.91	1.52	1.25	317,000	55,100	0	19,700	2.00
AUG PM	9,000	18.70	11.00	5.86	4.14	2.88	2.31	1.71	125,000	26,900	0	13,100	3.80
SEP PM	9,000	11.68	7.34	4.33	2.84	2.09	1.62	1.33	243,000	41,700	0	18,200	2.80
OCT AM	9,000	7.16	5.44	3.75	2.61	1.93	1.50	1.23	1,500,000	11,000	0	27,600	6.20
NOV AM	9,000	5.60	4.60	3.38	2.52	1.87	1.46	1.19	1,500,000	22,700	0	26,400	8.10
DEC AM	9,000	5.77	4.73	3.48	2.55	1.87	1.46	1.19	1,500,000	22,100	0	25,500	6.90

Table C8. Average Normalized Monthly Deflection Data for Site 9.

TTI MODULUS ANALYSIS SYSTEM SUMMARY REPORT

District: 8										MODULI RANGE (psi)			
County: Taylor										Minimum	Maximum		
Highway/Road: FM 1235										Pavement: 1.00	499,950	500,050	
Site: 9										Base: 8.00	5,000	100,000	
										Subbase: 0.00	0	0	
										Subgrade: 193.20	15,000		
Date	Load (lbs)	Measured Deflection (mils):							Calculated SURFACE (E1)	Moduli Values (psi):			ERROR/SENSOR %
		R1 0	R2 12"	R3 24"	R4 36"	R5 48"	R6 60"	R7 72"		BASE (E2)	SUBBASE (E3)	SUBGRADE (E4)	
FEB AM	9,000	25.02	12.67	6.55	4.21	2.85	2.05	1.62	500,000	62,400	0	12,900	2.10
MAR AM	9,000	29.16	13.70	7.01	4.58	3.05	2.21	1.75	500,000	48,500	0	12,100	2.40
APR AM	9,000	28.37	13.19	6.87	4.44	2.94	2.09	1.63	500,000	49,900	0	12,500	2.40
MAY AM	9,000	29.83	13.72	7.15	4.67	3.07	2.19	1.76	500,000	46,900	0	12,000	2.70
JUN AM	9,000	28.91	13.01	7.05	4.61	3.09	2.19	1.70	500,000	48,800	0	12,400	2.30
JUL AM	9,000	34.26	13.72	7.75	4.73	3.17	2.18	1.70	500,000	36,300	0	11,900	4.80
AUG AM	9,000	48.56	21.32	10.38	6.84	4.37	2.90	2.36	500,000	25,200	0	8,100	2.70
SEP PM	9,000	35.07	14.04	7.77	4.76	3.18	2.23	1.69	500,000	35,500	0	11,600	4.80
OCT AM	9,000	29.46	14.30	7.41	4.65	3.13	2.24	1.73	500,000	61,400	0	11,600	1.70
NOV AM	9,000	26.63	13.92	7.37	4.64	3.04	2.21	1.73	500,000	61,600	0	11,500	1.50
DEC AM	9,000	24.44	12.64	6.64	4.27	2.87	2.10	1.63	500,000	66,800	0	12,700	2.00

Table C9. Average Normalized Monthly Deflection Data for Site 11.

TTI MODULUS ANALYSIS SYSTEM SUMMARY REPORT

District: 8										MODULI RANGE (psi)			
County: Mitchell										Minimum		Maximum	
Highway/Road: IH 20										50,000		1,500,050	
Site: 11										5,000		100,000	
										0		0	
										15,000			
Station	Load (lbs)	Measured Deflection (mils):							Calculated Moduli Values (psi):				ERROR/SENSOR %
		R1	R2	R3	R4	R5	R6	R7	SURFACE (E1)	BASE (E2)	SUBBASE (E3)	SUBGRADE (E4)	
FEB AM	9,000	10.66	7.07	4.24	2.82	1.98	1.50	1.23	707,000	48,200	0	15,400	1.00
MAR AM	9,000	10.25	6.97	4.20	2.89	2.09	1.64	1.32	754,000	53,100	0	14,800	1.70
APR AM	9,000	10.56	6.90	4.10	2.83	2.07	1.59	1.31	597,000	55,500	0	15,000	2.00
MAY AM	9,000	10.70	6.67	3.86	2.66	1.95	1.50	1.26	480,000	57,400	0	16,100	2.20
JUN AM	9,000	11.89	6.50	3.74	2.63	1.97	1.54	1.27	240,000	64,100	0	16,300	2.80
JUL AM	9,000	12.28	6.17	3.64	2.55	1.92	1.55	1.21	133,000	85,800	0	15,400	8.40
AUG AM	9,000	14.85	8.80	4.66	3.58	2.57	2.07	1.52	214,000	54,100	0	11,500	7.50
SEP AM	9,000	11.78	6.90	3.94	2.65	1.99	1.60	1.27	280,000	66,400	0	14,600	8.00
OCT AM	9,000	10.95	6.71	3.88	2.62	1.96	1.54	1.22	644,000	58,200	0	15,200	1.90
NOV AM	9,000	9.53	6.73	4.06	2.81	2.00	1.57	1.27	980,000	52,500	0	15,400	1.70
DEC AM	9,000	8.08	5.65	3.75	2.67	1.93	1.50	1.19	1,026,000	79,100	0	15,300	0.20

Table C10. Average Normalized Monthly Deflection Data for Site 12.

TTI MODULUS ANALYSIS SYSTEM SUMMARY REPORT

District: 8										MODULI RANGE (psi)			
County: Mitchell										Minimum		Maximum	
Highway/Road: FM 1983										499,950		500,050	
Site: 12										5,000		100,000	
										0		0	
										15,000			
Date	Load (lbs)	Measured Deflection (mils):							Calculated Moduli Values (psi):				ERROR/SENSOR %
		R1	R2	R3	R4	R5	R6	R7	SURFACE (E1)	BASE (E2)	SUBBASE (E3)	SUBGRADE (E4)	
FEB AM	9,000	35.74	14.81	5.87	3.71	2.63	2.03	1.69	500,000	34,000	0	9,800	7.40
MAR AM	9,000	32.80	14.27	5.62	3.57	2.52	2.00	1.64	500,000	38,800	0	10,100	7.80
APR AM	9,000	34.25	13.63	5.50	3.58	2.54	1.97	1.64	500,000	34,900	0	10,600	8.30
MAY AM	9,000	33.04	13.38	5.38	3.43	2.47	1.85	1.64	500,000	36,600	0	10,800	7.70
JUN AM	9,000	33.22	13.15	5.24	3.38	2.45	1.88	1.55	500,000	35,500	0	11,100	8.10
JUL AM	9,000	33.74	12.88	5.20	3.23	2.41	1.87	1.53	500,000	33,900	0	11,400	7.50
AUG AM	9,000	49.19	19.51	7.13	4.67	3.09	2.43	1.74	500,000	22,200	0	7,800	9.00
SEP AM	9,000	33.60	13.84	5.59	3.42	2.48	1.94	1.58	500,000	36,300	0	10,400	6.60
OCT AM	9,000	35.00	14.41	5.56	3.58	2.65	2.02	1.65	500,000	36,600	0	10,500	8.40
NOV AM	9,000	33.77	14.18	5.72	3.72	2.64	2.07	1.68	500,000	37,100	0	10,000	7.80
DEC AM	9,000	35.27	14.50	5.97	3.89	2.81	2.17	1.76	500,000	35,300	0	9,700	8.20

APPENDIX D
BACKCALCULATION RESULTS

Table D1. Summary of the Backcalculation Results for Site 1.

Month	E _{Asphalt} (ksi)	E _{Base} (ksi)	E _{Subgrade} (ksi)	% Error per Sensor	Avg. Temp. (°F)
No Rigid Layer, Semi Infinite Subgrade					
Jan	1280	7.3	24.2	2.3	57
Feb	879	7.0	23.4	2.3	58
Mar	535	6.7	22.3	1.4	84
Apr	579	6.5	21.6	3.4	76
May	383	6.5	21.8	2.6	91
Jun	396	7.6	25.6	8.5	96
Jul	334	6.7	22.4	2.4	100
Aug	420	6.9	23.0	2.9	92
Sept	-	-	-	-	-
Oct	428	6.3	21.2	4.3	86
Nov	608	6.8	22.6	1.7	79
Dec	759	6.8	22.9	1.0	71
Year	600.1	6.8	22.8	3.0	
Rigid Layer at a Depth of 20 feet					
Jan	1066	44.5	16.7	2.1	57
Feb	594	48.5	16.2	1.5	58
Mar	339	36.3	15.6	2.7	84
Apr	521	19.0	15.3	1.7	76
May	303	19.0	15.6	3.8	91
Jun	322	17.0	17.8	4.8	96
Jul	247	19.4	15.9	3.9	100
Aug	340	20.0	16.4	5.1	92
Sept	-	-	-	-	-
Oct	398	14.2	15.2	2.9	86
Nov	451	30.8	15.8	2.7	79
Dec	534	40.9	15.9	3.0	71
Year	465	28.1	16.0	3.1	
Rigid Layer at a Predicted Depth of 6.1 feet (Selected Sensors)					
Jan	1243	18.6	12.4	5.3	57
Feb	549	62.0	10.1	0.9	58
Mar	366	56.6	10.3	0.9	84
Apr	433	59.7	9.5	0.1	76
May	372	25.9	10.4	0.9	91
Jun	355	26.3	11.9	4.1	96
Jul	277	32.4	10.5	1.4	100
Aug	414	29.3	10.8	1.4	92
Sept	-	-	-	-	-
Oct	487	21.2	9.8	0.6	86
Nov	492	50.9	10.2	0.7	79
Dec	659	50.0	10.3	0.6	71
Year	513.4	39.4	10.6	1.5	
E - Modulus of Elasticity					

Table D2. Summary of the Backcalculation Results for Site 2.

Month	E _{Asphalt} (ksi)	E _{Base} (ksi)	E _{Subgrade} (ksi)	% Error per Sensor	Avg. Temp. (°F)
No Rigid Layer, Semi Infinite Subgrade					
Jan	500	23.0	12.0	8.8	52
Feb	500	21.8	11.6	7.8	59
Mar	500	21.0	10.3	7.7	91
Apr	500	25.6	10.7	8.0	83
May	500	21.4	10.1	8.0	102
Jun	500	25.3	10.4	7.5	102
Jul	500	20.4	10.9	7.1	107
Aug	500	16.8	11.3	5.9	101
Sept	-	-	-	-	-
Oct	500	20.4	11.5	9.5	90
Nov	500	26.3	11.1	6.5	81
Dec	500	26.5	11.0	6.9	84
Year	500	22.6	11.0	7.6	
Rigid Layer at a Depth of 20 feet					
Jan	500	29.2	8.6	6.0	52
Feb	500	27.9	8.4	5.3	59
Mar	500	27.3	7.4	4.9	91
Apr	500	33.7	7.7	4.6	83
May	500	28.0	7.3	4.3	102
Jun	500	33.9	7.5	4.0	102
Jul	500	26.5	7.9	4.0	107
Aug	500	21.9	8.3	4.8	101
Sept	-	-	-	-	-
Oct	500	25.8	8.3	4.9	90
Nov	500	34.7	8.0	4.9	81
Dec	500	34.9	8.0	4.9	84
Year	500	29.4	7.9	4.8	
Rigid Layer at a Predicted Depth of 19.0 feet (Selected Sensors)					
Jan	500	29.4	8.5	5.4	52
Feb	500	27.2	8.5	3.4	59
Mar	500	26.5	7.5	3.3	91
Apr	500	32.7	7.7	3.2	83
May	500	27.1	7.4	2.6	102
Jun	500	31.6	7.7	2.2	102
Jul	500	25.0	8.2	1.5	107
Aug	500	19.7	8.8	1.4	101
Sept	-	-	-	-	-
Oct	500	26.2	8.1	5.1	90
Nov	500	32.4	8.3	2.2	81
Dec	500	32.9	8.2	2.4	84
Year	500	28.2	8.1	3.0	
E - Modulus of Elasticity					

Table D3. Summary of the Backcalculation Results for Site 4.

Month	E _{Asphalt} (ksi)	E _{Base} (ksi)	E _{Subgrade} (ksi)	% Error per Sensor	Avg. Temp. (°F)
No Rigid Layer, Semi Infinite Subgrade					
Jan	749	5.0	8.7	5.3	52
Feb	523	5.0	8.9	5.3	67
Mar	148	5.0	7.2	12.4	98
Apr	186	5.0	7.9	10.8	90
May	145	5.0	7.6	11.6	101
Jun	177	5.0	7.2	12.2	105
Jul	116	5.0	7.9	11.1	114
Aug	173	5.0	8.3	7.9	111
Sept	-	-	-	-	-
Oct	224	5.0	8.7	9.2	98
Nov	194	5.0	7.5	10.5	93
Dec	269	5.0	8.3	8.3	85
Year	264	5.0	8.0	9.5	
Rigid Layer at a Depth of 20 feet					
Jan	488	29.8	6.3	2.0	52
Feb	328	24.0	6.5	2.7	67
Mar	200	5.0	5.3	1.7	98
Apr	235	5.5	5.8	1.6	90
May	194	5.0	5.5	1.0	101
Jun	180	8.7	5.2	1.7	105
Jul	111	7.6	5.6	1.3	114
Aug	88	16.0	6.1	1.9	111
Sept	-	-	-	-	-
Oct	192	10.4	6.2	1.4	98
Nov	234	6.2	5.5	1.2	93
Dec	264	9.3	6.0	2.5	85
Year	228.5	11.6	5.8	1.7	
Rigid Layer at a Predicted Depth of 10.4 feet (Selected Sensors)					
Jan	423	48.1	5.3	0.3	52
Feb	292	36.8	5.5	0.6	67
Mar	142	13.1	4.2	0.6	98
Apr	167	14.6	4.7	0.6	90
May	131	13.3	4.5	3.0	101
Jun	110	20.8	4.3	1.1	105
Jul	59	18.2	4.7	1.8	114
Aug	52	29.5	5.2	0.8	111
Sept	-	-	-	-	-
Oct	129	22.4	5.2	0.8	98
Nov	175	14.9	4.5	0.7	93
Dec	229	17.5	5.0		85
Year	173.5	22.6	4.8	1.0	
E - Modulus of Elasticity					

Table D4. Summary of the Backcalculation Results for Site 5.

Month	E _{Asphalt} (ksi)	E _{Base} (ksi)	E _{Subgrade} (ksi)	% Error per Sensor	Avg. Temp. (°F)
No Rigid Layer, Semi Infinite Subgrade					
Jan	1492	28.2	14.9	1.4	55
Feb	1109	6.3	13.5	0.3	69
Mar	350	7.3	11.6	0.6	95
Apr	481	6.8	12.4	0.8	89
May	224	15.9	12.4	0.8	103
Jun	172	20.2	12.4	3.4	107
Jul	135	28.9	13.5	1.7	117
Aug	150	23.7	13.4	1.8	110
Sept	-	-	-	-	-
Oct	456	14.2	13.9	0.6	95
Nov	393	10.5	12.8	0.7	90
Dec	556	8.7	13.0	0.7	85
Year	501.6	15.5	13.1	1.2	
Rigid Layer at a Depth of 20 feet					
Jan	1197	24.2	11.9	11.1	55
Feb	961	33.5	9.6	3.6	69
Mar	202	43.4	8.5	5.4	95
Apr	270	50.0	8.9	4.5	89
May	139	60.7	9.3	7.1	103
Jun	108	70.7	9.4	7.0	107
Jul	103	78.5	10.3	8.8	117
Aug	102	71.0	10.2	8.3	110
Sept	-	-	-	-	-
Oct	291	72.2	10.3	6.0	95
Nov	245	55.5	9.4	6.1	90
Dec	323	62.0	9.5	4.9	85
Year	358.3	56.5	9.8	6.6	
Rigid Layer at a Predicted Depth of 11.5 feet (Selected Sensors)					
Jan	1036	47.1	10.4	8.6	55
Feb	836	57.2	8.4	1.4	69
Mar	234	37.0	7.7	3.3	95
Apr	294	46.8	8.0	2.7	89
May	140	57.1	8.6	4.5	103
Jun	111	64.6	8.6	6.2	107
Jul	97	72.8	9.7	5.9	117
Aug	108	62.9	9.6	5.1	110
Sept	-	-	-	-	-
Oct	275	71.5	9.4	3.2	95
Nov	341	28.4	9.0	0.9	90
Dec	417	37.5	8.8	0.5	85
Year	353.5	53.0	8.9	3.8	
E - Modulus of Elasticity					

Table D5. Summary of the Backcalculation Results for Site 6.

Month	E _{Asphalt} (ksi)	E _{Base} (ksi)	E _{Subgrade} (ksi)	% Error per Sensor	Avg. Temp. (°F)
No Rigid Layer, Semi Infinite Subgrade					
Jan	500	19.3	10.8	6.1	51
Feb	500	20.1	10.9	7.5	71
Mar	500	17.5	9.8	9.5	117
Apr	500	15.9	9.9	8.6	118
May	500	19.0	9.8	9.1	115
Jun	500	27.3	9.3	8.2	118
Jul	500	18.0	9.8	10.4	134
Aug	500	16.1	10.4	7.7	130
Sept	-	-	-	-	-
Oct	500	21.0	8.8	6.7	114
Nov	500	17.1	9.0	9.2	105
Dec	500	20.0	9.6	7.5	99
Year	500	19.2	9.8	8.2	
Rigid Layer at a Depth of 20 feet					
Jan	500	26.4	7.8	6.0	51
Feb	500	27.5	7.8	4.2	71
Mar	500	24.9	7.0	3.3	117
Apr	500	22.3	7.1	3.9	118
May	500	26.6	7.0	3.0	115
Jun	500	38.9	6.7	3.4	118
Jul	500	25.4	6.9	3.0	134
Aug	500	23.1	7.5	6.0	130
Sept	-	-	-	-	-
Oct	500	30.0	6.3	3.0	114
Nov	500	24.7	6.4	3.5	105
Dec	500	28.9	6.6	4.9	99
Year	500	27.1	7.0	4.0	
Rigid Layer at a Predicted Depth of 23.5 feet (Selected Sensors)					
Jan	500	23.2	8.7	1.7	51
Feb	500	24.7	8.5	0.8	71
Mar	500	21.8	7.6	3.1	117
Apr	500	19.5	7.8	2.3	118
May	500	24.1	7.5	0.9	115
Jun	500	35.1	7.2	2.3	118
Jul	500	23.3	7.4	2.0	134
Aug	500	19.1	8.4	5.0	130
Sept	-	-	-	-	-
Oct	500	27.0	6.8	1.4	114
Nov	500	21.3	7.0	2.9	105
Dec	500	24.1	7.6	3.2	99
Year	500	23.9	7.7	2.3	
E - Modulus of Elasticity					

Table D6. Summary of the Backcalculation Results for Site 7.

Month	E _{Asphalt} (ksi)	E _{Base} (ksi)	E _{Subgrade} (ksi)	% Error per Sensor	Avg. Temp. (°F)
No Rigid Layer, Semi Infinite Subgrade					
Jan	-	-	-	-	-
Feb	1500	22.8	28.7	4.5	47
Mar	1500	24.7	27.3	2.8	61
Apr	1321	9.1	30.4	0.8	76
May	1500	9.5	30.6	0.7	74
Jun	934	12.8	28.1	0.9	87
Jul	828	10.1	29.2	1.0	95
Aug	436	7.1	19.6	1.7	98
Sept	514	8.9	27.4	1.5	103
Oct	1500	13.3	28.9	1.0	73
Nov	1500	14.4	30.2	5.1	59
Dec	1500	13.9	29.2	4.5	60
Year	1184.8	13.3	28.1	2.2	
Rigid Layer at a Depth of 20 feet					
Jan	-	-	-	-	-
Feb	1500	11.8	24.8	13.2	47
Mar	1500	11.3	23.8	9.1	61
Apr	1500	15.8	20.3	2.0	76
May	1500	28.4	19.8	2.9	74
Jun	1006	29.0	18.7	1.6	87
Jul	870	21.6	19.2	1.6	95
Aug	445	15.1	13.0	3.2	98
Sept	483	21.1	18.1	1.2	103
Oct	1500	31.5	19.7	2.7	73
Nov	1500	11.7	24.7	11.4	59
Dec	1500	11.3	23.8	10.8	60
Year	1210	19.0	20.5	5.4	
Rigid Layer at a Predicted Depth of 9.1 feet (Selected Sensors)					
Jan	-	-	-	-	-
Feb	1500	15.4	19.3	13.6	47
Mar	1500	23.4	16.0	7.6	61
Apr	1387	28.1	13.9	1.2	76
May	1500	9.0	17.8	5.3	74
Jun	681	79.1	12.4	1.2	87
Jul	596	65.0	12.7	1.1	95
Aug	367	28.3	9.0	2.7	98
Sept	358	48.9	12.3	1.7	103
Oct	1500	9.7	18.2	7.2	73
Nov	1500	23.8	17.1	10.2	59
Dec	1500	9.7	18.8	11.5	60
Year	1126.3	30.9	15.2	5.8	
E - Modulus of Elasticity					

Table D7. Summary of the Backcalculation Results for Site 8.

Month	E _{Asphalt} (ksi)	E _{Base} (ksi)	E _{Subgrade} (ksi)	% Error per Sensor	Avg. Temp. (°F)
No Rigid Layer, Semi Infinite Subgrade					
Jan	-	-	-	-	-
Feb	1500	47.4	28.5	1.3	56
Mar	1365	38.9	28.0	1.0	66
Apr	762	36.6	28.3	1.3	81
May	796	43.6	27.0	0.9	74
Jun	457	54.0	27.2	1.3	89
Jul	328	43.1	26.7	1.3	99
Aug	138	20.2	17.7	3.6	115
Sept	260	31.1	24.5	0.9	106
Oct	1036	45.7	26.6	1.3	71
Nov	1500	45.6	28.7	0.9	60
Dec	1500	38.4	28.6	1.0	56
Year	876.5	40.4	26.5	1.3	
Rigid Layer at a Depth of 20 feet					
Jan	-	-	-	-	-
Feb	1351	100	19.5	2.3	56
Mar	1023	100	19.1	3.1	66
Apr	534	89.4	19.7	4.2	81
May	570	100	18.9	3.6	74
Jun	377	100	19.3	4.7	89
Jul	239	89.4	19.0	5.3	99
Aug	100	40.7	12.8	5.6	115
Sept	179	65.9	17.5	5.6	106
Oct	816	100	18.4	3.6	71
Nov	1325	100	19.6	2.5	60
Dec	1165	100	19.5	2.7	56
Year	698.1	89.6	18.5	3.9	
Rigid Layer at a Predicted Depth of 14.6 feet (Selected Sensors)					
Jan	-	-	-	-	-
Feb	1500	73.6	19.3	0.9	56
Mar	1500	34.1	21.5	2.6	66
Apr	752	49.4	20.2	2.0	81
May	748	62.3	19.1	1.0	74
Jun	448	68.0	19.7	2.0	89
Jul	317	55.1	19.7	2.0	99
Aug	125	26.9	13.1	3.8	115
Sept	243	41.7	18.2	2.8	106
Oct	1500	11.0	27.6	6.2	71
Nov	1500	22.7	26.4	8.1	60
Dec	1500	22.1	25.5	6.9	56
Year	921.2	42.4	20.9	3.5	
E - Modulus of Elasticity					

Table D8. Summary of the Backcalculation Results for Site 9.

Month	E _{Asphalt} (ksi)	E _{Base} (ksi)	E _{Subgrade} (ksi)	% Error per Sensor	Avg. Temp. (°F)
No Rigid Layer, Semi Infinite Subgrade					
Jan	-	-	-	-	-
Feb	500	48.3	18.1	8.3	56
Mar	500	38.2	16.9	8.2	73
Apr	500	38.9	17.7	9.5	78
May	500	36.9	16.8	8.7	77
Jun	500	39.2	17.0	8.6	86
Jul	500	28.9	16.8	10.7	112
Aug	500	18.8	12.0	12.8	107
Sept	500	27.7	16.6	10.7	115
Oct	500	46.2	16.5	8.9	78
Nov	500	45.7	16.6	9.6	68
Dec	500	51.2	17.8	8.1	61
Year	500	38.2	16.6	9.5	
Rigid Layer at a Depth of 20 feet					
Jan	-	-	-	-	-
Feb	500	66.4	12.9	3.0	56
Mar	500	51.9	12.0	2.7	73
Apr	500	53.0	12.6	1.7	78
May	500	50.3	12.0	2.4	77
Jun	500	54.5	12.1	3.0	86
Jul	500	39.6	11.9	2.4	112
Aug	500	25.0	8.6	3.2	107
Sept	500	37.7	11.8	1.7	115
Oct	500	63.9	11.8	3.1	78
Nov	500	63.2	11.8	2.6	68
Dec	500	71.3	12.7	3.1	61
Year	500	52.4	11.8	2.6	
Rigid Layer at a Predicted Depth of 16.1 feet (Selected Sensors)					
Jan	-	-	-	-	-
Feb	500	62.4	12.9	2.1	56
Mar	500	48.5	12.1	2.4	73
Apr	500	49.9	12.5	2.4	78
May	500	46.9	12.0	2.7	77
Jun	500	48.8	12.4	2.3	86
Jul	500	36.3	11.9	4.8	112
Aug	500	25.2	8.1	2.7	107
Sept	500	35.5	11.6	4.8	115
Oct	500	61.4	11.6	1.7	78
Nov	500	61.6	11.5	1.5	68
Dec	500	66.8	12.7	2.0	61
Year	500	49.4	11.8	2.7	
E - Modulus of Elasticity					

Table D9. Summary of the Backcalculation Results for Site 11.

Month	E _{Asphalt} (ksi)	E _{Base} (ksi)	E _{Subgrade} (ksi)	% Error per Sensor	Avg. Temp. (°F)
No Rigid Layer, Semi Infinite Subgrade					
Jan	-	-	-	-	-
Feb	1133	27.6	26.7	1.8	48
Mar	1046	34.2	25.1	1.0	66
Apr	852	36.3	25.5	1.2	71
May	660	39.7	26.8	1.0	79
Jun	325	46.9	26.9	0.7	95
Jul	231	51.6	27.8	1.3	95
Aug	317	33.9	20.8	4.3	100
Sept	451	40.5	26.2	0.7	90
Oct	848	40.5	25.3	0.5	76
Nov	1300	33.4	26.3	0.9	62
Dec	1500	45.4	27.6	2.0	52
Year	787.5	39.1	25.9	1.4	
Rigid Layer at a Depth of 20 feet					
Jan	-	-	-	-	-
Feb	822	44.7	19.1	2.8	48
Mar	834	52.9	18.0	3.3	66
Apr	678	54.7	18.3	3.3	71
May	535	57.7	19.4	3.8	79
Jun	290	64.2	19.4	4.3	95
Jul	215	68.7	19.9	4.6	95
Aug	274	47.3	15.0	3.9	100
Sept	376	57.0	19.0	4.5	90
Oct	703	60.1	18.2	3.9	76
Nov	1042	53.1	18.7	3.4	62
Dec	1500	66.7	19.6	1.6	52
Year	660.8	57.0	18.6	3.6	
Rigid Layer at a Predicted Depth of 10.4 feet (Selected Sensors)					
Jan	-	-	-	-	-
Feb	707	48.2	15.4	1.0	48
Mar	754	53.1	14.8	1.7	66
Apr	597	55.5	15.0	2.0	71
May	480	57.4	16.1	2.2	79
Jun	240	64.1	16.3	2.8	95
Jul	133	85.8	15.4	8.4	95
Aug	214	54.1	11.5	7.5	100
Sept	280	66.4	14.6	8.0	90
Oct	644	58.2	15.2	1.9	76
Nov	980	52.5	15.4	1.7	62
Dec	1026	79.1	15.3	0.2	52
Year	550.5	61.3	15.0	3.4	
E - Modulus of Elasticity					

Table D10. Summary of the Backcalculation Results for Site 12.

Month	E _{Asphalt} (ksi)	E _{Base} (ksi)	E _{Subgrade} (ksi)	% Error per Sensor	Avg. Temp. (°F)
No Rigid Layer, Semi Infinite Subgrade					
Jan	-	-	-	-	-
Feb	500	23.3	18.6	7.1	65
Mar	500	26.4	19.4	6.7	69
Apr	500	24.4	19.4	5.9	77
May	500	25.5	20.0	6.0	74
Jun	500	24.9	20.4	5.8	96
Jul	500	24.0	20.6	5.9	110
Aug	500	14.1	15.8	11.7	103
Sept	500	24.9	19.8	7.0	90
Oct	500	25.6	19.4	5.3	76
Nov	500	25.7	18.8	6.0	65
Dec	500	24.6	17.9	5.4	52
Year	500	23.9	19.1	6.6	
Rigid Layer at a Depth of 20 feet					
Jan	-	-	-	-	-
Feb	500	17.6	14.0	7.4	65
Mar	500	31.4	14.5	8.3	69
Apr	500	29.2	14.6	7.2	77
May	500	30.3	15.1	7.5	74
Jun	500	29.6	15.4	7.6	96
Jul	500	28.3	15.7	7.9	110
Aug	500	17.3	11.6	5.1	103
Sept	500	29.6	14.9	7.5	90
Oct	500	30.3	14.7	9.0	76
Nov	500	30.8	14.0	7.5	65
Dec	500	29.7	13.4	7.4	52
Year	500	27.6	14.4	7.5	
Rigid Layer at a Predicted Depth of 5.9 feet (Selected Sensors)					
Jan	-	-	-	-	-
Feb	500	34.0	9.8	7.4	65
Mar	500	38.8	10.1	7.8	69
Apr	500	34.9	10.6	8.3	77
May	500	36.6	10.8	7.7	74
Jun	500	35.5	11.1	8.1	96
Jul	500	33.9	11.4	7.5	110
Aug	500	22.2	7.8	9.0	103
Sept	500	36.3	10.4	6.6	90
Oct	500	36.6	10.5	8.4	76
Nov	500	37.1	10.0	7.8	65
Dec	500	35.3	9.7	8.2	52
Year	500	34.7	10.2	7.9	
E - Modulus of Elasticity					